DESIGN AND DEVELOPMENT OF TUMOR MICROENVIRONMENT RESPONSIVE PEGYLATED NANOPARTICLES FOR DRUG DELIVERY TO CANCEROUS SOLID TUMORS

A Dissertation
Submitted to the Graduate Faculty
of the
North Dakota State University
of Agriculture and Applied Science

By

Prajakta Satish Kulkarni

In Partial Fulfillment of the Requirements
for the Degree of
DOCTOR OF PHILOSOPHY

Major Department:
Pharmaceutical Sciences

July 2016

Fargo, North Dakota

North Dakota State University
Graduate School

Title

DESIGN AND DEVELOPMENT OF TUMOR MICROENVIRONMENT RESPONSIVE PEGYLATED NANOPARTICLES FOR DRUG DELIVERY TO CANCEROUS SOLID TUMORS

By

Prajakta Satish Kulkarni

The Supervisory Committee certifies that this ***disquisition*** complies with North Dakota State University's regulations and meets the accepted standards for the degree of

DOCTOR OF PHILOSOPHY

SUPERVISORY COMMITTEE:

Dr. Sanku Mallik
Chair

Dr. Bin Guo

Dr. Estelle Leclerc

Dr. Katie Reindl

Approved:

07/12/2016
Date

Dr. Jagdish Singh
Department Chair

ABSTRACT

Rapid growth of cancerous cells creates a biochemically distinct microenvironment in solid tumors. Leaky vasculature, lower pH, increased levels of proteolytic enzymes, hypoxia serve as hallmarks of tumor tissues. These changes in the tumor microenvironment present with opportunities to deliver drug at the targeted tumor tissues using stimuli responsive PEGylated nanoparticles. Stimuli responsive PEGylated nanoparticles extravasate into the tumor tissues through leaky vasculature developed at the tumor site. In the tumor tissue they undergo changes in the physico-chemical properties of the nanoparticle leading to stimuli responsive release of the entrapped chemotherapeutic/imaging agents. Clinical use of PEGylated liposomal doxorubicin formulation has encouraged multiple studies to improve the efficacy of the treatment and reduce side effects of chemotherapy. Liposomes and polymersomes are nanoparticles which form a lipid or polymeric bilayer allowing entrapment of hydrophilic molecules at the core and lipophilic molecules in the bilayer. These chemically engineered drug carriers allow targeting and drug delivery preferentially at the pathologically affected tissues. Stimuli responsive liposomes and polymersomes hold tremendous potential for drug delivery to solid tumors. We have prepared tumor microenvironment responsive PEGylated liposomes and polymersomes for efficient drug delivery to pancreatic cancer cells.

ACKNOWLEDGEMENTS

I would like to express my sincere gratitude towards my advisor Dr. Sanku Mallik for his constant support and guidance throughout my graduate studies. He always encouraged me to excel in academics and co-curricular activities. I would like to extend my genuine thanks to my graduate advisory committee members, Dr. Bin Guo, Dr. Estelle Leclerc, Dr. Katie Reindl for their valuable suggestions on my preliminary proposal. These suggestions steered my research in a right direction. I would also like to thank our department Chair Dr. Jagdish Singh for encouraging me to excel in the graduate studies.

I would also like to thank, Dr. D. K. Srivastava, Dr. K. Gange, Dr. W. Muhonen, Dr. J. Shabb, Dr. Yongki Choi, Dr. Seungyong You, Dr. Kausik Sarkar, Dr. Kalpana Katti, and Scott Payne for their guidance and help. I would also like to extend warm and sincere thanks to Dr. Manas Haldar, Rahul, Rinku, Erin, Mike and Fataneh for being excellent lab mates. I would like to acknowledge Janet Krom and Jean Trautmann for their help and assistance throughout my graduate studies. I would also like to thank my friends and fellow graduate students.

I gratefully acknowledge the financial support from the National Institute of Health (NIH), NSF and ND-EPSCoR. I would also like to acknowledge help of undergraduate and PharmD students - Preeya, Cortney, Anessa, Rayat, Matt, Cody and Chris who worked with me on various projects.

I would like to thank my parents, my husband Gaurav, my dad, family and friends for their support, patience and understanding during my entire graduate studies.

DEDICATION

To my loving parents and my supportive husband

TABLE OF CONTENTS

LIST OF TABLES

LIST OF FIGURES

LIST OF SCHEMES

LIST OF ABBREVIATIONS

ACS……..American Chemical Society

AFM…….Atomic Force Microscopy

ATCC……American Type Culture Collection

Avg……Average

C……Centigrade

CD…….....Circular Dichroism

cm…….....Centimeter

CYS……...Cysteine

dB…….....Decibel

DLS……....Dynamic Light Scattering

DSPC……..1,2-distearoyl-sn-glycero-3-phosphocholine

DSPE……..1,2-distearoyl-sn-glycero-3-phosphoethanolamine

EPR…….....Enhanced Permeation and Retention

Em……...Emission

Ex…….....Excitation

FDA…….....Federal Drug Administration

g……...Grams

GSH…….....Glutathione

h……...Hours

HBSS……...Hank's Blank salt solution

HBTU…….....O-Benzotriazole-N,N,N',N'-tetramethyl-uronium-hexafluoro-phosphate

HEPES…….4-(2-hydroxyethyl)-1-piperazineethanesulfonic acid

HOBT …….Hydroxybenzotriazole

HPLC……..High Performance Liquid Chromatography

LP…….Lipopeptide

M……..Molar

MALDI-TOF…….....Matrix-assisted laser desorption/ionization- Time of Flight

mg…….Milligrams

MHz……..Mega Hertz

mL…….Milliliters

mm……...…….Millimeters

mmol…….Millimolars

MMP…….Matrix Metalloproteinase

m-PEG……..Methoxy Polyethyleneglycol

MW……...Molecular Weight

n……Number

nm…….Nanometer

NMR…….Nuclear Magnetic Resonance

PBS……...Phosphate Buffered Saline

PDI…….....Polydispersity Index

PEG……...Polyethylene glycol

PLA……...Polylactic acid

PMDETA …….N,N,N′,N′,N″-pentamethyldiethylenetriamine

POPC…….....1-palmitoyl-2-oleoyl-sn-glycero-3-phosphocholine

POPE…….....1-palmitoyl-2-oleoyl-sn-glycero-3-phosphoethanolamine

RPMI……Roswell Park Memorial Institute medium

TEM…….Transmission Electron Microscopy

THF……..Tetrahydrofuran

µL…….Microliter

µmol…….Micromoles

UV ……...Ultravoilet

V ……..Volts

W……..Watts

3D…….Three dimensional

LIST OF APPENDIX TABLES

LIST OF APPENDIX FIGURES

1. INTRODUCTION AND DISSERTATION ORGANIZATION

Stimuli-responsive drug delivery increases the efficiency of chemotherapy treatment.[1] With the advances in nanomedicine and drug delivery carriers, chemotherapeutic agents can be targeted to the tumor tissues to enhance the effectiveness of the chemotherapy treatment and reduce side effects.[2] Extensive studies have reported increased drug accumulation and better tumor growth control with nanoparticulate drug delivery carriers compared to the conventional treatment.[3] However, the challenges in maintaining the chemical and structural stability of stimuli-responsive drug carriers in the normal tissues limit their clinical use. Stimuli-responsive carriers recognize changes in the biochemical or physical environment and deliver the drugs preferentially in the tumor tissues.[4] The internal stimuli are the abnormal biochemical patterns in the pathological conditions. However, external stimuli are externally applied. External stimuli include heat, light, ultrasound, and magnetic field.[5]

1.1. Tumor microenvironment and opportunities for drug delivery

The exponential growth of cancer cells generates a distinct microenvironment in the tumor tissues.[6] Rapid cell growth increases demands for blood flow, oxygen, and nutrients in the tumor microenvironment[7] and promotes irregular tissue architecture, biochemical variations, and altered vasculature. Irregularly developed vasculature presents endothelial lining with nanosized pores.[8] Nanoparticles circulating in the blood stream can extravasate through such leaky vasculature and accumulate in the tumor tissues.[9] Tumor tissues exhibit lower pH, elevated enzyme levels, overexpressed receptors, reducing environment, and hypoxic regions.[4] Drastic changes in the normal and pathological environments offer opportunities for targeted drug delivery in tumor tissues. Numerous studies report the ingenious chemical designs of nanoparticles which interact with tumor microenvironment and deliver the drugs.[4, 10] Drastic structural and biochemical

changes in the tumor tissues inspire the design and development of stimuli-responsive nanoparticles.

1.2. Stimuli-responsive nanoparticles

Stimuli-responsive nanoparticles are designed to be stable in normal tissues but release the drugs only in the tumors.[11, 12] Such nanoparticles undergo chemical changes in response to biochemical or physical stimulus and disintegrate to deliver the encapsulated drug.[13] These nanoparticles are broadly classified as external, and internal stimuli-responsive based on the trigger used to release the encapsulated drug. External stimuli-responsive nanoparticles use an applied physical energy (e.g., heat, light, ultrasound) to release the encapsulated content.[14, 15, 16] The internal stimuli-responsive nanoparticles undergo chemical transitions in response to biochemical changes observed in pathologically affected tissue. Elevated proteolytic enzymes, reduced pH, reducing environment, and hypoxia in the tumor tissues act as excellent internal triggers for tumor-specific drug delivery.[17]

1.2.1. pH-responsive nanoparticles

Human tumors are acidic due to lactic acid accumulation in rapidly growing cells, insufficient blood supply, and poor lymphatic drainage.[6] This acidic tumor pH has been exploited to achieve high local drug concentrations and to minimize overall systemic exposure. The pH-responsive nanoparticles change the physical, and chemical properties (such as by swelling and an increase in solubility) in response to local pH levels.[18]

1.2.2. Reduction-sensitive nanoparticles

Tumor tissues show high concentrations of the reducing tripeptide glutathione.[19] The sulfhydryl group glutathione engages in thiol transfer reactions with disulfide bonds. Stimuli-responsive lipids or polymers incorporating disulfide bonds undergo thiol exchange reactions and

reduction in the tumor microenvironment.[20] Hence, nanoparticles comprising of reduction sensitive disulfide linker undergo reduction in the presence of elevated levels of glutathione and release the encapsulated drug.

1.2.3. Proteolytic enzyme responsive nanoparticles

Tumor tissues present high level of proteolytic enzymes such as MMP-2 and MMP-9. The enzyme responsive nanoparticles use a synthetic substrate "bait" which the enzyme recognizes and cleaves. Various peptides and small synthetic molecules have been designed to respond to elevated enzymes and trigger the drug release from the drug carrier.[21, 22]

1.2.4. Hypoxia responsive nanoparticles

Hypoxia or lower oxygen levels are often observed in solid tumors because of poorly developed tumor vasculature. Hypoxia promotes biochemical remodeling of the tumor microenvironment. Hypoxia is developed in the tumor tissue because of irregular blood supply and insufficient drainage from tumor tissues.[23] These hypoxic regions form far from the leaky vasculature. Hypoxia responsive carriers have a high potential for efficient drug delivery, albeit this approach is less explored. Nitroimidazole and azobenzene derivatives undergo reduction in the hypoxic environment and hence act as hypoxia responsive materials.[24]

1.3. Tumor targeting strategies

1.3.1. Active targeting

For active targeting, the nanoparticles are conjugated to a chemical ligand to interact with overexpressed receptors on the cancer cells.[25] For example, in many breast cancer patients, the HER-2 receptor is overexpressed.[26] The drug Herceptin (Trastuzumab, a recombinant DNA-derived humanized monoclonal antibody), acts as a ligand for the HER-2 receptor.[27] When a patient is diagnosed with breast cancer, further test is conducted to determine the expression levels

of the HER-2 receptor. If overexpression of the receptors is observed, patients receive targeted treatments in the clinics.[28] The folate receptor is overexpressed in various solid tumors.[29] When the folic acid-drug conjugate is administered, it targets the overexpressed folate receptors on the cancer cells to delivers the drug preferentially to the cancer cells.[30] Numerous active targeting approaches have been found to improve the treatment *in-vivo* and *in-vitro*.

1.3.2. Passive targeting

Tumor tissues show irregular vasculature with leaky endothelial lining. Nanoparticles circulating in the blood stream extravasate in the tumor tissue through the gaps between the endothelial lining by the enhanced permeation and retention (EPR) phenomenon.[31] It is different from active targeting in multiple ways. a) Nanoparticles targeted by EPR effect, infiltrate the tumor tissues irrespective of the receptor expression level. b) The nanoparticulate drug carriers can be targeted by the passive targeting, and not the small drug molecules. c) Nanoparticles utilize the leaky vasculature developed in the tumors to gain entry into the tumor tissues.[6, 32] Passively targeted nanoparticles are designed to be intact in healthy tissues to minimize the side effects associated with intravenously injected chemotherapeutic agents.[33]

It is also important that the long-circulating drug carrier avoids the reticuloendothelial system to prevent premature delivery of the loaded drug at non-targeted sites. Nanoparticles designed to follow the 'Trojan horse' approach, show better passive targeting to the tumor tissues.[34] Various hydrophilic polymer coatings on the nanoparticles have been developed to impart long circulating characteristics to the nanoparticles.[35,36] However, the most reliable results are observed by coating the nanoparticles with poly (ethylene glycol) (PEGylation). The hydrophilic PEG coating makes the nanoparticles long circulating by avoiding the deposition of opsonins on the surface.[37] This helps in avoiding interaction with the reticuloendothelial system

and immature release of encapsulated drugs. A PEGylated liposomal formulation encapsulating doxorubicin is approved by the US FDA for clinical use. [38, 39]

1.4. Nanocarriers

Multiple polymer and lipid based nanosized drug carriers have been developed to extravasate the tumor tissue through the EPR effect. Liposomes, polymersomes, micelles, nanosilica, and nanoceria are a few examples of nanocarriers for drug delivery to tumor tissues.[40] The bilayer membranes of liposomes and polymersomes encapsulate hydrophilic drugs in the core and entrap hydrophobic drugs in the bilayer.[41]

1.4.1. Liposomes as drug carriers

Liposomes are nano-sized lipid vesicles capable of encapsulating the hydrophilic drug in their core and hydrophobic drugs in the lipid bilayer. Liposomes are the most experimented form of nanoparticles.[42] The versatility of the lipids allows various chemical strategies to design a liposome.[43] [44] Simple conjugation of PEG polymer to the lipids gives the liposomes long circulating characteristics.[45] The US Food and Drug Administration (FDA) has approved multiple liposomal formulations for human use.[46] Liposomes encapsulating the cytotoxic drug doxorubicin is used clinically for the treatment of cancer under the brand names Doxil and lipodox. Recently, FDA has approved Onivyde (irinotecan liposome injection), in combination with fluorouracil and leucovorin, to treat patients with advanced (metastatic) pancreatic cancer who have been previously treated with gemcitabine-based chemotherapy.[47]

1.4.2. Polymersomes as drug carriers

Polymersomes are nanoparticles prepared from amphiphilic block copolymers which self-assemble into spherical particles encapsulating the hydrophilic drug in the core and hydrophobic drug in the bilayer.[48] Polymersomes form rigid membranes, making them more stable than

liposomes. The stimuli-responsive polymersomes release the encapsulated drugs at the targeted site.[49]

Stimuli-responsive nanoparticles are promising drug carriers. Multiple external stimuli-responsive nanoparticles are in clinical trials. However, internal stimuli-responsive nanoparticles remain less explored. In our studies, we have developed stable nanoparticles and internal stimuli-responsive nanoparticles.

1.5. Organization of the Thesis

We have designed PEGylated stimuli-responsive liposomes and polymersomes to release the encapsulated drug in the tumor microenvironment. This is a paper-based thesis. All chapters are intended for publication in peer-reviewed journals (Section 2,3 and 4 are published). These are the abstracts for each of the sections.

2. MMP-9 responsive PEGylated nanovesicles for drug delivery to solid tumors

Significant differences in biochemical parameters between normal and tumor tissues offer an opportunity to chemically design drug carriers which respond to these changes and deliver the drugs at the desired site. For example, overexpression of the matrix metalloproteinase-9 (MMP-9) enzyme in the extracellular matrix of tumor tissues can act as a trigger to chemically modulate the drug delivery from the carriers. In this study, we have synthesized an MMP-9-cleavable, collagen mimetic lipopeptide which forms nanosized vesicles with the POPC, POPE-SS-PEG, and cholesteryl-hemisuccinate lipids. The lipopeptide retains the triple-helical conformation when incorporated into these nanovesicles. The PEG groups shield the substrate lipopeptides from hydrolysis by MMP-9. However, in the presence of elevated glutathione levels, the PEG groups are reductively removed, exposing the lipopeptides to MMP-9. The resultant peptide-bond cleavage disturbs the vesicles' lipid bilayer, leading to the release of encapsulated contents. These

PEGylated nanovesicles are capable of encapsulating the anticancer drug gemcitabine with 50% efficiency. They were stable in physiological conditions and in human serum. Effective drug release was demonstrated using the pancreatic ductal carcinoma cells (PANC-1 and MIAPaCa-2) in two-dimensional and three-dimensional "tumor-like" spheroid cultures. A reduction in tumor growth was observed after intravenous administration of the gemcitabine-encapsulated nanovesicles in the xenograft model of athymic, female nude mice.

(MMP-9 responsive nanovesicles for efficient delivery of chemotherapeutics to pancreatic cancer, Molecular Pharmaceutics, 2014, 11 (7): 2390–2399)

(http://pubs.acs.org/doi/abs/10.1021/mp500108p)

3. Hypoxia responsive, tumor penetrating lipid nanoparticles for delivery of chemotherapeutics to pancreatic cancer cell spheroids

The solid tumors are often poorly irrigated due to the structurally compromised microcirculation. Uncontrolled multiplication of cancer cells, insufficient blood flow, and the lack of enough oxygen and nutrients lead to the development of hypoxic regions in the tumor tissues. As the partial pressure of oxygen drops below the necessary level (10 psi), the cancer cells modulate their genetic makeup to survive. Hypoxia triggers tumor progression by enhancing angiogenesis, cancer stem cell production, remodeling of the extracellular matrix, and epigenetic changes in the cancer cells. However, the hypoxic regions are usually located deep in the tumors and are usually inaccessible to the intravenously injected drug carrier or the drug. Considering the designs of the reported nanoparticles, it is likely that the drug is delivered to the peripheral tumor tissues, close to the blood vessels. In this study, we prepared lipid nanoparticles (LNs) comprising the synthesized hypoxia-responsive lipid and a peptide-lipid conjugate. We observed that the resultant nanoparticles penetrated to the hypoxic regions of the tumors. Under low oxygen partial

pressure, the hypoxia-responsive lipid undergoes reduction, destabilize the lipid membrane, and release the encapsulated drugs from the nanoparticles. We demonstrated the results employing spheroidal cultures of the pancreatic cancer cells BxPC-3. We observed that the peptide-decorated, drug encapsulated LNs reduced the viability of pancreatic cancer cells of the spheroids to 35% under hypoxic conditions.

(Hypoxia responsive, tumor penetrating lipid nanoparticles for delivery of chemotherapeutics to pancreatic cancer cell spheroids, Bioconjugate Chemistry, 2016, 27 (8), 1830–1838)

(http://pubs.acs.org/doi/abs/10.1021/acs.bioconjchem.6b00241)

4. Hypoxia responsive polymersomes for drug delivery to hypoxic pancreatic cancer cells

Hypoxia in tumors contributes to overall tumor progression by assisting in epithelial-to-mesenchymal transition, angiogenesis, and metastasis of cancer. In this study, we have synthesized a hypoxia-responsive, diblock copolymer poly(lactic acid)−azobenzene−poly(ethylene glycol), which self- assembles to form polymersomes in an aqueous medium. The polymersomes did not release any encapsulated contents for 50 min under normoxic conditions. However, under hypoxia, 90% of the encapsulated dye was released in 50 min. The polymersomes encapsulated the combination of anticancer drugs gemcitabine and erlotinib with entrapment efficiency of 40% and 28%, respectively. We used three-dimensional spheroid cultures of pancreatic cancer cells BxPC-3 to demonstrate hypoxia-mediated release of the drugs from the polymersomes. The vesicles were nontoxic. However, a significant decrease in cell viability was observed in hypoxic spheroidal cultures of BxPC-3 cells in the presence of drug encapsulated polymersomes. These polymersomes have potential for future applications in imaging and treatment of hypoxic tumors.

(Hypoxia-responsive polymersomes for drug delivery to hypoxic pancreatic cancer cells, Biomacromolecules 2016, *17* (8), 2507–2513)

(http://pubs.acs.org/doi/abs/10.1021/acs.biomac.6b00350)

5. Hypoxia responsive echogenic polymersomes for drug delivery to hypoxic pancreatic cancer cells

Echogenic polymersomes allow ultrasound assisted tracking of the drug carrier as it delivers the drug at the targeted site. Hypoxia in tumor tissue modulates tumor microenvironment and extracellular matrix to promote angiogenesis and metastasis. We have prepared echogenic hypoxia responsive polymersomes using azobenzene conjugated PLA-PEG polymer to allow the release of the encapsulated drug in hypoxic cancer cells. Polymersomes are surface functionalized with a cyclic peptide iRGD to allow deep penetration into the tumor tissues. These polymersomes were observed to encapsulate anticancer drug gemcitabine with 50% entrapment efficiency. Polymersomes were observed to be echogenic at diagnostic ultrasound frequencies. Under hypoxic conditions, up to 65% of the encapsulated content released. Treatment with drug encapsulated polymersomes resulted in decreased cell viability in hypoxic monolayer and spheroidal cultures of BxPC-3 cells. Improved penetration was observed with iRGD peptide conjugated polymersomes in the layered culture of pancreatic cancer cells BxPC-3.

(Manuscript under preparation)

2. MMP-9 RESPONSIVE PEGYLATED NANOVESICLES FOR DRUG DELIVERY TO SOLID TUMORS[1]

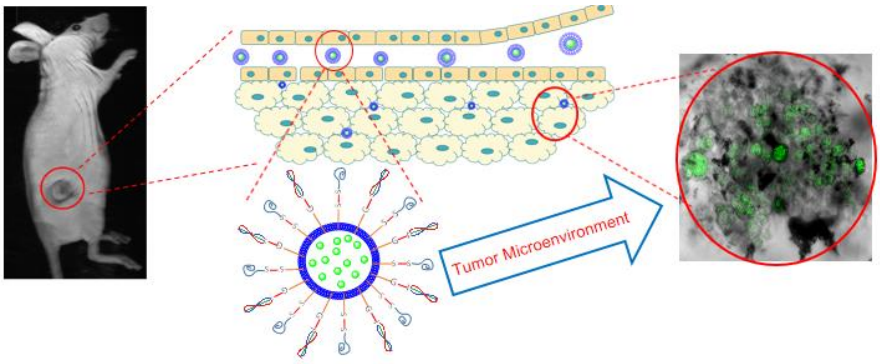

Figure 2.1. Graphical abstract

2.1. Introduction

Stimuli-responsive nanomaterials deliver encapsulated drugs preferentially at the target site, enhancing the therapeutic benefits and minimizing drug-related cytotoxicity.[50] Several extraneous sources of energy, such as temperature, light, magnetic field, ultrasound, etc., have been used to release the encapsulated drugs from the nanomaterials.[51] Internal stimuli-responsive carriers use the inherent biochemical differences between physiological and cancerous tissues

[1] This section is coauthored by Kulkarni, Prajakta; Haldar, Manas; Nahire, Rahul; Katti, Preeya; Ambre, Avinash; Muhonen, Wallace; Shabb, John; Padi, Sathish; Singh, Raushan; Borowicz, Powel; Srivastava, D. K.; Katti, Kalpana; Reindl, Katie; Guo, Bin; Mallik, Sanku.
Prajakta had primary responsibility to conduct all the experiments listed in the section, analyze the data and write the manuscript. Manas had primary responsibility for synthesizing reduction sensitive lipid. Wallace and Muhonen recorded MALDI mass spectrum for synthesized compounds. Rahul and Sathish assisted in animal studies, Avinash imaged the liposomes with AFM, Raushan synthesized recombinant MMP-9. Preeya helped in cellular experiments. Drs. Borowicz, Powel; Srivastava, D. K.; Katti, Kalpana; Reindl, Katie; Guo, Bin; Mallik, Sanku verified the data and advised on experimental designs.

when delivering the drugs to the affected site.[52] Because several enzymes are overexpressed in the cancerous tissues, the enzymes have been used as triggers to release the contents from appropriate carriers.[53]

The extracellular matrix-metalloproteinase (MMP) proteolytic enzymes are overexpressed in many types of tumors and play a crucial role in cancer invasion and metastasis.[54] MMP-2 and MMP-9 have been investigated as triggers by employing enzyme-responsive peptides on the surface of the carriers.[55] However, in a dynamic physiological environment, the drug carrier needs to be stable before it reaches the tumor site. Coating the nanoparticles with polyethyleneglycol polymer (PEGylation) reduces the unintended interactions with circulating proteins.[56] This PEG coating reduces the interfacial tension and hinders protein adsorption on the nanoparticles' surface.[47] Hence, PEGylated nanoparticles accumulate at the tumor site due to the enhanced permeation and retention (EPR) effect.[57] However, at the tumor site, the PEG layer needs to be removed from the carriers to elicit the desired effects.[58]

Matrix-metalloproteinase levels are often elevated in the extracellular matrix of various cancers, including pancreatic cancer.[59] In the present study, we have synthesized an MMP-9-cleavable, collagen mimetic lipopeptide which formed nanosized vesicles with 1-palmitoyl-2-oleoyl-*sn*-glycero-3-phosphocholine (POPC), cholesteryl-hemisuccinate, and the synthesized reduction sensitive, PEGylated 1-palmitoyl-2-oleoyl-*sn*-glycero-3-phosphoethanolamine lipid (POPE-SS-PEG_{5000}). The PEG_{5000} in POPE-SS-PEG_{5000} was incorporated to render long circulating characteristic to nanovesicles. In the extracellular matrix of the tumors, we anticipated that the POPE-SS-PEG_{5000} polymer would undergo reduction by glutathione and shed the PEG chains. The de-PEGylation from the surface of nanovesicles will expose the MMP-9-responsive, collagen mimetic lipopeptides to enzymatic hydrolysis. The resultant destabilization of the

nanovesicles will trigger the release of the encapsulated drugs (Figure 2.2). We note that, besides MMP-9, the increased levels of extracellular MMP-2 and intracellular glutathione (GSH) in tumors have been used to shed PEG from the surface of the drug carrier for *in-vitro* studies.[47, 58, 60]

We validated and optimized this delivery strategy by monitoring the release profiles of the encapsulated dye carboxyfluerescein in the presence of physiologically relevant concentrations of GSH and MMP-9. Subsequently, the anticancer drug gemcitabine was encapsulated in the optimized nanovesicles, and cytotoxicity was determined by employing two-dimensional monolayer cultures of human pancreatic cancer cells. However, we note that the conventional monolayer cultures of cancer cells lack the three-dimensional, cell-cell interactions that are encountered with the *in-vivo* environments.[61] Three-dimensional, spheroid cell cultures have been proposed to bridge this gap between conventional monolayer cultures and animal-model studies.[62] The human pancreatic cancer cell line PANC-1 forms such spheroids which can provide the three-dimensional architecture encountered by drug carriers *in-vivo*.[63] In this study, we tested the cytotoxicity of gemcitabine-encapsulated nanovesicles in PANC-1 cell spheroids and also in a mouse xenograft model.

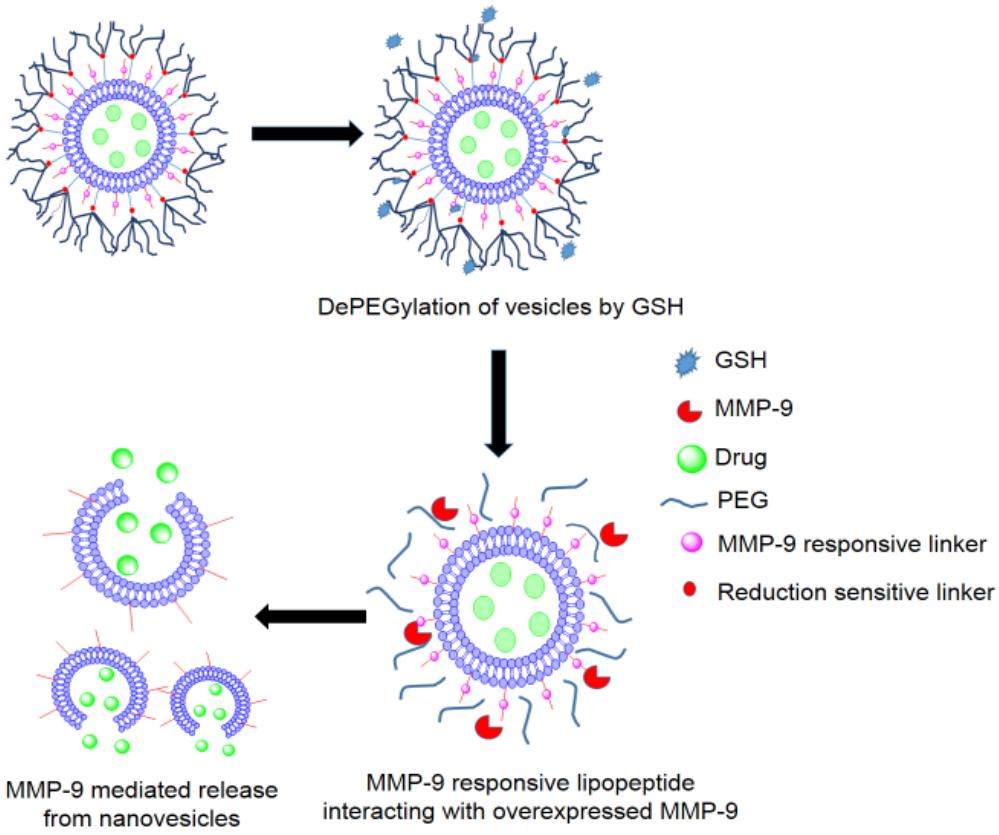

Figure 2.2. Schematic representation of nanovesicles incorporating MMP-9 substrate lipopeptides and reduction-sensitive POPE-SS-PEG which render the nanovesicles responsive to extracellular, elevated levels of MMP-9 and GSH.

2.2. Materials and Methods

The POPE-S-S-PEG disulfide lipid was synthesized as shown in Scheme 2.1. Synthetic details for this lipid, as well as for the **LP** lipopeptide, are provided in the Supporting Information.

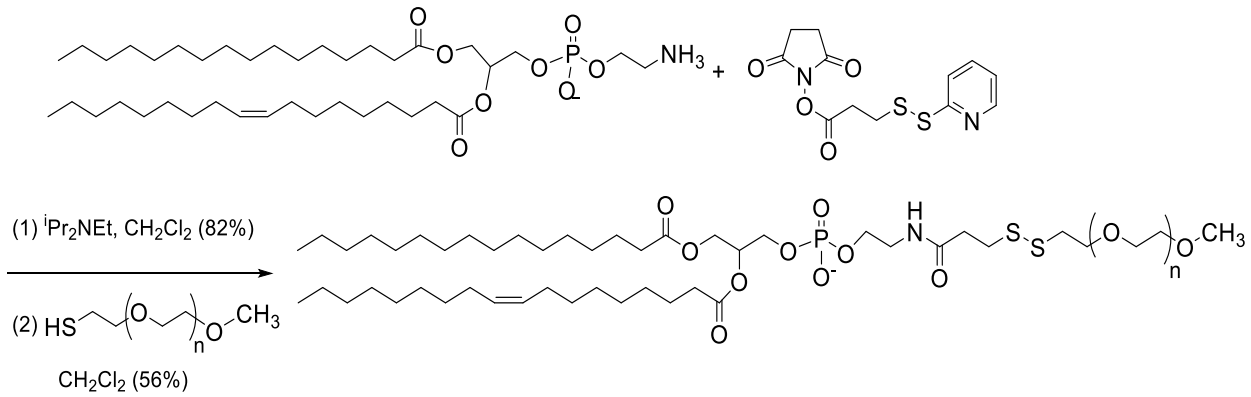

Scheme 2.1. Synthetic scheme for POPE-SS-PEG.

2.2.1. Preparation of carboxyfluorescein encapsulated nanovesicles

The nanovesicles (liposomes) were prepared by mixing POPC lipid (Avanti Polar Lipids), synthesized lipopeptide **LP**, POPE-SS-PEG$_{5000}$ and cholesteryl hemisuccinate in molar proportions of 60:30:5:5, respectively. All the lipids were dissolved in chloroform. The chloroform was removed using a rotary evaporator to form a thin lipid film in a round-bottom flask. The film was further vacuum dried overnight inside a desiccator. The film was then hydrated at 60 ºC for 2 hours with 100 mM carboxyfluorescein solution prepared in HEPES buffer (pH 7.4). The formed vesicles were subjected to ultrasonication for 45 minutes using an Aquasonic bath sonicator (Model: 250D, power level 9). The resulting vesicles were then extruded through 0.8 µm and, subsequently, 0.2 µm filters to obtain vesicles with a uniform size. To remove the unencapsulated dye, the vesicles were passed through a Sephadex G50-size exclusion column, and an orange band of carboxyfluorescein-encapsulated nanovesicles was collected. These vesicles were used for the release and imaging experiments. Since a large excess of carboxyfluorescein was used, we did not estimate the percentage of the dye encapsulated.

2.2.2. Preparation of gemcitabine-encapsulated nanovesicles

Gemcitabine was encapsulated in the nanovesicles with the pH gradient method.[64] Nanovesicles of lipid composition POPC (Avanti Polar Lipids), **LP**, POPE-SS-PEG, cholesteryl hemisuccinate and lissamine rhodamine lipid (Avanti Polar Lipids) were prepared by dissolving them in chloroform in the molar proportions of 59:30:5:5:1, respectively. Chloroform was then evaporated under reduced pressure, and the resulting thin film of lipids was dried under a vacuum desiccator. This film was hydrated with 2 mL of 20-mM citric-acid buffer (pH 4). The resulting vesicles were subjected to ultrasonication for 45 minutes (at power level 9) and were then extruded through a 0.2-μm filter. Nanovesicles were collected after passing them through a Sephadex G50 gel-filtration column. Lissamine rhodamine lipid (1 mol %) was incorporated in these nanovesicles to impart color, and to aid in visualizing the vesicles during size exclusion chromatography. These eluted nanovesicles (pH 7.4) were incubated with 1 mg/mL aqueous solution of gemcitabine at 60 ^{o}C for 2 hours. The gemcitabine solution was added to the nanovesicles to create a lipid-drug ratio of 10:1. Drug-carrying nanovesicles were again passed through the Sephadex G50 column to remove non-encapsulated gemcitabine. Entrapment efficiency of the nanovesicle was then calculated to be 50% (Supporting Information). These nanovesicles were used for cytotoxicity studies.

2.2.3. Size and Morphology Analysis

The hydrodynamic diameters of the vesicles were measured using a Dynamic Light Scattering (DLS) instrument (Malvern Zetasizer Nano-ZS90). Measurements were conducted at a scattering angle of 90^{o} using a polystyrene, latex disposable cuvette. An equilibration time of 120 seconds was kept constant for all measurements. For each sample, 6 readings were recorded averaging 6 runs for the same sample. In order to observe size changes in the presence of added

MMP-9 and GSH, the nanovesicles that encapsulated gemcitabine were incubated with MMP-9 and GSH. Size changes were monitored for 24 hours with DLS, and the morphology change was observed using an atomic force microscope (AFM). For AFM imaging, the nanovesicles were deposited on a mica sheet and were imaged using Multimode™ atomic force microscope with a Nanoscope IIIa controller and a J-type piezo scanner (Veeco Metrology Group, Santa Barbara, CA). An antimony (n) doped Si tip was used for obtaining images in the Tapping Mode.™

2.2.4. Release studies

The release of the encapsulated dye was monitored with a fluorescence spectrophofluorometer (Spectramax-M5, Molecular Devices, Inc.). Carboxyfluorescein (100 mM) was encapsulated in liposomes, and the release was monitored as function of time (excitation: 480 nm; emission: 515 nm). Release from the nanovesicles was recorded for 60 minutes in 30-second intervals. The experiments were carried out in a 96-well plate (6 repeats for each measurement). Each well contained 20 µL of nanovesicles and 160 µL of HEPES buffer (pH 8) with added Ca^{2+} and Zn^{2+} ions (10 mM, osmolarity adjusted to 290 with NaCl). Recombinant human MMP-9 was prepared in our laboratory, as described previously.[65] Contents released in response to added recombinant MMP-9 (2 µM) and GSH (50 µM) were monitored for 60 minutes. Release in human serum (10%) was also monitored for 60 minutes. After 60 minutes, Triton-X100 was added to each well to disrupt the nanovesicles, and emission intensity was measured. This intensity was considered to be for complete release of the encapsulated dye, and the percentage released for each experiment was calculated using the following formula:

$$\text{Percent Release} = \frac{\text{Emission intensity observed after 60 min} - \text{Initial intensity before treatment}}{\text{Emission intensity after triton treatment} - \text{Initial intensity before treatment}} \text{ X } 100$$

2.2.5. Cell culture

Pancreatic-cancer cell lines PANC-1 and MIAPaCa-2 were obtained from American Type Culture Collection (Manassas, VA). PANC-1 cells were cultured in RPMI media (without phenol red) that were supplemented with 2% antibiotics (penicillin, streptomycin) and 10% v/v fetal bovine serum. The MIAPaCa-2 cells were cultured in DMEM media that were supplemented with 2% horse serum and 2% antibiotics. All cell lines were grown at 37 ºC in a humidified atmosphere containing 5% CO_2.

2.2.6. Alamar Blue assay with a monolayer cell culture

Cytotoxicity of the encapsulated gemcitabine was measured by treating the PANC-1 and MIAPaCa-2 cells with nanovesicles. The cells were incubated (1,000 per well) in a 96-well plate after trypsinizing the flask and making a cell suspension. RPMI media (100 µL) were added to each well. Cells were allowed to grow for one doubling time. The plate was divided into three groups: control, gemcitabine treated and gemcitabine-encapsulated nanovesicles treated. Six replicates were recorded for each sample. The control group did not receive any treatment. Phosphate buffer saline (PBS) encapsulated liposomes were also employed as control for cell viability studies. Gemcitabine-treated cells received 5 µM, 10 µM and 20 µM of gemcitabine, and nanovesicle-treated cells received an equivalent amount of encapsulated gemcitabine. The treatment was carried out for 3 days, and cell toxicity was recorded after 72 hours with the Alamar Blue assay by following the supplier's (Life Technologies) protocol. Alamar Blue solution (10 µL) was added to all the wells and incubated for 2 hours, and the absorbance was recorded at 585 nm for cytotoxicity calculation. Toxicity of PBS encapsulated nanovesicles was observed by incubating MIAPaca-2 cells (1000 per well) in 96 well plate with nanovesicles representing lipid

concentrations ranging from 5 µg/mL to 100 µg/mL. Alamar blue assay was carried out to observe cell viability of MIAPaca-2 cells after incubating for 72 hours with the nanovesicles.

2.2.7. Estimation of cell-secreted MMP-9 concentration

Conditioned media from confluent cultures of PANC-1 and MIAPaca-2 cells were collected, and a concentration of secreted MMP-9 was estimated by using a commercially available MMP-9 ELISA kit (RayBio Tech). The manufacturer's instructions were followed to estimate the MMP-9 secreted by the cells.

2.2.8. Three-dimensional spheroid cell culture

Based on the ELISA results, the PANC-1 cell line was selected for the spheroid culture because it showed the highest levels of secreted MMP-9. In order to prepare the cell spheroids, agar molds, each having the capability to form 96 spheroids of uniform size, were created. To prepare the plates, a slightly modified protocol provided by Microtissues™ (http://www.microtissues.com/3dcellculture_protocols/Casting_Equilibrating_and_Seeding_the_3D_Petri_Dish.pdf) was used. The prepared plates were equilibrated with RPMI media for 1 hour at 37 ºC and placed in 6-well plates, and 2 mL of RPMI media were added to each well to provide nutrition for the cells seeded in the plates. Agar plates were then seeded with 75 µL of cell suspension containing 10,000 cells in each plate which formed spheroids after 3 days of incubation at 37 ºC. These spheroids were used for cell-viability and oxidative-stress studies.

2.2.9. Lactate dehydrogenase (LDH) assay

LDH was measured using a kit supplied by G-Biosciences (Cytoscan™ LDH Cytotoxicity assay). The manufacturer's instructions were followed to measure the LDH released in response to cytotoxicity caused by the release of gemcitabine from the nanovesicles. This assay was carried out using 1-day, 3-day and 5-day old spheroids.

2.2.10. Alamar Blue assay with 3-D cell culture

Plates containing 96 spheroids molds were prepared, and cells were allowed to grow for 5 days in order to form spheroids. These plates were divided into 3 groups on the basis of the treatment they received: control, drug treated and drug-encapsulated nanovesicles. Each group contained 6 plates with 96 spheroids. The control group received the same nutrition media as the other groups. The drug-treated group received 10 μM of gemcitabine, and the test group received drug-encapsulated nanovesicles (encapsulating 10 μM of gemcitabine). Spheroids in all groups received the treatment for 72 hours. Subsequently, all the media surrounding the micro-mold were removed. The spheroids were treated with TryPLE (Life Technologies) and were incubated for 1 hour at 37 ºC to ensure dissociation of all the cells in the spheroid. RPMI media (3 mL) were added to each plate and were triturated to remove all the cells from the plate. From the cell suspension obtained, 100 μL from each plate were seeded on a new clear-bottom, 96-well plate (repeated 6 times for each well). Additional growth medium (100 μL) was added to all the wells receiving the cell suspension. The cells were allowed to grow for one doubling time, and the Alamar Blue assay was carried out per the manufacturer's protocol, as described before.

2.2.11. Confocal fluorescence microscopic imaging

Carboxyfluorescein-encapsulated nanovesicles were used to visualize the release of contents in 7-day-old spheroids of PANC-1 cells. Nanovesicles devoid of lipopeptide **LP** were used as a control. The spheroids were treated in the plate with the control and sample nanovesicles by incubating for 4 hours at 37 ºC. The spheroids were then washed (3X) with culture media. Spheroid-holding plates were then centrifuged to dislodge spheroidsin the media. These spheroids were then imaged using a Zeiss AxioObserver Z1, inverted microscope with an LSM700 laser-scanning head attachment and a 20X 0.4 LD Plan-Neofluar objective. The first and last appearance

of the fluorescence in the sample-treated spheroids was set as the scanning range. The same comparison range was selected for the control spheroids. Images were processed with Zeiss AxioVision Rev. 4.8.1 image-analysis software (Carl Zeiss, Thornwood, NY).

2.2.12. *In-vivo* imaging

For *in-vivo* imaging, athymic, Nude-Foxn1 (female, 5-6 week old), nude mice were used. PANC-1 cells (3 million) were injected subcutaneously. A well-developed tumor was observed after 21 days, and this animal was used for the imaging studies. Carboxyfluorescein-encapsulated (50 mM) nanovesicles (60 µL) were injected *via* the tail vein. Images were recorded using a reflectance imaging system (Kodak *in-vivo* system FX, Carestream Health, Inc., Rochester, NY). The whole-body fluorescence images were acquired using the FITC channel (excited at 480 nm and recorded at 680/720 nm) after 5 seconds of exposure. Images were recorded to monitor the release of carboxyfluorescein at the tumor site 6 hours and 24 hours after injection. The images were further processed using Kodak Molecular Imaging software (version 4.0).

2.2.13. *In-vivo* studies

In-vivo studies were carried out using a xenograft model for athymic, Nude-Foxn1 (female, 5-6 week old), nude mice (IACUC-approved protocol number A13066). PANC-1 cells (3 million) were injected subcutaneously into the nude mice, and the cells were allowed to grow at the injected site for 15 days. After the tumors developed, mice were divided into the control, positive control and test groups (n = 3 for each group). The control group received a phosphate buffer (pH 7.4, osmolarity 325 mOsm/kg), animals in positive control group received gemcitabine (10 mg/kg/week) encapsulated in PEGylated liposomes devoid of **LP** and the test group received a 10-mg/kg/week dose of gemcitabine-encapsulated in the deigned MMP-9 responsive PEG cleavable nanovesicles. The treatment was administered for 4 weeks *via* tail-vein injection. The tumor size

was recorded each week, and the tumor volume was calculated using the following formula: volume = $(\text{width})^2$ x length/2. The mice's weights were recorded throughout the study, and the mice were closely monitored for any sign of toxicity.

2.3. Results and discussion

Coating the drug carriers with a layer of polyethylene glycol or another hydrophilic polymer imparts the long-circulating property. However, efficient interactions between the drug carrier and tumor microenvironment require the removal of the protective PEG coating from the surface of the carrier at the target site.[66] In order to impart this feature to the nanovesicles, we synthesized a reduction-sensitive PEGylated lipid POPE-SS-PEG_{5000} (Scheme 2.1). The product was confirmed by NMR and MALDI mass spectral analysis (Figure A3). We anticipated that the long PEG chains would protect the MMP-9 substrate lipopeptide **LP** from cleavage in the presence of low levels of MMP-9 (50-100 nM; found in the blood), and would provide long-circulating characteristics to the nanovesicles. Increased oxidative stress often results in elevated levels of glutathione (GSH) in tumor tissues.[67] The sulfhydryl group of reduced glutathione participates in the thiol-exchange,[68] and this reaction is expected to reduce the disulfide bonds of the POPE-SS-PEG_{5000} lipid. We anticipate that the resultant exposure of the collagen mimetic, substrate lipopeptides to the elevated MMP-9 levels in the tumor extracellular matrix will initiate the hydrolysis of the lipopeptides, leading to destabilization of the nanovesicles.

The lipopetide **LP** was designed to act as a substrate for the extracellular enzyme MMP-9.[69] We have previously demonstrated that **LP** can be successfully incorporated into liposomal lipid bilayer and that the resultant vesicles undergo "uncorking" in the presence of elevated levels of catalytically active MMP-9, releasing the encapsulated contents.[65a] We have also established that other cancer-associated MMPs, which do not hydrolyze triple helical peptides (e.g., MMP-7,

MMP-10), are ineffective in releasing contents from these liposomes.[65b, 69] However, MMP-2 and MMP-9 have similar substrate selectivity,[70] and is likely to hydrolyze **LP**. The collagen-mimetic, MMP-9, cleavable **LP** was synthesized by microwave-assisted, solid-phase peptide synthesis and was purified by reverse-phase HPLC. The MMP-9 cleavage site for **LP** is located between the amino acids Glycine and Isoleucine.[69] The collagen-mimetic, triple-helical structural characteristic of purified **LP** was confirmed by CD spectroscopy, showing a positive peak at 220 nm and a negative peak at 198 nm.[71]

LP retained its triple helical structure when incorporated into nanovesicles composed of POPC (65%), POPE-SS-PEG (5%) and cholesteryl hemisuccinate (5%) (Figure 2.3A, black trace). We observed that the triple helicity of nanovesicle-incorporated **LP** was unchanged upon treatment with GSH (50 μM) for 1 hour (Figure 2.3A, red trace). However, the triple helicity of **LP** was considerably reduced when incubated with 2 μM of recombinant human MMP-9 for 60 minutes (Figure 2.3B, red trace).

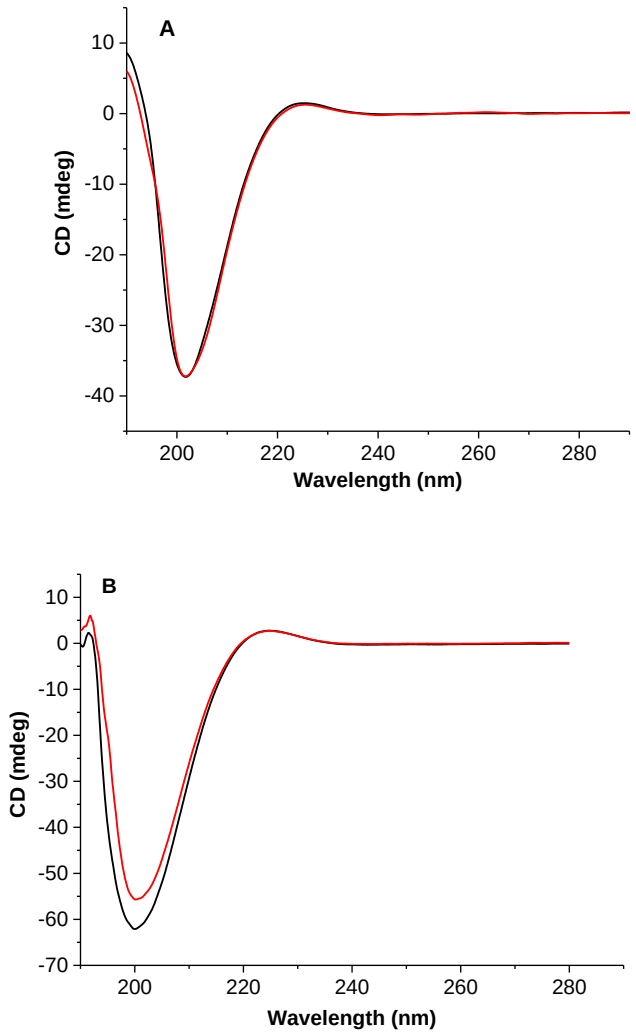

Figure 2.3. CD spectra of nanovesicles (black trace) and nanovesicles treated with 50 µM of GSH (red trace) did not show any change in triple helicity (A), but treatment with MMP-9 (red trace) showed changes in the triple helicity of the nanovesicles (black trace) (B).

The nanocarriers' size is crucial for passive tumor targeting because the drug carriers accumulate at the target site by infiltration through the leaky vasculature.[72] The nanovesicles composed of POPC: LP: cholesteryl hemisuccinate: POPE-SS-PEG (60:30:5:5) were prepared with the freeze-drying method, followed by sonication and extrusion. The size of the prepared nanovesicles was assessed by dynamic light scattering at a 90º angle. The size of the vesicles

immediately after passing through the size-exclusion column was observed to be 86 ± 18 nm with a polydispersity index (PDI) of 0.3. The size of these nanovesicles was retained for 24 hours at room temperature. Treatment with MMP-9 (2 μM) and GSH (50 μM) for 24 hours at room temperature increased the average size to 109 ± 20 nm with a PDI of 0.4 (Figure 2.4). Treatment with 50 μM GSH only led to a slight reduction in the sizes of the liposomes – possibly indicating the removal of the PEG groups (Figure A4). Treatment with only MMP-9 (2 μM) resulted in a slight increase in the liposomal size (Figure A4). A similar size increase was also observed when we repeated the experiment at 37 ^{o}C (Table A1).

This change in size upon incubation with MMP-9 indicates that the hydrolysis of the triple-helical substrate peptides by MMP-9 leads to substantial structural changes in the vesicles, resulting in the increased average diameter. The size change was also observed in the AFM imaging (Figure 2.5). The observed size of the nanovesicles increased after 24 hours of treatment with MMP-9 and GSH at room temperature. Although, the nanovesicles were expected to decrease in size as result of leakage through the bilayer, we observed an increase in the size of the nanovesicles treated with MMP-9 and GSH. After cleavage of the lipopeptides by MMP-9, nanovesicles undergo ‘uncorking’, and release the encapsulated contents. This leads to the loss of integrity of the nanovesicles, possibly resulting in non-specific aggregates of larger size. The liposomes which were not treated with MMP-9 showed less variation in size after 24 hours.

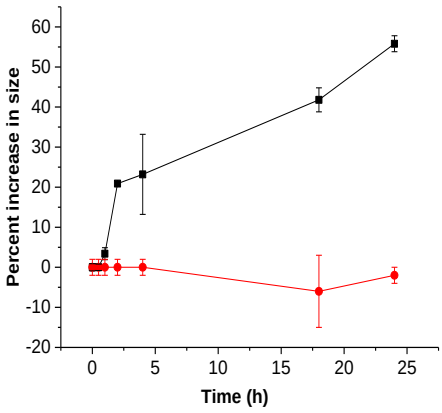

Figure 2.4. Nanovesicles treated with the MMP-9 (2µM) and GSH (50 µM) showed an increased size with time (black squares, n = 6). The size of the untreated nanovesicles was not affected at room temperature (red circles, n = 6). The straight lines connecting the observed data points are shown in the plot.

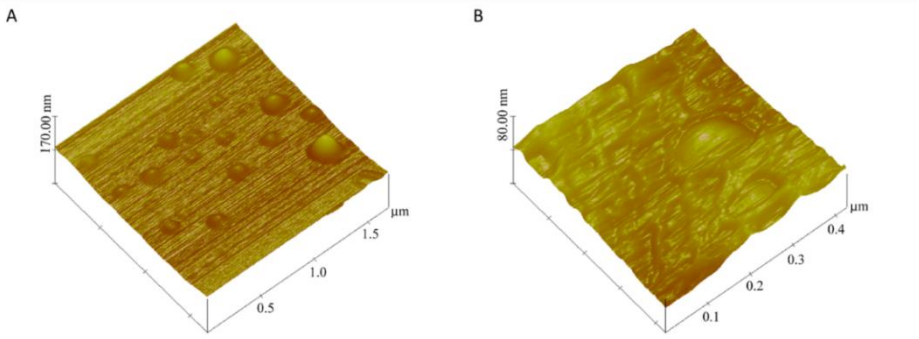

Figure 2.5. AFM images for the gemcitabine-encapsulated nanovesicles (A) before and (B) after 24 hours of incubation with GSH (50 µM) and MMP-9 (2 µM).

For quantitative estimation of contents release from the nanocarrier we encapsulated carboxyfluorescein (100 mM) in the nanovesicles. The release was monitored as a function of time in the presence of added GSH (50 µM) and MMP-9 (2 µM) in pH 8.0 buffer. We have previously demonstrated that the release of liposomal contents requires catalytically active MMP-9.[65b] An increased release was observed with both the GSH and MMP-9 treatments. The nanovesicles exhibited about a 5% release over 1 hour, in the presence of basal concentration of

GSH observed in circulation (2-μM) (Figure 2.6, black squares). However, up to 22% of the encapsulated carboxyfluorescein was released after 1 hour of exposure to elevated levels of GSH found in tumor extracellular microenvironment (50 μM, Figure 2.6, red circles). To mimic the tumor's extracellular matrix environment, the nanovesicles were exposed to elevated levels of MMP-9 (2 μM) and GSH (50 μM). In these conditions, we observed a 45% content release in 60 minutes (Figure 2.6, blue triangles). These release profiles can be fitted with a single exponential-rate equation with rate constants of $(12.5 \pm 0.6) \times 10^{-2}$ s^{-1} for 2 μM of MMP-9, $(11.1 \pm 2.2) \times 10^{-2}$ s^{-1} for 2 μM of GSH and $(80.5 \pm 0.1) \times 10^{-2}$ s^{-1} in the presence of 2 μM of MMP-9 and 50 μM of GSH. Note that the rate of content release was substantially higher in the presence of MMP-9 and GSH, as observed in the extracellular microenvironment of tumors. Based on literature reports[73] and these observations, we conclude that the elevated levels of GSH is reductively removing the PEG groups from the POPE-S-S-PEG lipids. This facilitates the hydrolysis of **LP** by MMP-9, leading to the release of liposomal contents. We observed similar results when the release experiments were conducted at 37 ^{o}C (Figure A4). As another control, we incubated the liposomes (without any added GSH and MMP-9) in buffers of different pH values (5.0, 6.0, 7.0, and 8.0) at room temperature, and at 37 ^{o}C. We did not observe any significant release from the liposomes as a function of pH (release < 5 %).

A major challenge in designing an internal, stimuli-sensitive system is the stability of the carriers in circulation before reaching the target site. To test the stability of the prepared nanovesicles, we monitored the release of carboxyfluorescein in the presence of 10% human serum. The nanovesicles exhibited less than 5% release over a period of 1 hour in 10% human serum (Figure A2). The stability of nanovesicles in human serum was suggestive of the designed nanovesicles' stability in circulatory conditions.

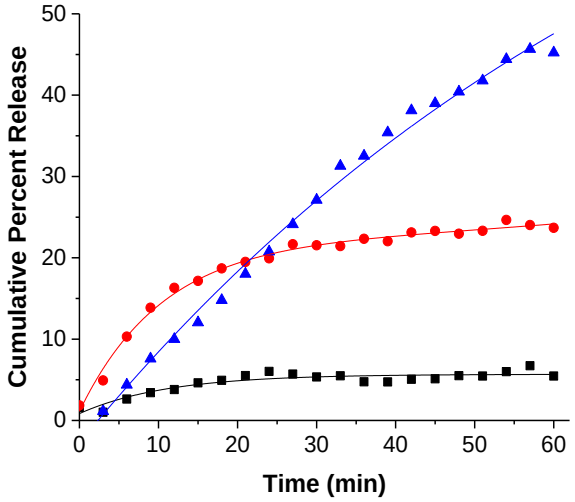

Figure 2.6. Cumulative release profiles from nanovesicles under circulatory conditions (2 μM GSH, black squares), in response to MMP-9 (2 μM, red circles), and with an extracellular tumor mimicking the environment comprised of MMP-9 (2 μM) and GSH (blue triangles). The traces represent the fitted curves using a single exponential-rate equation.

Having demonstrated the release of encapsulated dye, the *in-vitro* and *in-vivo* studies were carried out using gemcitabine-encapsulated nanovesicles. Gemcitabine was encapsulated in the nanovesicles with the pH gradient method, and entrapment efficiency was observed to be 50%. These nanovesicles were used to assess cytotoxicity for the pancreatic cancer cells (PANC-1 and MIAPaCa-2) in the monolayer cultures. The cells were treated with gemcitabine and gemcitabine-encapsulated nanovesicles for 72 hours, and cell viability was measured with Alamar Blue dye. Both free and encapsulated gemcitabine showed similar toxicity for the PANC-1 (viability: 30-35%; Figure 2.7, blue bars) and MIAPaCa-2 cells (viability: 45-50%; Figure 2.7, green bars). No apparent cytotoxicity was observed from nanovesicles themselves (Figure A5). However, both free and liposome-encapsulated gemcitabine showed similar and dose-dependent toxicity (Figure 2.7C). We quantified the levels of secreted MMP-9 from these two cell lines by employing a commercially available ELISA kit. The results showed a higher concentration of MMP-9 in the

conditioned media of PANC-1 cells (126 ± 23 pg/mL) compared to MIAPaCa-2 cells (8 ± 4 pg/mL). It is likely that the encapsulated gemcitabine was released from the nanovesicles by the MMP-9 secreted into the conditioned culture media. Hence, free and encapsulated gemcitabine demonstrated similar cytotoxicity, and the effect was more for the PANC-1 cells compared to the MIAPaCa-2 cells. To corroborate this hypothesis, we repeated the liposomal contents release experiments in the presence of the conditioned culture media of the brain endothelial cells bEnd-3. These cells do not express and secrete MMP-9 in the extracellular media.[74] We observed minimal contents release from the liposomes in the presence of conditioned media from the bEnd-3 cells (Table A2).

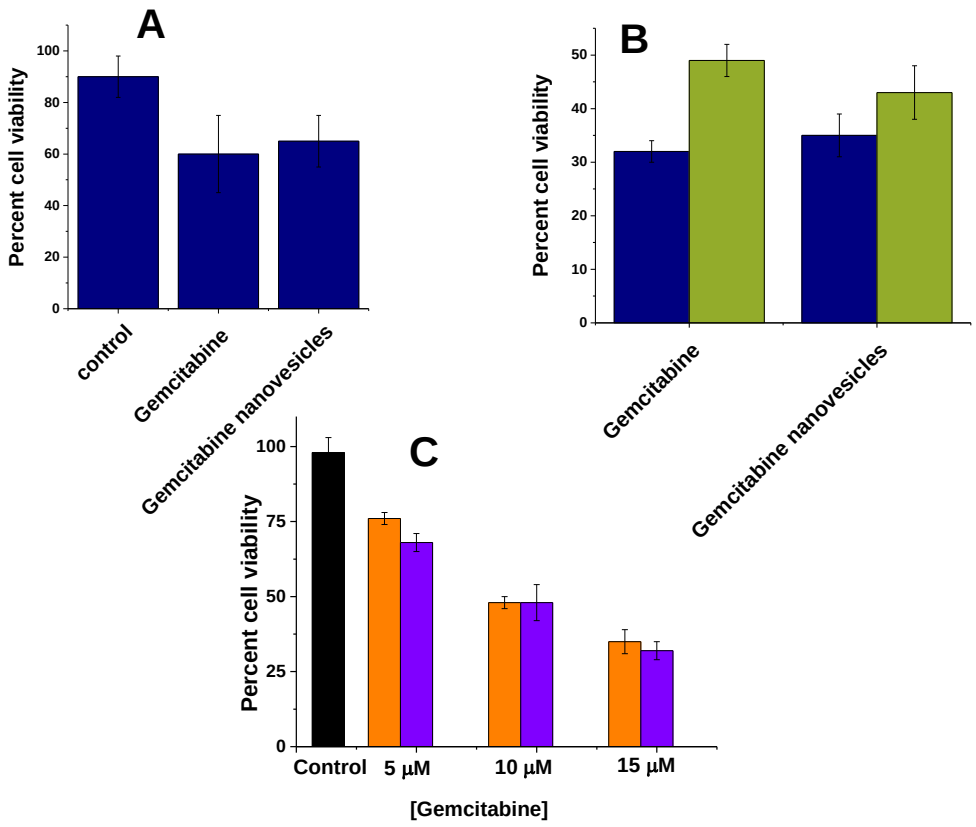

Figure 2.7. Cell viability observed in the monolayer (A) (n = 6) and spheroid (B) cultures (n = 3) of PANC-1 (blue) and MIAPaca-2 cells (green) after gemcitabine (10 µM), gemcitabine nanovesicles (encapsulating 10 µM of gemcitabine), and control nanovesicles encapsulating PBS (20 mM, pH 7.4) treatment for 72 hours. No significant difference was observed in cell viability of PANC-1 cells in 2-D and 3-D cultures when treated with gemcitabine or gemcitabine nanovesicles. Concentration dependent decrease in cell viability (C) was observed when the MIAPAca-2 cells were treated with free gemcitabine (violet) or gemcitabine encapsulated nanovesicles (orange) for 72 hours.

Subsequently, we cultured spheroids of uniform size by using micro-molds in each well of a 6-well microplate. After seeding the PANC-1 cells, the spheroid growth was monitored for 7 days. With the increased size, the cells in the spheroid core undergo apoptosis due to a lack of oxygen and nutrients, mimicking the hypoxic conditions observed in tumor tissues.[75] This cell death in the spheroid core is reflected in increased LDH levels in the culture media.[76] We also

observed a similar effect in the spheroid cultures of the PANC-1 cells (Figure 2.8). Subsequently, we repeated the cytotoxicity assays with free and nanovesicle-encapsulated gemcitabine, employing the PANC-1 spheroids. We observed that the cell viability was similar in spheroids treated with the free and encapsulated drug (Figure 2.7B). We saw that the cytotoxicity for the encapsulated gemcitabine was less in spheroids compared to the two-dimensional cultures of the PANC-1 cells.

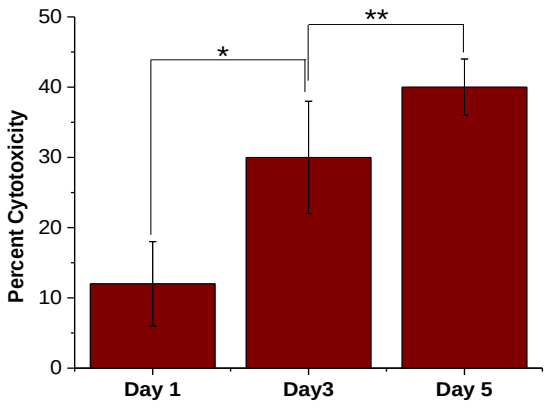

Figure 2.8. LDH released in response to cell death due to the hypoxic conditions in the spheroid core after 1, 3 and 5 days. (n = 6, *p < 0.001, **p < 0.05)

To ascertain that the encapsulated contents were released from the nanovesicles and internalized in the PANC-1 cell spheroids, we monitored the uptake with confocal fluorescence microscopy. For easier visualization, these experiments were conducted with carboxyfluorescein-encapsulated nanovesicles. We prepared analogous liposomes without incorporating the MMP-9 substrate peptide **LP** and used these nanovesicles as the control. Since our objective was to demonstrate that the encapsulated dye is released by the tumor spheroids, we did not add any GSH to the culture media. We observed that the control nanovesicles failed to release the contents, and

no significant dye internalization was detected (Figure 2.9, Panel A). However, the nanovesicles with **LP** efficiently released the encapsulated carboxyfluorescein and that the dye was internalized in the spheroids (Figure 2.9, Panel B).

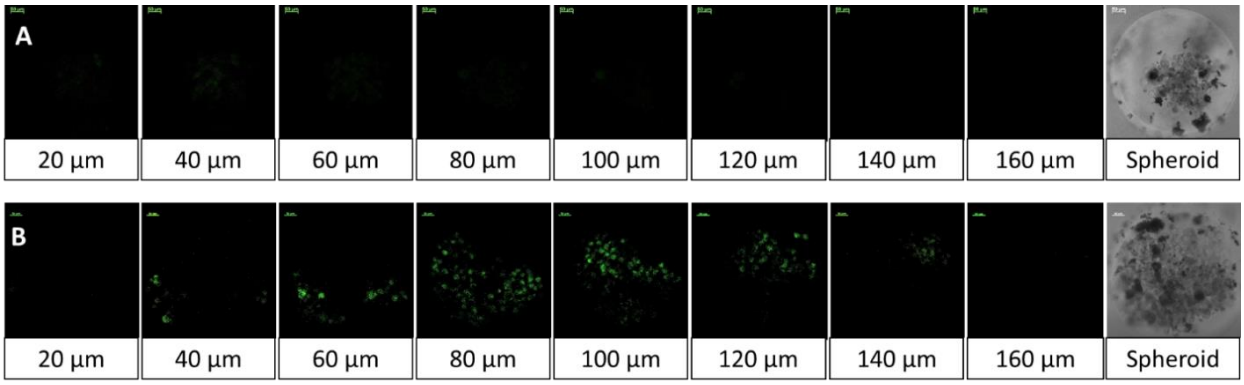

Figure 2.9. Uptake of released carboxyfluorescein by the spheroids of the PANC-1 cells. Spheroids treated with MMP-9-responsive nanovesicles showed an enhanced uptake of carboxyfluorescein released from the nanovesicle (B) as compared to nanovesicles that lacked the MMP-9 responsive lipopeptide (A).

The nanovesicles were observed to be stable in 10% human serum, suggesting stability in circulation before reaching the tumor site (Figure A2). Live-animal imaging after 6 hours and 24 hours of tail-vain administration of carboxyfluorescein-encapsulated nanovesicles confirmed the stability and the effective release capability at the tumor site (Figure 2.10).

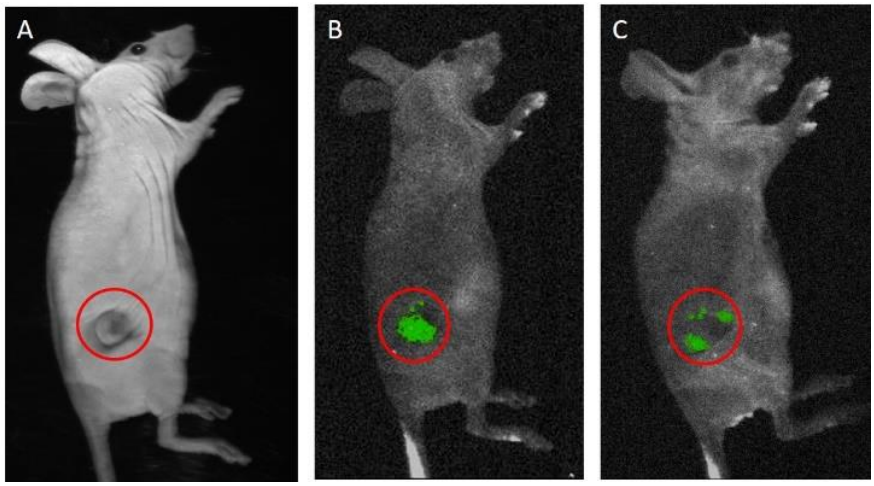

Figure 2.10. Carboxyfluorescein release from nanovesicles was observed after 6 hours (B) and 24 hours (C) of injection *via* the tail vein in nude mice. Panel A represents a white-light image, and the red circles indicate the tumor-bearing site.

Subsequently, we proceeded to demonstrate the effectiveness of the proposed delivery strategy by employing a xenograft mouse model of human pancreatic cancer. For these studies, we used 9 athymic, female, Nude-Foxn1nu mice (5-6 weeks old). The mice were divided in three groups (control, positive control and test), and were injected with 3 million PANC-1 cells subcutaneously. Tumors developed in the animals, 15 days after subcutaneous injections. The objective of this study was to demonstrate the release of encapsulated gemcitabine from the PEGylated nanovesicles in response to elevated levels of proteolytic enzyme MMP-9 in tumor extracellular matrix. Studies on the in-vivo toxicity of gemcitabine, and benefit of using gemcitabine encapsulated liposomes are already reported.[77,78] Hence, for our studies, the control group received the weekly injections (*via* the tail vain) of buffer. The animals in positive control and test groups received injections of gemcitabine-encapsulated nanovesicles (without and with **LP**, respectively, dose: 10 mg/kg/week) for 4 weeks. The animals from both the groups showed lesser tumor growth as compared to the control (Figure 2.11). However, we observed that the

animals receiving gemcitabine encapsulated in PEGylated MMP-9 responsive nanovesicles showed more pronounced reduction in tumor growth (Figure 2.11, blue triangles) as compared to animals receiving gemcitabine encapsulated in PEGylated liposomes without **LP** (Figure 2.11, red circles). Weight for all the animals receiving gemcitabine nanovesicles did not decrease during and after the treatment – indicating the lack of toxicity for the nanovesicle formulations (Figure A4). After 4 weeks of treatment, we observed that the increased tumor volumes for the treated mice were substantially less compared to the control group (Figure 2.11).

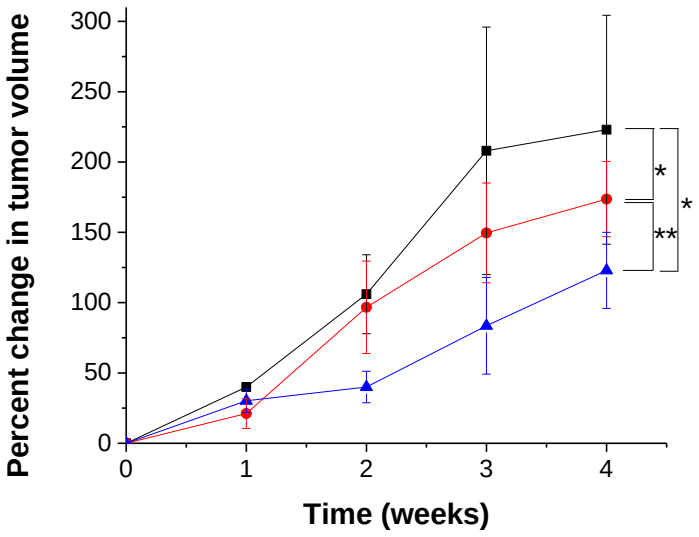

Figure 2.11. The percentage increase in tumor volume for the test group (blue triangles, n = 3) was lower in LP incorporated nanovesicle-treated mice as compared to the control (black squares, n = 3), and positive control treated mice (red circles, n = 3). (*p < 0.05, ** p < 0.05)

2.4. Conclusion

We have successfully demonstrated that the elevated levels of MMP-9 and GSH in the extracellular matrix of tumor tissues can be used to trigger contents release from suitably-constructed nanovesicles. These liposomes incorporate disulfide linked PEG groups on the surface.

At the tumor site, elevated levels of glutathione reductively removes the PEG groups, exposing the MMP-9 substrate peptide towards enzymatic hydrolysis. The resultant destabilization of the lipid bilayer leads to rapid release of encapsulated contents. We have successfully encapsulated the anticancer drug gemcitabine and demonstrated that the cytotoxicity of the released drug to pancreatic cancer cells (in monolayer and spheroid cultures) is comparable to that for the non-encapsulated drug. Internalization studies carried out using pancreatic cancer cell spheroids showed that the incorporated MMP-9-responsive lipopeptide triggers the drug release in the tumor's extracellular matrix. *In-vivo* imaging studies with the designed, long-circulating nanovesicles exhibited circulatory stability. *In-vivo* studies also confirmed the release of encapsulated gemcitabine in the tumor microenvironment, showing a reduction in tumor growth rate in nude mice. We observed better control over tumor growth with the MMP-9 responsive nanovesicles compared to the PEGylated vesicles without the MMP-9 substrate lipopeptide.

3. HYPOXIA RESPONSIVE, TUMOR PENETRATING LIPOSOMES FOR DELIVERY OF CHEMOTHERAPEUTICS TO PANCREATIC CANCER CELL SPHEROIDS[2]

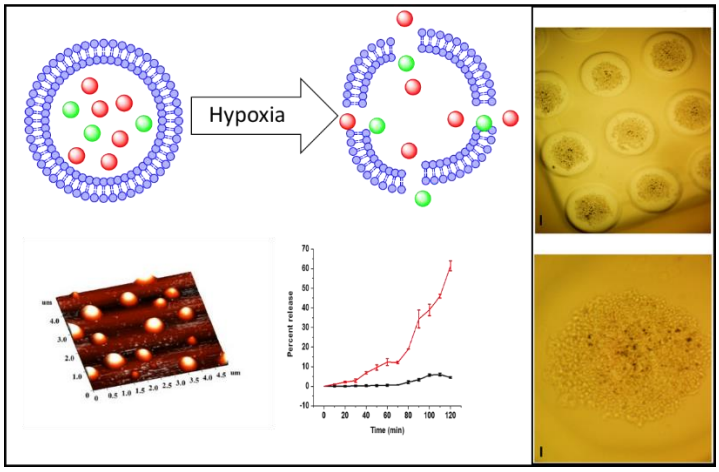

Figure 3.1. Graphical abstract

3.1. Introduction

Stimuli-responsive nanoparticles show tremendous potential to deliver anticancer chemotherapeutics to the targeted tumor site with enhanced efficacy and reduced side effects.[79] Liposomes are the most popular lipid-based bilayer vesicles approved by the US Food and Drug Administration (FDA) for the treatment of various cancers.[43] Compared to the conventional chemotherapy, the anticancer drug encapsulated, polyethylene glycol-coated (PEGylated) liposomes show reduced side effects.[80] However, the slow release of the encapsulated drugs from

[2] This section is coauthored by Prajakta Kulkarni, Manas K. Haldar, Preeya Katti, Courtney Dawes, Seungyong You, Yongki Choi, Sanku Mallik. Prajakta had primary responsibility to conduct all the experiments listed in the section, analyze the data and write the manuscript. Manas had a primary role of synthesizing the hypoxia responsive lipid, Preeya and Courtney assisted in isolation of microsomes, Seungyong and Dr. Choi were involved in AFM imaging studies. Dr. Mallik verified the results and edited the manuscript for publication.

the clinically-approved liposomal formulations have stimulated intense research on tumor microenvironment responsive, PEGylated drug carriers.

After intravenous administration, the PEGylated nanoparticles accumulate in the tumor tissues due to the leaky vasculature and poor lymphatic drainage (the Enhanced Permeation and Retention or EPR effect).[81] The abnormal tumor microenvironment (such as, reduced pH, elevated enzyme and reducing agent levels, high cell surface receptor density) acts as triggers for stimuli-responsive nanoparticles to release the encapsulated drugs.[6] *In-vivo* studies demonstrate better control over tumor growth by the drug-encapsulated, stimuli-responsive nanoparticles compared to the conventional treatment.[82] Considering the designs of the reported nanoparticles, it is likely that the drug is delivered to the peripheral tumor tissues, close to the blood vessels.

The solid tumors are often poorly irrigated due to the structurally compromised microcirculation.[83] Uncontrolled multiplication of cancer cells, insufficient blood flow, and the lack of enough oxygen and nutrients lead to the development of hypoxic regions in the tumor tissues. As the partial pressure of oxygen drops below the necessary level (10 psi), the cancer cells modulate their genetic makeup to survive.[84] Hypoxia triggers tumor progression by enhancing angiogenesis, cancer stem cell production, remodeling of the extracellular matrix, and epigenetic changes in the cancer cells.[85] However, the hypoxic regions are usually located deep in the tumors and are usually inaccessible to the intravenously injected drug carrier or the drug.[86] The cyclic iRGD peptide is reported to interact with the overexpressed integrin and neuropilin receptors[87] – increasing the penetration of nanoparticles in tumor tissues.[88]

In this study, we prepared lipid nanoparticles (LNs) comprising a synthesized hypoxia-responsive, PEGylated lipid and an iRGD peptide conjugated lipid. We hypothesized that the resultant LNs would penetrate to the hypoxic regions of the tumors. Under low oxygen partial

pressure, the hypoxia responsive lipid will undergo reduction, destabilize the lipid membrane, and release the encapsulated drugs from the LNs. We validated our hypothesis employing spheroidal cultures of the pancreatic cancer cells BxPC-3. The BxPC-3 cells form coherent spheroids with hypoxic cores – making them ideal for *in-vitro* studies.[63] We observed that the iRGD peptide-decorated, drug encapsulated LNs reduced the viability of pancreatic cancer cells of the spheroids to 35% under hypoxic conditions. To the best of our knowledge, this is the first report of the hypoxia-triggered release of liposomal anticancer drugs.

3.2. Materials and Methods

3.2.1. Materials

The amino acids and the resins for peptide synthesis were purchased from Peptides International. The lipids, 1,2-distearoyl-*sn*-glycero-3-phosphocholine (DSPC), 1,2-dipalmitoyl-*sn*-glycero-3-phosphoethanolamine-N-lissamine rhodamine B sulfonyl ammonium salt (rhodamine lipid), and palmitoyl oleoyl phosphatidylethanolamine (POPE) were purchased from Avanti Polar Lipids. The 1,2-distearoyl-*sn*-glycero-3-phosphoethanolamine (DSPE)-PEG-N_3 (molecular weight 5,000) was purchased from Nanocs. The pancreatic cancer cell line BxPC-3 was purchased from ATCC. The cell culture media, fetal bovine serum, and antibiotics were purchased from Lonza. All other chemicals used were laboratory grade.

3.2.2. Synthesis and characterization of hypoxia responsive lipid PEG–azobenzene–POPE

Following a reported procedure,[89] the amine terminated $mPEG_{2000}$ was conjugated with the azobenzene-4,4' dicarboxylic acid. NMR spectrum confirmed formation of the product.[89] ^{1}H NMR (400 MHz, CHLOROFORM-*d*) δ ppm 0.00 - 0.01 (m) 1.08 - 1.36 (m) 3.37 - 3.38 (m) 3.53 - 3.63 (m) 3.77 - 3.91 (m) 5.25 - 5.38 (m) 7.27 (s) 7.93 - 8.07 (m). The resultant Polymer attached diphenyl azacarboxylate (100 mg, 0.046 mmol) was reacted with POPE (35 mg, 0.048 mmol)

employing HBTU (19 mg, 0.048 mmol), HOBt (7 mg, 0.050 mmol), and diisopropylethyl amine (18 mg, 0.138 mmol) in DMF (20 mL) under inert conditions overnight. After removal of the solvent under reduced pressure, the semisolid was dissolved in dichloromethane, washed with 10% citric acid solution, and 0.5 N NaOH solution. The clear organic phase was dried over sodium sulfate and evaporated under reduced pressure. The resulting semisolid was subjected to chromatographic purification (R_f = 0.7 in 10% methanol in dichloromethane) affording 105 mg (79%) of the final product. ^{1}H NMR (400 MHz, CHLOROFORM-*d*) δ ppm 0.80 - 0.92 (m) 1.16 - 1.40 (m) 1.52 - 1.64 (m) 1.97 - 2.22 (m) 2.24 - 2.32 (m) 2.91 - 3.08 (m) 3.35 - 3.50 (m) 3.54 - 3.75 (m) 3.90 - 4.07 (m) 4.09 - 4.22 (m) 5.19 - 5.38 (m) 7.27 (s) 7.91 - 8.03 (m). ^{13}C NMR (100 MHz, CHLOROFORM-*d*) δ ppm 14.12, 22.69, 27.22, 29.32, 29.53, 29.71, 45.60, 59.04, 70.57, 71.95, 76.71, 77.03, 77.35, 119.07, 128.51, 133.30, 153.08, 167.2, 173.79.

3.2.3. Synthesis and characterization of the iRGD peptide

The peptide was synthesized using a microwave-assisted, solid-phase peptide synthesizer (Liberty Blue with Discover microwave unit, CEM Corporation) employing the CLEAR Amide resin as the solid support (0.2 g, 0.1 mmol/g). The sequence hexynoic acid-Cys(Acm)-Arg(Pbf)-Gly-Asp(OBu^{t})-Lys(Boc)-Gly-Pro-Asp(OBu^{t})-Cys(Acm)-OH was synthesized without the final deprotection. To cyclize the product, thallium trifluoroacetate (55 mg, 0.1 mmol) in DMF (5 mL) was stirred with the resin conjugated protected peptide for 3 hours. The resin was washed with DMF (3X) and dichloromethane (3X). Subsequently, the peptide was cleaved from the resin with trifluoroacetic acid (19 mL), and distilled water (0.5 mL) for 2 hours. The resin was filtered through a Whatman filter paper. To the filtrate, 15 mL cold diethyl ether was added, and the obtained precipitate was dried in a vacuum desiccator. The obtained product was characterized by MALDI-TOF mass spectrometry (Observed mass: 1042.36, Expected Mass: 1042.43, (Figure B1)

and circular dichroism spectroscopy. CD spectra were recorded using 1 mg/mL solution of the iRGD peptide in phosphate buffer (4 mM, pH = 7.5, Figure B2).

3.2.4. Synthesis of iRGD peptide-lipid conjugate

The lipid DSPE-PEG-N_3 was reacted with the hexynoic acid conjugated iRGD peptide using the "Click" reaction. To conjugate the alkyne of the peptide to the azide group of the lipid, the compounds were reacted in 1:2 molar ratio. The hexynoic acid conjugated peptide (40 mg) and DSPE-PEG-N_3 (50 mg) were dissolved in 3 mL water. The copper complex was prepared by mixing copper (II) sulfate with N, N, N', N', N''-pentamethyl diethylenetriamine (PMDETA) for 2 hours at room temperature. The ascorbic acid solution was prepared in water. The copper complex (53 mM $CuSO_4$ solution in water and 2 mmol PMDETA stirred for 2 hours) and sodium ascorbate (1.4 µmol) were added to the reaction mixture and stirred for 24 hours at room temperature. The sample was then transferred to a dialysis cassette with a molecular weight cut-off of 3,000. The reaction mixture was dialyzed against water for 72 hours to remove the catalyst and unreacted iRGD peptide. The product was then analyzed by CD spectroscopy (Figure B3).

3.2.5. Preparation of LNs for release studies

LNs were prepared by the thin film hydration method. DSPC, hypoxia-sensitive POPE-azobenzene-PEG, and iRGD conjugated DSPE lipid were dissolved in chloroform in a round bottom flask (molar ratio 50:40:10 respectively). Chloroform was then evaporated using a rotary evaporator to form a thin film at the bottom of the flask. The thin film was dried overnight in a vacuum desiccator. The dry film was hydrated with a carboxyfluorescein (100 mM) solution (prepared in 25 mM HEPES buffer, pH 7.4) for 1 hour at 60 °C. The multi-lamellar LNs formed were then subjected to ultrasonication for 1 hour at level 9 on a bath sonicator (Aquasonic, model 250D). The formed LNs were then extruded 11 times through 0.8 µm Whatman filter paper using

an extruder (Avanti Polar Lipids). To reduce the size, the LNs were again extruded 11 times through 0.2 μm Whatman filter. Excess of carboxyfluorescein (unencapsulated) was removed by a Sephadex G100 size exclusion column. The eluted LNs were used for release studies.

3.2.6. Size analysis

The hydrodynamic diameter of the LNs was measured by dynamic light scattering, using a Malvern Zetasizer. All measurements were performed employing 1 mL sample with 6 runs and 6 repeats.

3.2.7. Release studies

LNs (20 μL of 1 mg/mL total lipid concentration) encapsulating carboxyfluorescein were taken in 25 mM HEPES buffer of pH 7.5 (180 μL). Rat liver microsomes were isolated and (10 μL of 790 μg/mL) were added to this solution along with NADPH (100 μM) as a cofactor.[90] The LNs were subjected to normoxic and hypoxic conditions to measure the release of the encapsulated dye. Normoxic conditions were maintained by bubbling air through the buffer containing the LNs. Hypoxic conditions were created by bubbling nitrogen through the reaction mixture. Emission intensity of the mixture was measured at 515 nm as a function of time (excitation: 485 nm).

$$Percent\ release = \frac{(Emission\ intensity\ after\ release - Intensity\ before\ release)}{(Intensity\ after\ treatment\ with\ triton - Intensity\ before\ release)} \times 100$$

3.2.8. Atomic force microscopic imaging

An atomic force microscope (AFM) was used to image the LNs on a mica surface. The AFM measurements were carried out in non-contact mode at a scanning rate of 0.7 Hz and a resonance frequency of 145 kHz using an NT-MDT NTEGRA (NT-MDT America, Tempe, AZ). The cantilever was made of silicon nitride and was 100 μm long. The scanning areas were 5 x 5

or 20 x 20 μm at the resolution of 512 or 1024 points per line, respectively. The LN solution was dropped on top of a freshly cleaved mica surface and kept for 10 minutes at room temperature. The remaining solution was rinsed with water and dried extensively with an air blow gun. The mica substrate was glued on top of a sapphire substrate (sample holder) using Scotch double sided tape, and cleaved with Scotch tape to obtain a debris-free and flat surface. The images were flattened by a first order line correction and a first order plane subtraction to compensate for the sample tilt.

3.2.9. Preparation of gemcitabine encapsulated LNs

Gemcitabine was encapsulated in LNs by the active loading method.[82] The lipid DSPC, hypoxia-sensitive POPE-azobenzene-PEG, iRGD conjugated DSPE, and POPE-lissamine rhodamine were dissolved in chloroform in a round bottom flask (molar ratio of 49:40:10:1 respectively). The lipid thin film was prepared as described before. The thin film was hydrated with 25 mM citrate buffer (pH 4) for 1 hour at 60 °C. Subsequently, the formed LNs were sonicated in a bath sonicator (Aquasonic 250D, Power level 9) for 1 hour. The LNs were then extruded through a 0.2 μm Whatman Nucleopore membranes for 11 times and were passed through Sephadex G100 column to build the pH gradient across the membrane. Gemcitabine was encapsulated in these LNs by incubating the drug (lipid: drug ratio 9:1) with the LNs for 3 hours at 60 °C. The absorbance spectrum of the LNs was recorded. From a standard curve, the amount of gemcitabine was determined. Percent entrapment and encapsulation efficiency for gemcitabine were calculated using the following formula:

$$Percent\ extrapment = \frac{\text{gemcitabine before gel filtration (mg)} - \text{gemcitabine after gel filtration (mg)}}{\text{gemcitabine before gel filtration (mg)}} \times 100$$

$$Encapsulation\ efficiency = \frac{\text{Gemcitabine encapsulated in LNs (mg/mL)}}{\text{Weight of of the lipids (mg/mL)}} \times 100$$

3.2.10. Cellular studies

The cellular studies were carried out with the pancreatic cancer cell line BxPC-3 in RPMI media (supplemented with 10% FBS and 1% antibiotics). The cells were grown as monolayer and as three-dimensional spheroids. Spheroids grown on 96 well agarose microwell plate were used for cell viability assay. To study the penetration ability of the LNs, BxPC-3 cells were grown on stacks of wet strengthened Whatman filter paper (number 114).

3.2.11. Cell viability studies in monolayer cultures

In a 96 well clear bottom plate, the BxPC-3 cells (2000 per well) were seeded. The cells were allowed to attach to the surface and grow for 24 hours at 37 °C in an incubator supplemented with 5% CO_2. The cells received treatment with hypoxia responsive, iRGD peptide-decorated LNs encapsulating gemcitabine (20 µM) for 3 days. LNs devoid of hypoxia-sensitive lipid and without iRGD conjugated lipid were used as controls. Gemcitabine (20 µM) in aqueous solution was used as a positive control. After 3 days of treatment, the conditioned media was removed from the plate (to discard the fluorescent LNs) and was replaced with 200 µL of fresh medium supplemented with 20 µL Alamar Blue (Invitrogen). The plates were incubated for 2 hours, and fluorescence was measured (excitation wavelength 560 nm, emission wavelength 590 nm).

3.2.12. Cell viability study in spheroid cultures

The BxPC-3 cell spheroids were prepared by seeding the 2 x 10^6 cells in each of the 96 well agarose scaffolds. To make the scaffold, an aqueous agarose solution (2% W/V) was sterilized in an autoclave for 45 minutes. The mold was purchased from Microtissues, and the scaffolds were prepared using manufacturer's protocol. The cells were seeded on 36 scaffolds and were incubated for 7 days. Media on the scaffolds was changed every 2 days. The scaffolds were then divided

equally into two groups (18 scaffolds per group). One group of scaffold was allowed to grow under normoxic conditions, and another group was incubated in a hypoxic chamber maintained at an oxygen level of 1% (hypoxic conditions) for 24 hours. After establishing normoxic and hypoxic cultures, the scaffolds were treated with gemcitabine, gemcitabine encapsulated hypoxia-sensitive LNs, gemcitabine encapsulated iRGD functionalized hypoxia responsive LNs, and gemcitabine encapsulating LNs devoid of iRGD and stimuli responsive lipids. Treatment with buffer and buffer encapsulating LNs was used as a control. The scaffolds were divided equally into each of these treatment groups (3 scaffolds in each treatment group). The cell spheroids were treated under normoxic and hypoxic conditions for 72 hours. After the treatment, the cells in each spheroid scaffold were dissociated by using a Tryple solution (1 mL for each scaffold) for 10 minutes. The scaffolds were then washed with 3 mL of cell culture medium to harvest the cells. The harvested cells from each scaffold were then dissociated and plated directly in 6 wells of 96 well plate. This step converted the 3-dimensional cell culture to a monolayer culture. It was crucial to keep the dilution of the cells exactly same for each treatment group to keep the relative ratios of cell viability in each treatment group. The cell viability was then measured by the Alamar Blue assay.

3.2.13. Cellular uptake in spheroid cultures

To facilitate the hypoxic microenvironment of tumors, we cultured the BxPC-3 cells as layers. To grow the layered cells, a stack of wet strengthened Whatman filter paper (No. 114) was used.[91] This setup allowed us to image the depth of penetration of the iRGD peptide-decorated LNs. We cut these papers as 1" diameter circles using a commercially available hole punch. The cut circles were then wrapped in aluminum foil and were autoclaved for 45 minutes. We designed a culture apparatus (using the CAD software Creo Parametric) to hold the paper stack in place. The assembly was then 3D printed using poly(lactic acid) as the "ink". Our apparatus had four

components – base, paper stack insert, paper press insert attached to a media transfer tube, and a cover (Figure 3.2).

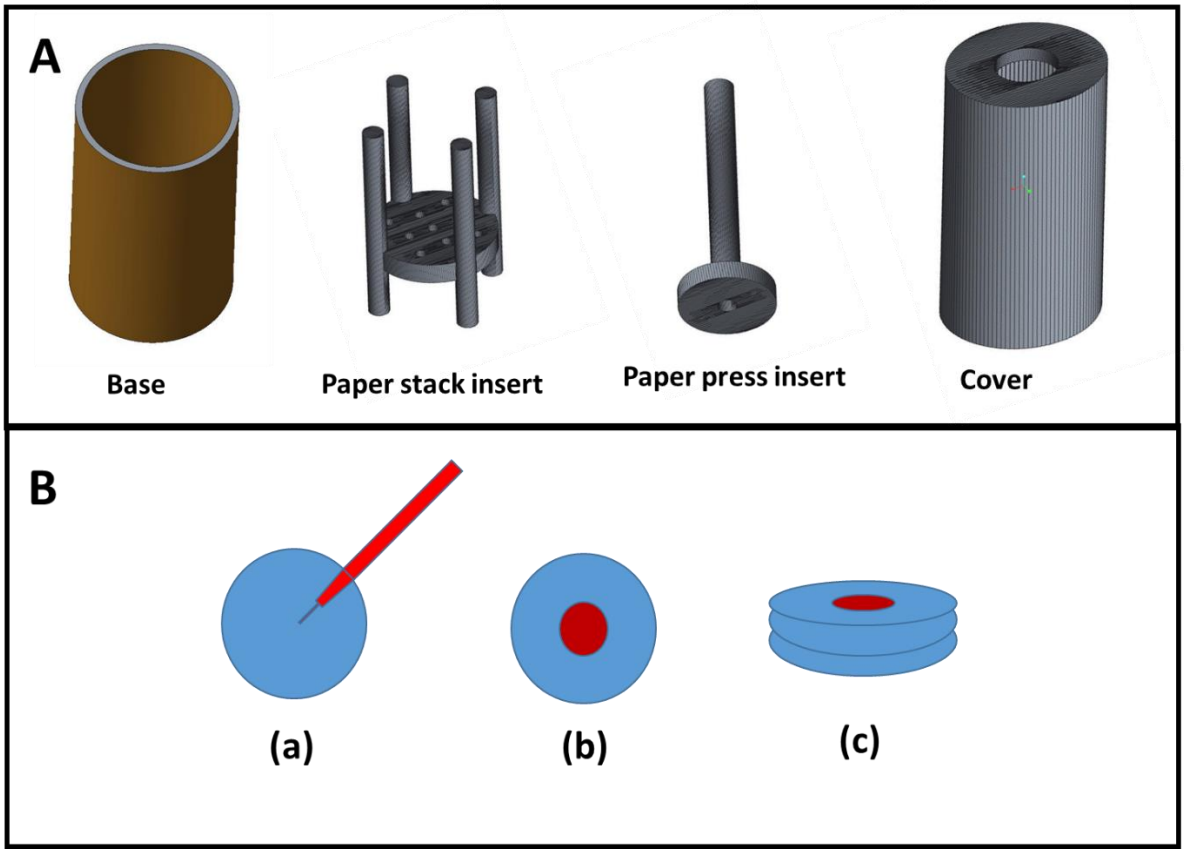

Figure 3.2. (A) The 3D printed parts for the cell culture apparatus to hold the stacks of Whatman filter paper. (B) (a) The sterilized filter papers were inoculated with BxPC-3 cells embedded in agarose and sodium alginate, (b) stacked with other filter papers, and (c) incubated together for layered cell culture.

The trypsinized BxPC-3 cells were centrifuged, and 100,000 cells were suspended in 500 µL culture medium. A solution of agarose and sodium alginate (1:2) was autoclaved, cooled to 40 °C, and the cells suspension was added. After mixing, 20 µL of this suspension was applied at the center of each paper circle. The cell-seeded papers were stacked together on the 3D printed paper stack insert with the paper press insert on the top. The assembly was inserted in the base, and the cover was placed. Two apparatus were then incubated under normoxic conditions, and two were

incubated in 1% oxygen for three days. The cell stacks in normoxic and hypoxic incubators received treatments with 20 μL of carboxyfluorescein encapsulated LNs (delivered through the hollow tube of the paper press insert) with and without the iRGD on the surface. The cell stacks were treated for 2 hours in respective incubation conditions (normoxic/hypoxic), the paper racks were removed, and were submerged in HBSS solution to wash excess of carboxyfluorescein. After washing the stacks 3 times, they were again immersed in cell culture medium before imaging. To image the cells with a fluorescence microscope, the papers from the stack were peeled one at a time and fluorescence was measured in each paper layer. The fluorescence intensity and the depth of penetration of polymersomes were measured using an Olympus laser scanning confocal microscope. The images were analyzed with the ImageJ software.

3.3. Results and discussion

Hypoxia alters the tumor microenvironment through the overexpressed HIF-1α and contributes to the overall cancer progression and metastasis.[92,93] The azobenzene group is reduced in the presence of elevated levels of reducing enzymes in the hypoxic tumor microenvironment (Figure 3.3).[94] We synthesized a hypoxia-sensitive lipid by conjugating POPE to polyethylene glycol (PEG_{1900}) through the azobenzene linker (Scheme 3.1). We incubated a solution of the purified lipid under simulated hypoxic conditions (100 μM NADPH, rat liver microsomes, and nitrogen gas bubbling) for 2 hours. We observed that the fluorescence emission intensity from the azobenzene group was substantially reduced after the hypoxic treatment. We did not observe any reduction in the emission intensity of the lipid under normoxic conditions (100 μM NADPH, rat liver microsomes, and nitrogen air bubbling).

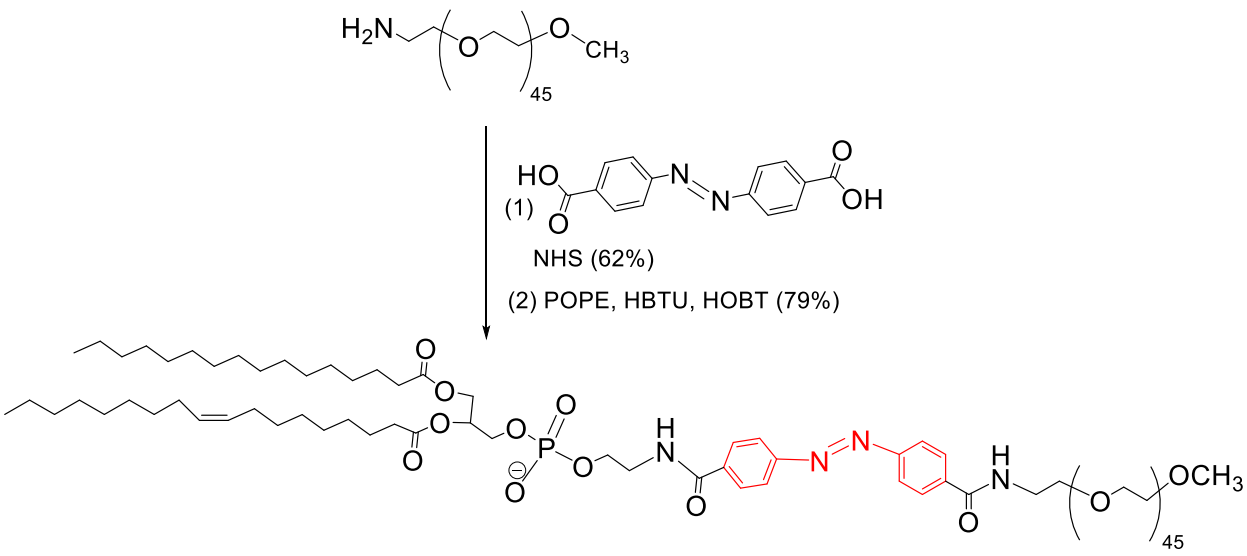

Scheme 3.1. Synthesis of the hypoxia responsive POPE-azobenzene-PEG_{1900} lipid. The hypoxia-responsive linker is indicated in red.

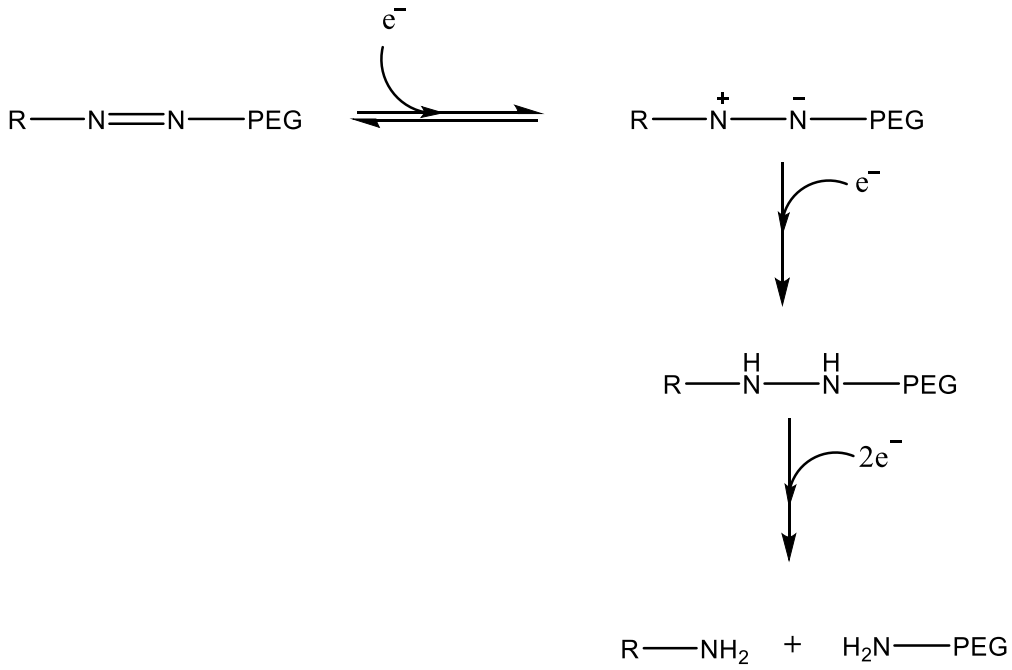

Figure 3.3. Mechanism of reduction of azobenzene under hypoxic reducing environment, where R represents POPE.[94]

Tumor tissues develop hypoxia in the regions with inadequate blood flow due to the irregularly formed vasculature.[93] These areas are usually less accessible to passively targeted drug

carriers. The cyclic iRGD peptide has been previously used to enhance accumulation of the drugs or nanoparticles in the tumor tissues.[88, 95] The iRGD peptide functionalized nanoparticles preferentially accumulate and penetrate deep into the tumor tissue.[96]

We synthesized the hexynoic acid conjugated iRGD peptide by employing a microwave assisted, solid-phase peptide synthesizer. The alkyne of hexynoic acid allowed conjugation of the synthesized peptide to the surface of the LNs by the "Click" chemistry. To confirm the cyclization of the peptide, we recorded the CD spectrum in the absence and presence of 10 mM glutathione. Thiol-sulfhydryl exchange and the reduction of the disulfide bond in the peptide resulted in a shift of the negative peak in the CD spectra from 199 nm to 195 nm (B2). The peptide was then conjugated to the lipid DSPE-PEG-N_3 by using the copper catalyzed [2+3]-cycloaddition reaction (Scheme 3.2). The product was confirmed by CD spectroscopy (B3). This lipid was then incorporated into the LNs to enhance the tissue penetration depth of the vesicles.

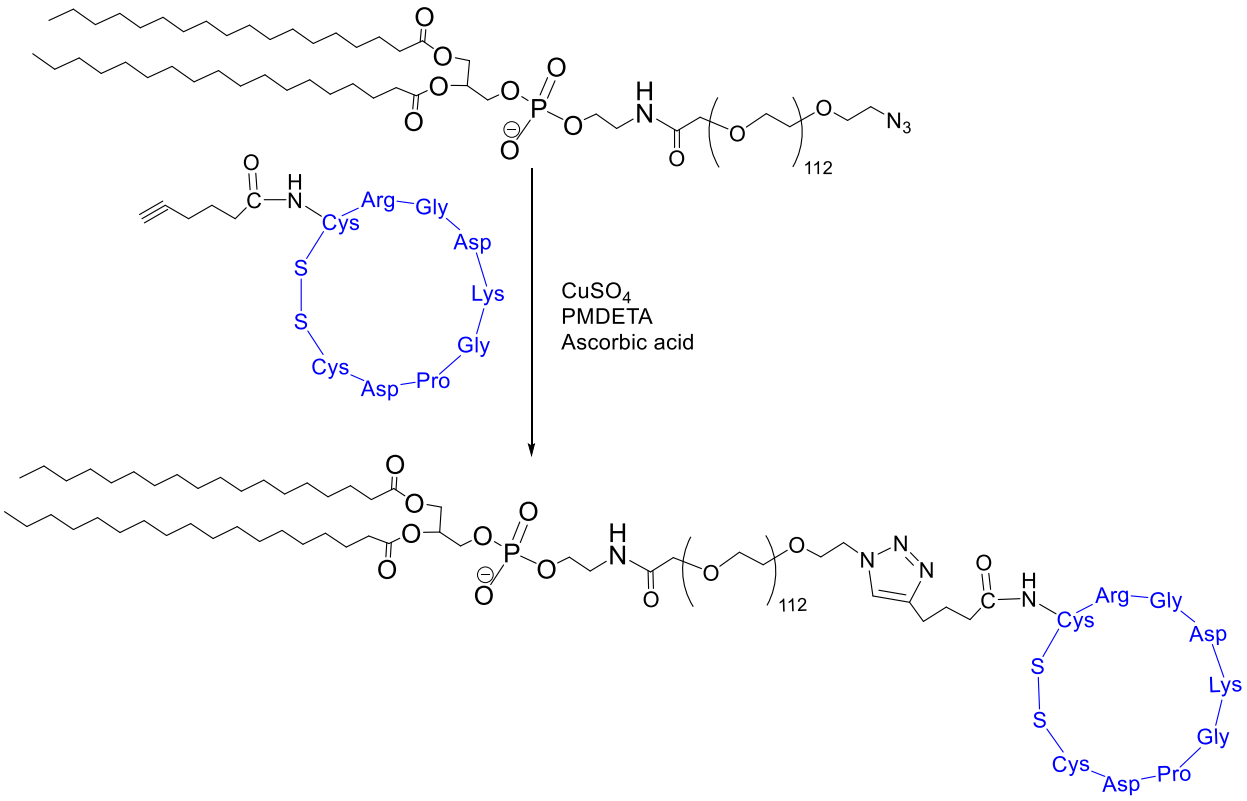

Scheme 3.2. Synthesis of iRGD peptide conjugated DSPE lipid. The iRGD peptide is shown in blue.

The stability of the nanoparticles in the absence of a stimulus is critical for drug delivery applications. To impart stability, we incorporated the saturated DSPC along with the synthesized hypoxia responsive and iRGD conjugated lipid in the LNs. We optimized the relative ratio of these lipids such that the LNs are stable in normoxic circulatory conditions but disintegrate in the hypoxic environment to release the encapsulated contents. We encapsulated the self-quenching dye carboxyfluorescein in the LNs and monitored its release employing fluorescence spectroscopy (excitation: 485 nm, emission: 515 nm). The optimum stability and release characteristics were observed with the lipid composition DSPC: POPE-azobenzene-PEG_{1900}: DSPE-PEG-iRGD in the molar percentage of 40:50:10. Under normoxic conditions, the release from these LNs was

observed to be less than 5% in 2 hours (Figure 3.4, black squares). However, under hypoxic conditions, the LNs released 66% of the encapsulated dye within 2 hours (Figure 3.4, red triangles).

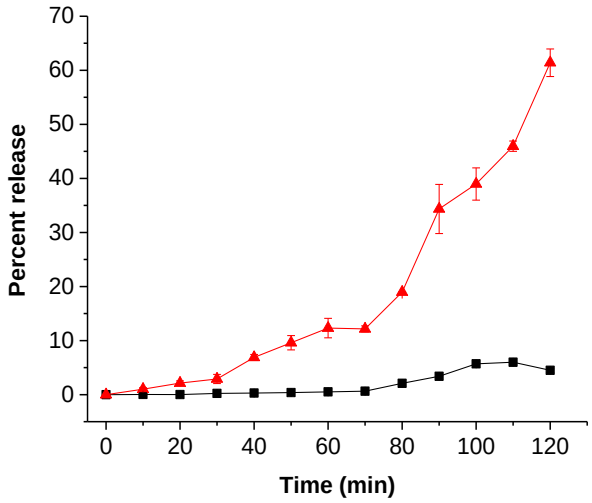

Figure 3.4. Dye release profiles from the LNs in hypoxic (red triangles) and normoxic (black squares) environment. The lines connecting the observed data points are shown (n = 3).

The LNs were less than 250 nm in size with a polydispersity index (PDI) of less than 0.3. A typical size distribution pattern, as measured by dynamic light scattering, is shown in Figure 3.5. Table 3.1 shows the size analysis of the LNs as determined by dynamic light scattering.

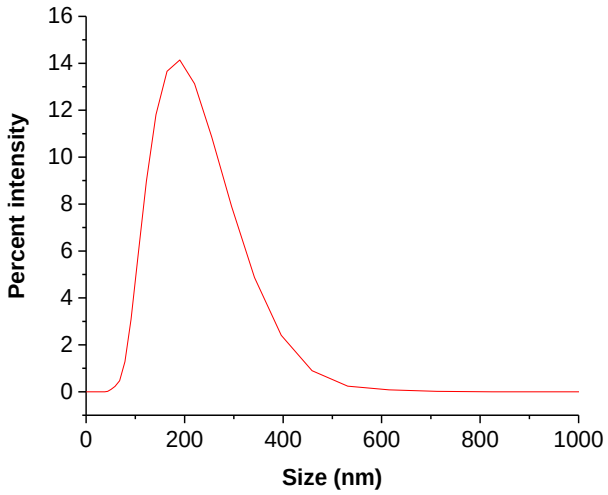

Figure 3.5. Size distribution of LNs as determined by the dynamic light scattering. The mean diameter was (180 $\pm$ 3) nm with a polydispersity index of 0.23 $\pm$ 0.01.

Table 3.1. Size analysis by dynamic light scattering for the test and the control LNs.

	Lipid composition (molar percentage)	**Encapsulated content**	**size (nm) ± std. dev.**	**PDI ± std. dev.**
DSPC	DSPC (100)	gemcitabine	178 ± 3.6	0.15 ± 0.02
Test LNs	POPE-azobenzene-PEG (50): DSPC (39): DSPE-PEG-iRGD (10): Lissamine rhodamine (1)	gemcitabine	180 ± 3.4	0.23 ± 0.01
LNs without iRGD	POPE-AZB-PEG (50): DSPC (49): Lissamine rhodamine (1)	gemcitabine	121 ± 1.5	0.12 ± 0.01
Test LNs	POPE-AZB-PEG (50): DSPC (40): DSPE-PEG-iRGD (10):	carboxyfluorescein	235 ± 2.3	0.20 ± 0.04

We imaged the LNs by atomic force microscopy (AFM) to determine any structural changes in the hypoxic environment. In this endeavor, we prepared the LNs in 25 mM HEPES buffer (pH 7.4) and added NADPH and rat liver microsomes. The control samples were exposed to normal atmospheric oxygen levels while nitrogen gas was bubbled through the test reaction mixture for 2 hours. We observed that the LNs under normoxic conditions retained the spherical structures (Figure 3.6, Panel A). However, hypoxic conditions distorted the shapes of the vesicles (Figure 3.6, Panel B), indicating structural changes in the lipid bilayer.

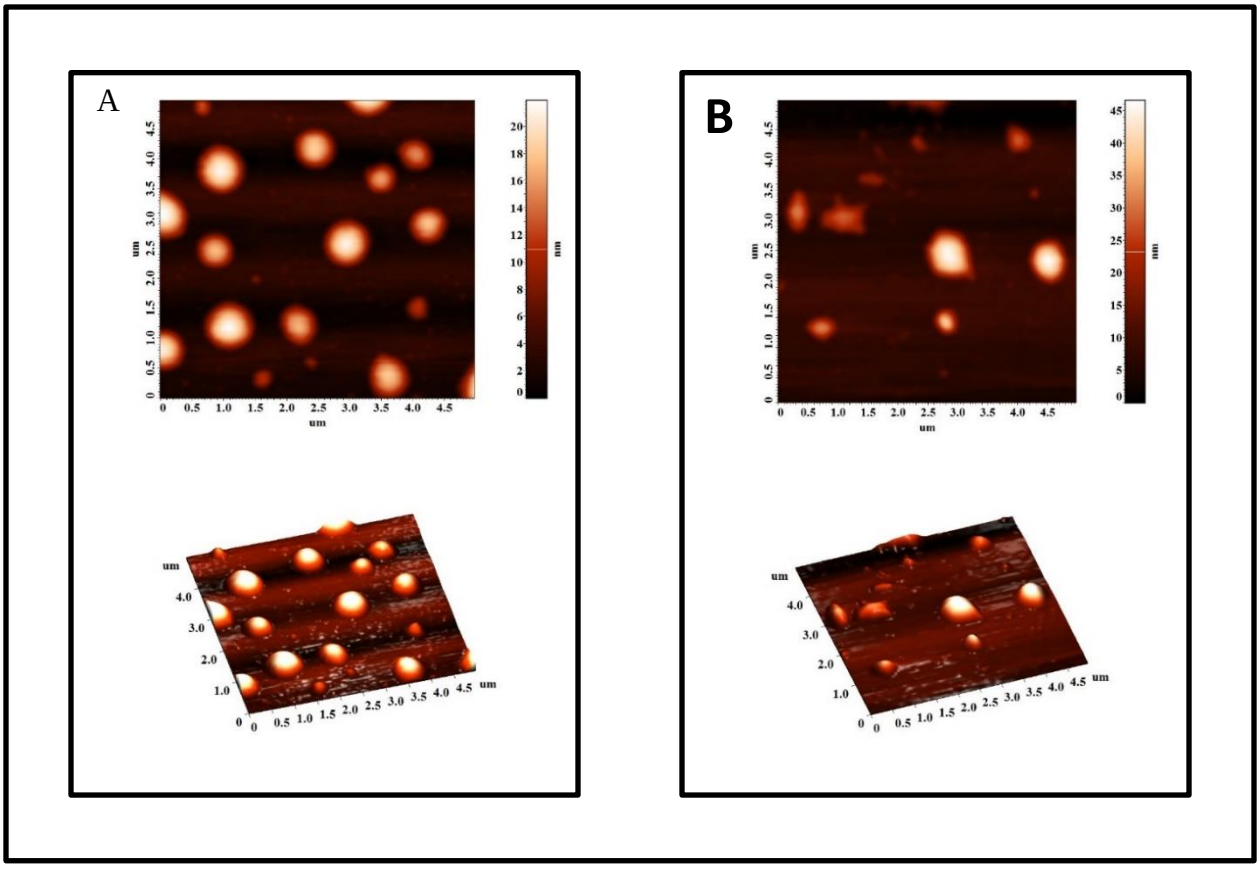

Figure 3.6. AFM images of LNs under normal oxygen levels (A) and after 2 hours of hypoxia treatment in the presence of NADPH and rat liver microsomes (B).

After confirming the hypoxia responsive characteristics of the LNs, we encapsulated the anticancer drug gemcitabine by the active loading method.[82] Gemcitabine is the first line of treatment for pancreatic cancer. Since gemcitabine in a solution is colorless, we incorporated 1% of the fluorescent lipid 1,2-dipalmitoyl-*sn*-glycero-3-phosphoethanolamine-N-(lissamine rhodamine B sulfonyl) (lissamine rhodamine lipid) in the LNs (molar ratio of DSPC: POPE-azobenzene-PEG_{1900}: DSPE-PEG-iRGD: lissamine rhodamine lipid 39:50:10:1) for visualization. To encapsulate gemcitabine, a pH gradient was developed across the lipid bilayer with inside pH of 4 and outside pH of 7.4. After the active loading, we used gel filtration to remove any

unencapsulated drug. The entrapment efficiency for these LNs was found to be about 40% with a drug loading capacity of 8% (by absorption spectroscopy).

The effectiveness of the drug encapsulated LNs was tested using monolayer and three-dimensional spheroid cultures of the pancreatic cancer cells BxPC-3. We observed that the viability of cells in monolayer cultures decreased in the presence of LNs encapsulating gemcitabine under both normoxic and hypoxic conditions. However, the response of three-dimensional tumor tissues cannot be predicted from monolayer cells cultures.[97] Hence, we cultured the BxPC-3 cells as spheroids in agarose scaffolds (Figure 3.7).

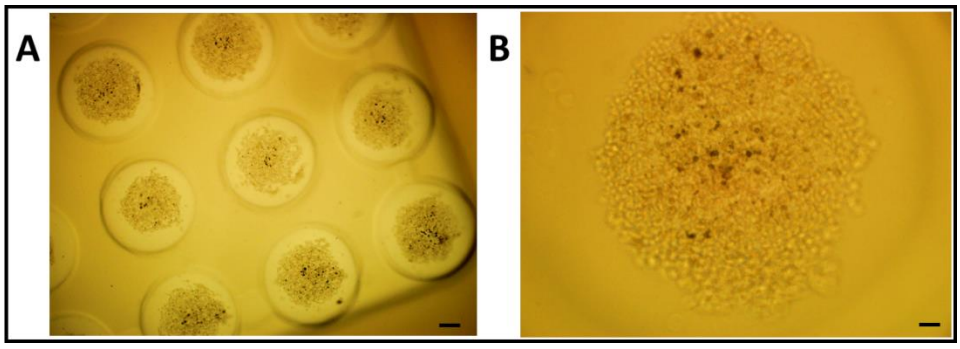

Figure 3.7. Optical microscopic images of the cultured spheroids of BxPC-3 cells in agarose molds at (A) 4X magnification (scale bar: 200 µm), and (B) 10X magnification (scale bar: 50 µm).

We divided the BxPC-3 cell spheroids into two groups and cultured them in normoxic and hypoxic (1% oxygen) conditions for 72 hours. Both the groups received treatments with gemcitabine encapsulating iRGD functionalized hypoxia-sensitive LNs, gemcitabine encapsulating LNs without the iRGD peptide on the surface, free gemcitabine, and gemcitabine encapsulating LNs devoid of hypoxia responsive lipid (prepared with DSPC). We measured the cell viability by the Alamar Blue assay.[82] To make a valid comparison between the groups, we ensured the gemcitabine concentration was 20 µM for all the treatments. Results indicated that

the cell viability in monolayer cultures (Figure 3.8A) was unaffected after treatment with drug encapsulated LNs under normoxic and hypoxic conditions. However, we observed significant decrease in cell viability in the group of cells treated with iRGD conjugated LNs under hypoxic conditions as compared to the cell viability observed in cells treated under normoxic conditions ($p \leq 0.05$). In spheroidal cultures of BxPC-3 cells we observed decreased cell viability after treatment with gemcitabine encapsulated LNs under normoxic as well as hypoxic conditions (Figure 3.8B). Cell viability in spheroids treated with DSPC LNs, gemcitabine free drug and LNs devoid of iRGD peptide showed decrease in cell viability under normoxic as well as hypoxic conditions. The reduction in cell viability under normoxic spheroids may be due to reduction of azobenzene and release of the drug gemcitabine in hypoxic core of the BxPC-3 cell spheroids. The treatment with iRGD conjugated, hypoxia-responsive LNs decreased the cell viability in hypoxic spheroidal culture to 25% (Figure 3.8B) showing significant decrease in cell viability as compared to the spheroidal cultures treated under normoxic conditions. We speculate that the enhanced cytotoxicity is due to the penetration ability of iRGD conjugated LNs. As the LNs penetrate deep inside the core of the spheroids, they are likely to encounter a hypoxic microenvironment and release the encapsulated drugs. The reduced effectiveness of the other liposomal formulations and the free gemcitabine is probably due to less penetration in the spheroids.

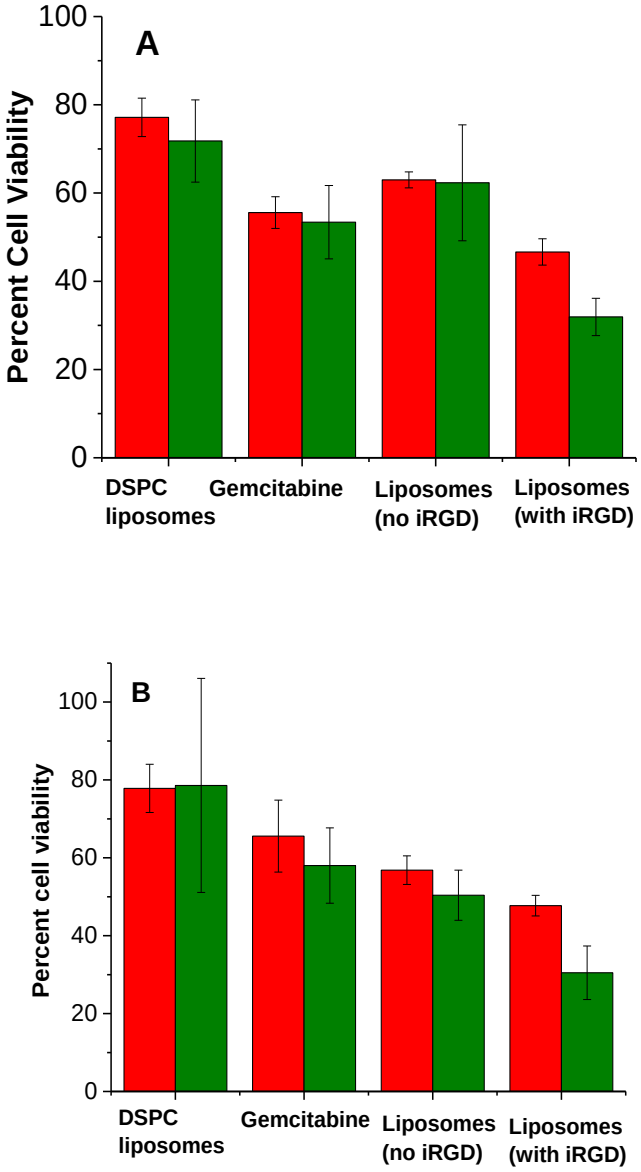

Figure 3.8. Viability of BxPC-3 cells cultured as monolayers (A) and three-dimensional spheroids (B) after treatment with DSPC LNs encapsulating gemcitabine (20 μM), free gemcitabine (20 μM), gemcitabine encapsulated hypoxia-responsive LNs devoid of surface iRGD peptide, and the hypoxia-sensitive LNs with the iRGD under normoxic (red bars) and hypoxic conditions (green bars).

The cell viability studies in the spheroidal cultures indicated that the hypoxia-responsive LNs were able to release the encapsulated drug in the hypoxic BxPC-3 cells. To observe the

penetration depth facilitated by iRGD peptide on the surface, we cultured the BxPC-3 cells in a paper stack as a tumor tissue[91] using our 3D printed apparatus (Figure 3.2). We delivered 20 μL of carboxyfluorescein encapsulated, hypoxia-sensitive LNs through the hollow tube of the paper stack insert, and incubated for 2 hours under normoxic and hypoxic conditions. Subsequently, the apparatus was disassembled, the filter papers were separated, and imaged under a fluorescence microscope. We observed very low fluorescence under normoxic conditions after 2 hours, even from the top filter paper (Figure 3.9A, Normoxic Panel). However, under hypoxic conditions, considerably higher fluorescence intensity was observed (Figure 3.9B, Hypoxic Panel) from the top filter paper, indicating the release of the LN encapsulated carboxyfluorescein dye. We also noted that the LNs conjugated to the iRGD peptide penetrated deeper into the cultured tumor tissues. LNs devoid of the iRGD peptide were unable to reach the 8^{th} layer of the stack under hypoxic conditions (Figure 3.9A, Hypoxic Panel). However, LNs functionalized with the iRGD peptide penetrated deeper into the stack, reaching the 12^{th} layer of the culture from the top (approximately 1.8 mm in depth, Figure 3.9B, Hypoxic Panel).

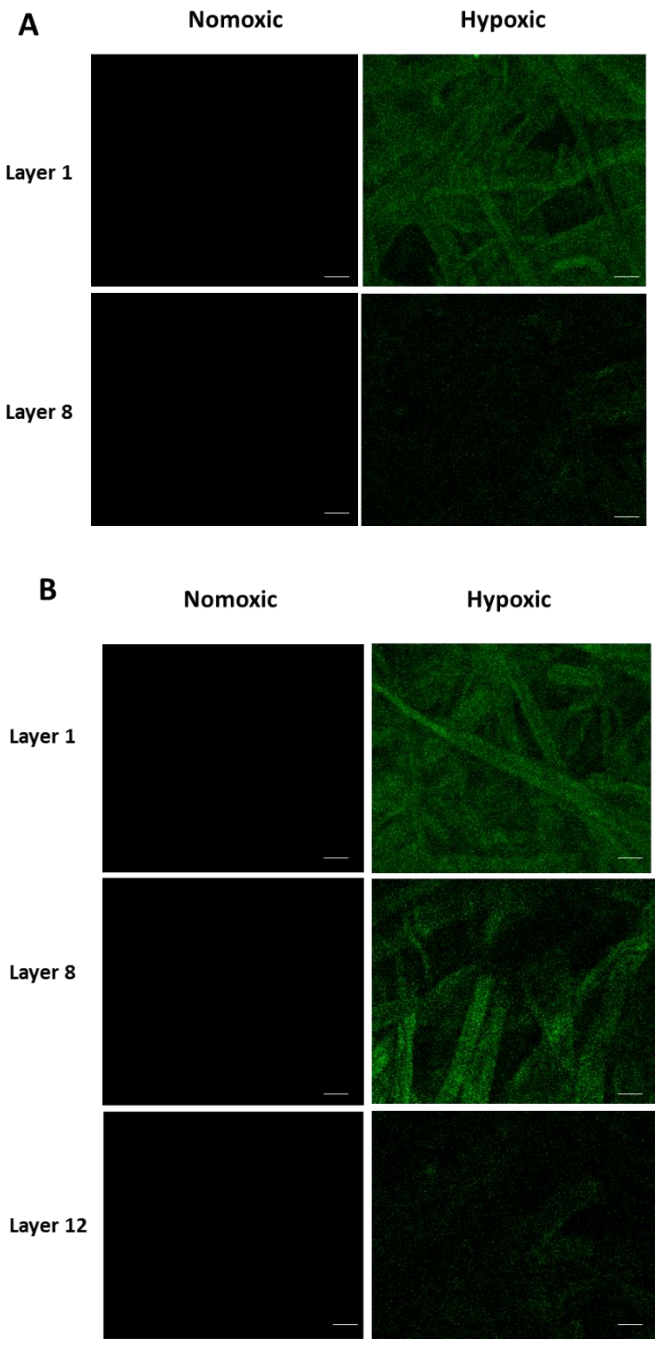

Figure 3.9. Fluorescence microscopic images of layers of cells indicating carboxyfluorescein release from the LNs under normoxic and hypoxic conditions without (A) and with (B) the iRGD peptide functionalization (scale bar: 100 μm).

3.4. Conclusion

In conclusion, we have successfully synthesized a hypoxia-sensitive lipid and prepared iRGD peptide functionalized, hypoxia-responsive LNs encapsulating the anticancer drug gemcitabine in the aqueous core. The LNs released 65% of the encapsulated contents under hypoxic conditions in 2 hours. The pancreatic cancer cells BxPC-3 treated with the LNs showed decreased cell viability compared to the free drug and DSPC LNs. The iRGD peptide on the surface allowed the LNs to penetrate deeper and deliver the anticancer drug to the hypoxic cores, resulting in enhanced cytotoxicity for the cultured pancreatic cancer cell spheroids.

4. HYPOXIA-RESPONSIVE POLYMERSOMES FOR DRUG DELIVERY TO HYPOXIC PANCREATIC CANCER CELLS[3]

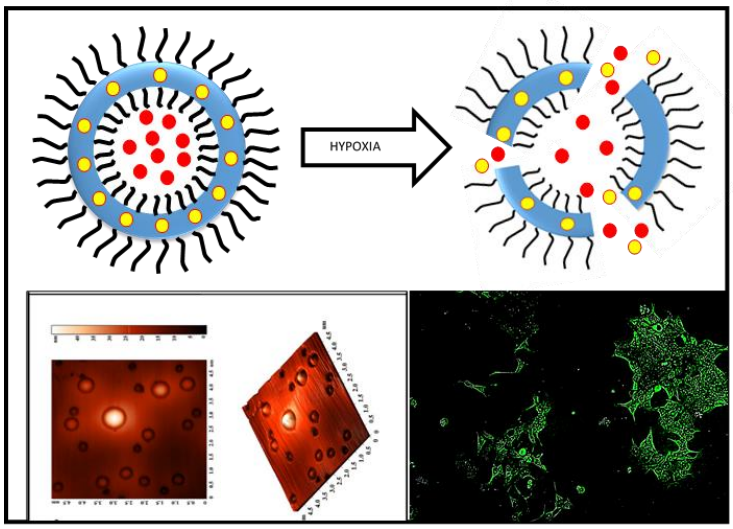

Figure 4.1. Graphical abstract

4.1. Introduction

Rapid cell division, exponential growth, and insufficient blood supply create oxygen gradients in solid tumors.[98] Oxygen partial pressure in the tumors decreases from the surface to the interior, reaching as low as 0 – 2.5 mm of Hg in some regions.[99] These hypoxic areas assist disease progression by remodeling the extracellular matrix, initiating the epithelial-to-mesenchymal transition, and altering the overall biochemical environment around the cells.[100]

[3] This section was coauthored by Kulkarni, Prajakta; Haldar, Manas; You, Seungyong; Choi, Yongki and Mallik, Sanku. Prajakta had primary responsibility to conduct all the experiments listed in the section, analyze the data and write the manuscript. Manas had primary role of synthesizing hypoxia responsive polymer. Seungyong and Dr. Choi were involved in AFM imaging studies. Dr. Mallik had a primary role of verifying the results and editing the manuscript for publication.

Hypoxia also plays a significant role in developing resistance to radio and chemotherapy in cancer patients.[101]

Hypoxia develops in the solid tumors of the breast, colon, prostate, and pancreatic cancers.[102] This problem is exacerbated in pancreatic cancer due to the formation of the dense extracellular matrix (desmoplasia) and the early development of hypoxia.[7] The hypoxic regions and desmoplasia make the treatment ineffective for pancreatic cancer, leading to a dismal five-year survival rate of about 5%.[103, 104,105]

Hypoxic and normoxic tissues show remarkably different micro-environments – providing an opportunity for tumor-specific drug delivery with reduced oxygen partial pressure as the trigger.[92] Polymersomes are vesicles formed from amphiphilic di-block copolymers capable of encapsulating hydrophilic compounds in the core and hydrophobic drugs in the bilayer.[49] The relative ratio of the hydrophobic and hydrophilic polymer blocks determines the formation of polymersomes.[49] The reported tumor-targeted polymersomes deliver the encapsulated drugs at the targeted site in response to the elevated levels of enzymes, reducing agents, reduced pH, etc.[12] However, hypoxia-responsive polymeric drug carriers are less explored. Polymeric nanoparticles with the nitroimidazole pendant groups released the encapsulated doxorubicin in a hypoxic environment.[24] The reducible azobenzene group has been used to prepare imaging agents and polymeric micelles responsive to the reducing microenvironment of hypoxia.[106, 94]

In this study, we have synthesized a hypoxia-responsive, amphiphilic, diblock copolymer by conjugating polylactic acid (PLA) with polyethylene glycol (PEG) via an azobenzene linker. We prepared polymersomes from the synthesized copolymer, encapsulating the anticancer drug gemcitabine and the epidermal growth factor receptor (EGFR) inhibitor erlotinib. Gemcitabine is the first choice anticancer drug for pancreatic cancer.[107] The EGFR receptor inhibitors aid in

restricting the disease progression.[108] Clinical trials indicate improved survival of pancreatic cancer patients when gemcitabine is combined with erlotinib.[105] However, erlotinib is more hydrophobic compared to gemcitabine. Hence, encapsulation of both drugs in polymersomes has the potential to increase the effectiveness of the treatment. We expected that hypoxic conditions will reduce the azobenzene group to amines.[94] Herein, we demonstrate that the resultant destabilization of the polymer bilayer releases the encapsulated drugs from the polymersomes to the cultured, hypoxic, spheroids of the pancreatic cancer cells BxPC-3.

4.2. Materials and Methods

4.2.1. Synthesis and characterization of the copolymer

4.2.1.1. Reaction of PEG-diphenylazacarboxylate with 1- aminopropanol

Polymer m-PEG$_{1900}$-amine was conjugated to azobenzene-4,4'-dicarboxylic acid by following a previously published protocol.[106] The PEG-diphenylazacarboxylate (1 g, 0.46 mmol) was dissolved in pyridine (25 mL). To this solution, EDC (134 mg, 0.69 mmol) and NHS (80 mg, 0.69 mmol) were added followed by excess of 1-aminopropanol (175 mg, 2.32 mmol). The reaction mixture was stirred overnight. The solvent was then removed under reduced pressure. The residue obtained was dissolved in dichloromethane, washed with 0.5 N HCl, and 0.5 N NaOH. The clear organic solution was dried over Na_2SO_4, evaporated, and subjected to chromatographic purification (R_f = 0.6, 10 % MeOH in dichloromethane) yielding 677 mg (66%) of the yellow semisolid product. ^{1}H NMR (400 MHz, CHLOROFORM-*d*) δ ppm: 0.02 - 0.01 (m) 1.08 - 1.36 (m) 3.37 - 3.38 (m) 3.53 - 3.63 (m) 3.77 - 3.91 (m) 5.25 - 5.38 (m) 7.27 (s) 7.93 - 8.07 (m).

4.2.1.2. Synthesis of the block copolymer

The product obtained from the previous step (150 mg, 0.068 mmol) was taken into toluene (30 mL) and was subjected to azeotropic distillation for 6 hours employing a Dean-Stark apparatus.

After cooling to room temperature under nitrogen, D, L-lactide (450 mg, 3.17 mmol) and tin (II) ethoxyhexanoate (15 mg) were added, and the solution was heated to reflux under nitrogen for 14 h. After cooling to room temperature, the reaction mixture was added dropwise to the cold ether. After 3 h, the clear supernatant was decanted, and the precipitate was dried under vacuum. The yellow viscous semi-solid product obtained (405 mg, 67%) was analyzed by ^{1}H NMR spectroscopy for purity. NMR: ^{1}H NMR (400 MHz, CHLOROFORM-d) δ ppm: 0.00 - 0.11 (m) 1.40 - 1.61 (m) 1.68 - 1.78 (m) 1.81 - 2.11 (m) 3.62 - 3.89 (m) 3.92 - 4.16 (m) 5.08 - 5.35 (m).

4.2.2. Preparation of polymersomes encapsulating carboxyfluorescein dye

The synthesized hypoxia responsive polymer PLA_{80}-azobenzene-PEG_{47} was dissolved in tetrahydrofuran (10 mg/mL), and the solution (200 µL) was added dropwise to a stirred solution of (2 mL) carboxyfluorescein dye (100 mM) in HEPES buffer (25 mM, pH 7.4). After stirring for 1 h, the THF was evaporated by bubbling air through the solution to form the carboxyfluorescein encapsulated polymersomes. The formed polymersomes were then sonicated for 1 hour in a bath sonicator (Aquasonic 250D, level 9), and dialyzed (molecular cutoff 1000) overnight in iso-osmolar HEPES buffer (25 mM, pH 7.4) to remove unencapsulated carboxyfluorescein. The polymersomes were then passed through Sephadex G100 gel filtration column to remove the remaining unencapsulated carboxyfluorescein. The polymersomes collected were used for the release and cellular uptake studies.

4.2.3. Preparation of polymersomes encapsulating gemcitabine and erlotinib

The synthesized polymer PLA_{80}-azobenzene-PEG_{47} was dissolved in tetrahydrofuran (10 mg/mL) and a fluorescent lipid, 1,2-dipalmitoyl-sn-glycero-3-phosphoethanolamine-N-lissamine rhodamine B sulfonyl ammonium salt (rhodamine lipid) was dissolved in chloroform (0.01 mg/mL). To an empty vial, rhodamine lipid solution was added, and chloroform was evaporated

from the bottle. To the same vial, the polymer solution (200 µL, 2 mg) was added to adjust the polymer to lipid molar ratio of 95:5. The solvent was evaporated from the vial by passing air through it, and 200 µL THF was added to make the concentration of polymer 10 mg/mL. In another vial, erlotinib was dissolved in 200 mM citrate buffer (pH 4) to make drug concentration 0.2 mg/mL. Polymers dissolved in THF were then added dropwise to an erlotinib-citrate buffer solution (2 mL). The mixture was stirred for 1 hour at room temperature. THF was evaporated by passing air through the mixture for 45 minutes. The polymersomes formed were then sonicated using a bath sonicator (Aquasonic model 250D, level 9) for 45 minutes, and the polymersomes were passed through SephadexG-100 gel filtration column saturated with HEPES buffer (25 mM, pH 7.4). This protocol generated a pH gradient across the polymersome membrane (surrounding pH 7.4, core pH 4). Gemcitabine was added to these polymersomes (polymer to drug ratio 5:1 by weight), and the resulting mixture was stirred for 4 hours at room temperature. The polymersomes were again passed through the SephadexG-100 gel filtration column to remove unencapsulated drugs. Drug encapsulation was determined from the UV spectra for the polymersomes (270 nm for gemcitabine and 247 nm for erlotinib). The amount of drug encapsulated was measured from the standard curves. To calculate entrapment efficiency and loading capacity of the polymersomes, following equations were used.

$$\text{Percent Entrapment efficiency} = \frac{\text{amount of drug added- amount of drug encapsulated}}{\text{amount of drug added}} \times 100$$

$$\text{Percent Loading efficiency} = \frac{\text{Total weight of drug loaded in polymersomes}}{\text{Total weight of polymer}} \times 100$$

4.2.4. Size analysis

The hydrodynamic diameters of polymersomes were measured using a Dynamic Light Scattering (DLS) instrument (Malvern Zetasizer Nano-ZS90). Measurements were conducted at a scattering angle of 90^{o} using disposable polystyrene cuvette. An equilibration time of 120 s was maintained for all the measurements. For each sample, 6 readings were recorded averaging 6 runs for the same reading.

4.2.5. Transmission electron microscopy

Copper TEM grids (300-mesh, formvar-carbon coated, Electron Microscopy Sciences, Hatfield, Pennsylvania, USA) were prepared by applying a drop of 0.01% poly-L-lysine, allowing it to stand for 30 seconds, wicking off the liquid with torn filter paper, and allowing the grids to air dry. A drop of the suspension diluted 1:100 was placed on a prepared grid for 30 seconds and wicked off; grids were allowed to air dry again. Phosphotungstic acid 0.1%, pH adjusted to 7-8, was dropped onto the grid containing the sample, allowed to stand for 2 min, and wicked off. After the grids had been dry, images were obtained using a JEOL JEM-2100 LaB6 transmission electron microscope (JEOL USA, Peabody, Massachusetts) running at 200 keV.

4.2.6. Release studies

Carboxyfluorescein encapsulated polymersomes (200 µL) were added to 1.6 mL of iso-osmolar HEPES buffer (25 mM, pH 7.4). To this solution, 100 µL of rat liver microsomes were added along with 100 µM NADPH. The rat liver microsomes were isolated using a reported protocol.[90] Air was bubbled through the reaction mixture to create normoxic conditions. For hypoxic conditions, nitrogen gas was bubbled through the reaction mixture. The emission intensity was recorded every 5 minutes for 1 hour using a spectrofluorimeter at the emission wavelength of 515 nm (excitation: 480 nm). After 1 hour of normoxic/hypoxic treatment, 20 µL of Triton was

added to disintegrate the polymersomes, and release the encapsulated dye. Fluorescence intensity was measured for the total release after complete disintegration. Percent release was calculated using following formula:

$$\frac{(\text{Emission intensity after release-Intensity before release})}{(\text{Intensity after treatment with triton-Intensity before release})} \times 100$$

Cumulative percent release profile was plotted as a function of time.

4.2.7. Atomic force microscopic (AFM) imaging

A drop of polymersome solution was placed on top of a freshly cleaved mica surface. The surface was evenly coated with the polymersomes using spin coater at 2000 rpm and then dried. The AFM imaging was carried out in non-contact mode at a scanning rate of 0.7 Hz and a resonance frequency of 145 kHz using an NT-MDT NTEGRA (NT-MDT America, Tempe, AZ). The mica substrate was glued on top of a sapphire substrate, which is a sample holder, using Scotch double sided tape and cleaved with Scotch tape to obtain a debris-free and flat surface. The cantilever was made of silicon nitride and was 100 μm long. The scanning areas were 5 x 5 or 20 x 20 μm at the resolution of 512 or 1024 points per line, respectively. The images were flattened by a first order line correction and a first order plane subtraction to compensate a sample tilt.

4.2.8. Cell culture

The pancreatic cancer cell line BxPC-3 was purchased from American Type Culture Collection (Manassas, VA). The BxPC-3 cells were cultured in RPMI media (Hyclone) supplemented with 10% fetal bovine serum (Gibco) and 2% antibiotics (Corning). The cells were grown at 37 ºC in a humidified atmosphere containing 5% CO_2 for normoxic conditions. Hypoxia was induced in the cells by culturing in Biospherix C21 hypoxic chamber supplemented with 1% oxygen.

4.2.9. Cell viability assay

Cytotoxicity of the gemcitabine and erlotinib encapsulated polymersomes was tested on BxPC-3 cells. The cells were incubated (2,000 per well) in a 96-well sterile plate. RPMI media supplemented with 10% FBS were added to each well (200 µL) and the cells were allowed to grow for one doubling time. The plate was divided into three groups: control, drug treated, and test polymersomes treated. The control polymersomes (Control P) were prepared using $PLLA_{5000}$-PEG_{2000} polymer (Polyscitech). This polymer has similar chain length for hydrophilic and hydrophobic portions as observed in the synthesized polymer, and can act as a good control in hypoxic conditions due to its non-responsiveness to hypoxic environment. Six replicates were recorded for each sample. The control group received buffer encapsulated polymersomes. Polymersomes prepared for treatment were prepared in iso-osmolar buffer with the cell culture medium to avoid premature leakage from the polymeric vesicles. Drug-treated cells received the gemcitabine (20 µM)-erlotinib (7.5 ± 1 µM) solution equivalent to the encapsulated drug concentration. Test polymersomes treated cells received an equivalent amount of encapsulated gemcitabine (20 µM) and erlotinib (7.5 ± 1 µM). The cells were treated for 3 days, and cell toxicity was recorded after 72 hours with the Alamar Blue assay by following the supplier's (Life Technologies) protocol. Alamar Blue solution (10 µL) was added to all the wells and incubated for 2 hours. Fluorescence was recorded (excitation/emission wavelength: 585/615 nm) for cytotoxicity calculation. The viability was determined for the normoxic and the hypoxic BxPC-3 cells.

4.2.10. Cellular uptake

The BxPC-3 cells were seeded (5,000 per well) on two 6 well plates. The cells in one plate were allowed to grow in a normoxic environment, and the other was incubated in the hypoxic

chamber maintained at 1% oxygen level. The cells cultured in both the plates were allowed to grow for two doubling times. Cells in both the plates were treated with carboxyfluorescein encapsulated polymersomes for 1, 2 and 3 hours under normoxic or hypoxic conditions. The uptake of carboxyfluorescein encapsulated polymersomes, and the released dye was observed by fluorescence microscopy. Images were analyzed by ImageJ software.

4.2.11. Cell viability in spheroidal cultures

The BxPC-3 cells were cultured as three-dimensional spheroids on agarose molds. Briefly, purchased mold (#24-35, Microtissues) was used to cast a 35 well agarose scaffold. Scaffolds were seeded with BxPC-3 cells (10,000 cells per scaffold) and were incubated at 37 °C in a CO_2 incubator for 5 days. As the spheroids are formed, the scaffolds were divided into two groups (18 scaffolds in each group). One group was incubated in a normoxic environment (supplemented with 21% oxygen, 37 °C), and the other group was incubated in a hypoxic environment (supplemented with 1% oxygen, 37 °C). After 3 days of incubation, the spheroids were treated with the control polymersomes (encapsulating buffer), gemcitabine and erlotinib combination (concentrations equivalent to test polymersomes), and polymersomes encapsulating gemcitabine and erlotinib (20 µM gemcitabine and 7.5 ± 1 µM erlotinib). The cells received treatment for 3 days under normoxic or hypoxic conditions. To measure the cell viability after the treatment, the spheroids were dislodged from the scaffolds with centrifugation (1000 g, 37°C), and treated in 15 mL centrifuge tubes containing 3 mL of Tryple (recombinant trypsin). The tubes were then incubated at 37 °C for 20 minutes to allow dissociation of attached cells. The cells were then suspended in 10 mL culture media and plated on 6 wells of 96 well plate. Similarly, the cells from all scaffolds were collected and seeded in 96 well plates (n = 6 for each group). The cells were allowed to grow in a

CO_2 incubator at 37 °C for 24 hours. After the treatment, the Alamar Blue assay was carried out following manufacturer's protocol to estimate cell viability for each group.

4.3. Results and discussion

Polymersomes are more stable drug carriers compared to micelles and liposomes. The ratio of the hydrophilic and hydrophobic blocks of the amphiphilic polymers is critical for the formation of spherical, bilayer vesicles. [109] We synthesized the azobenzene linked polymer PLA_{80}-(AZB)-PEG_{47} (Scheme 4.1) and characterized by NMR spectroscopy. The azobenzene group linking the PEG and PLA act as the hypoxia responsive unit in the synthesized polymer.[89,110] The PEG groups on the surface of the polymersomes impart long circulating and passive targeting characteristics.[111] The amphiphilic nature of the polymersomes allows encapsulation of hydrophilic drugs in the aqueous core and hydrophobic drugs in the membrane. Since the polymer molecules in the bilayer do not flip-flop, the structures are considerably more stable compared to the liposomes.[49,48] However, under reducing hypoxic conditions, the azobenzene linker undergoes reduction (mechanism shown in Figure 4.2) and disrupts the polymer membrane, allowing the release of encapsulated drugs.[94]

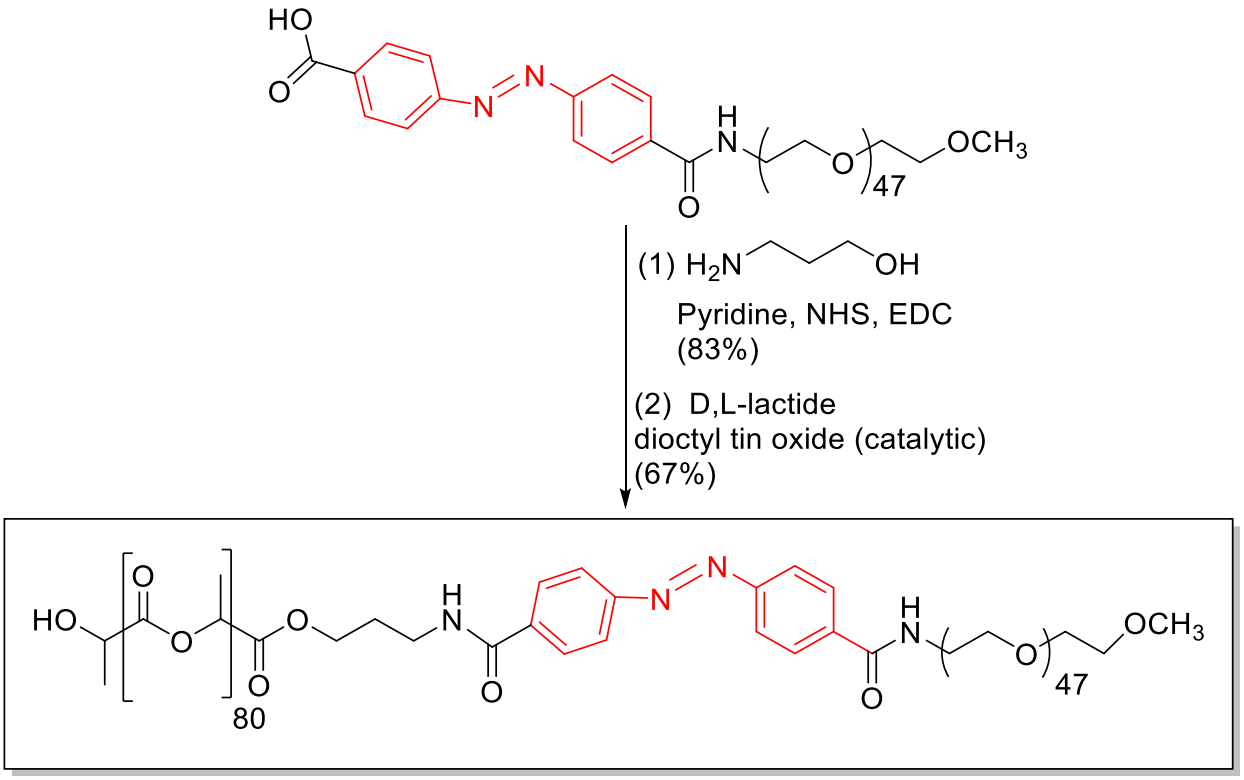

Scheme 4.1. Synthesis of the azobenzene incorporated, hypoxia-responsive polymer. The hypoxia-responsive unit is shown in red.

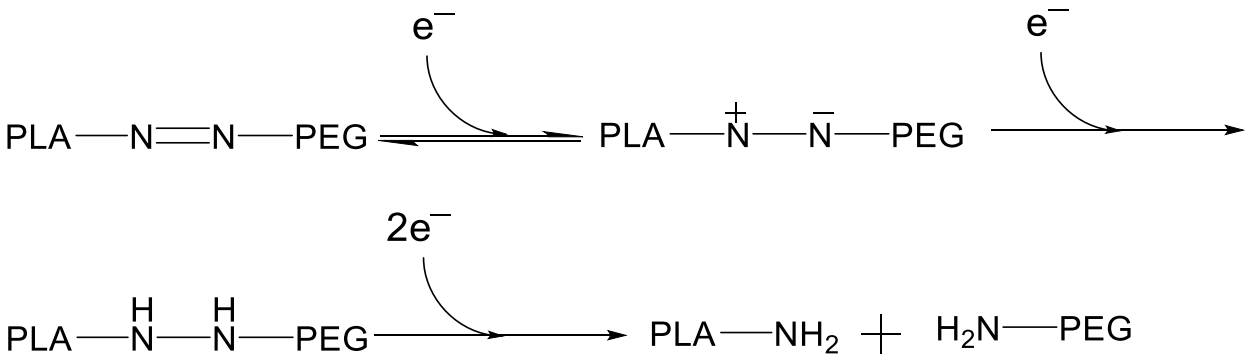

Figure 4.2. The proposed mechanism of azobenzene reduction in hypoxic, reducing environment.[94]

The polymersomes were prepared using the synthesized, hypoxia-responsive polymer by the solvent exchange method (Materials and Methods).[112] The size of the gel-filtered

polymersomes was observed to be (83 ± 2) nm with a polydispersity index (PDI) of 0.3 (by dynamic light scattering). A typical size distribution for the polymersomes is shown in Figure 4.3. Encapsulation of a dye or the two drugs increased the size of the polymersomes to (262 ± 30) nm. The polydispersity index (PDI) for all the batches was observed to be less than 0.4. (Table 4.1)

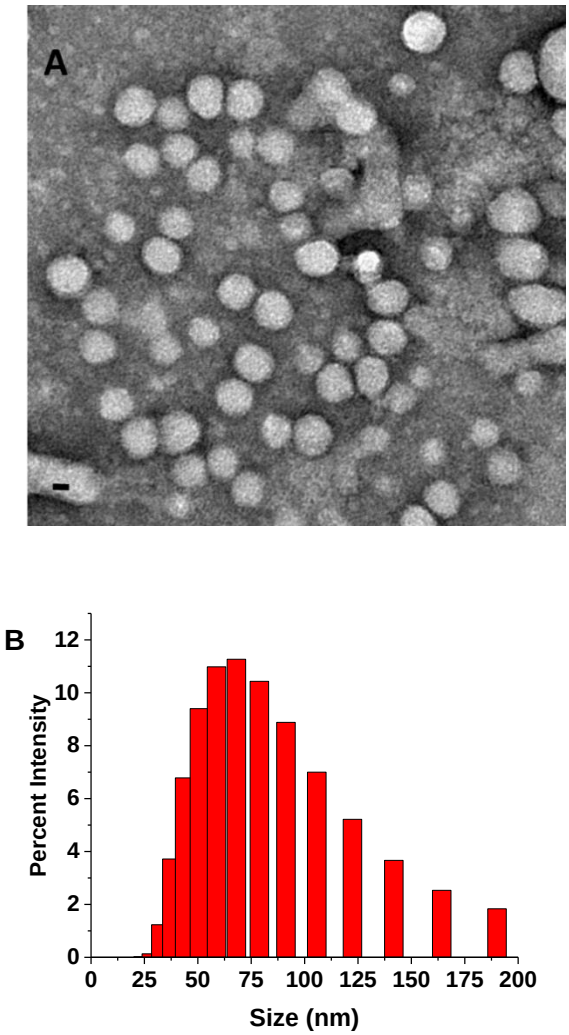

Figure 4.3. Transmission electron microscopic (TEM) image of polymersomes (scale bar: 20 nm) (A) and the size distribution profile by DLS (B).

Table 4.1. The hydrodynamic diameters and the PDI for polymersome formulations determined by DLS.

Formulation	Average diameter (nm) ± Std. dev.	PDI ± Std. dev.
Buffer encapsulated polymersomes	83.6 ± 1.9	0.30 ± 0.02
Carboxyfluorescein encapsulated polymersomes	136.4 ± 1.1	0.25 ± 0.03
Drug encapsulated polymersomes	262.6 ± 30	0.35 ± 0.06

To test the stimuli responsiveness of azobenzene incorporated polymersomes, a self-quenching dye (carboxyfluorescein) was encapsulated. Under hypoxia, the polymersomes released 90% of the encapsulated dye within 50 minutes (Figure 4.4, green squares). No significant release was observed from these vesicles under normoxic conditions (Figure 4.4, red circles).

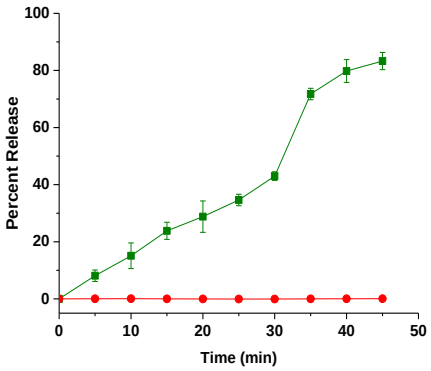

Figure 4.4. Cumulative release of encapsulated carboxyfluorescein from polymersomes under normoxic (red circles) and hypoxic conditions (green squares). The lines connecting the data points are also shown (N = 3).

Atomic force microscopy indicated that the polymersomes lost their spherical morphology after 1 hour under hypoxia (Figure 4.5A and B). The treated sample showed irregular shapes – showing the disintegration of the vesicle structures (Figure 4.5B). We also observed (by dynamic light scattering) a reduction in the hydrodynamic diameter of the polymersomes (from 90 nm to 55 nm) and an increase in the polydispersity index (from 0.3 to 0.7) under hypoxia.

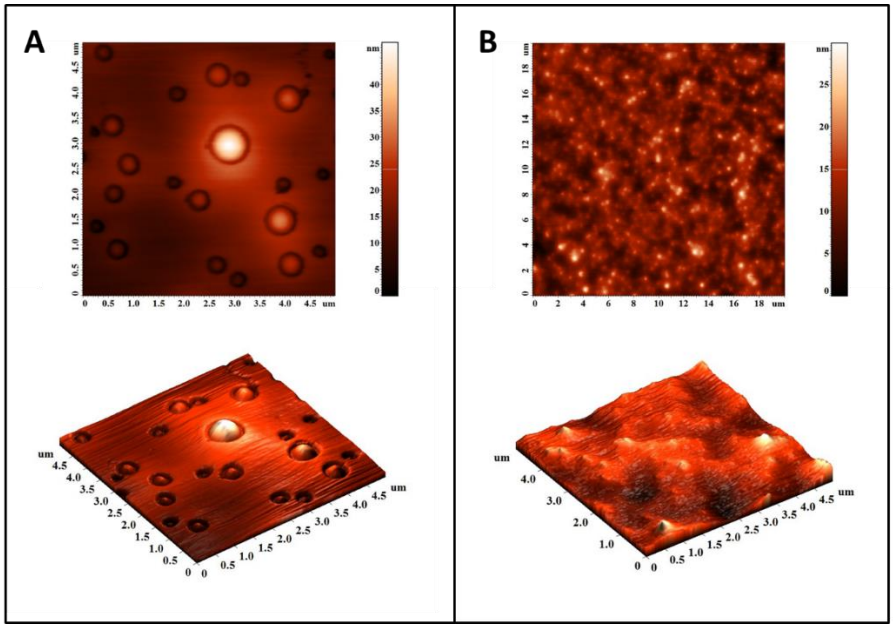

Figure 4.5. Atomic force microscopic images of the polymersomes under normoxic (A) and hypoxic conditions (B).

To demonstrate the content release in biological systems, we incubated the BxPC-3 cells with the dye-encapsulated polymersomes in a hypoxia chamber supplemented with 1% oxygen. Although we seeded an equal number of cells in the hypoxic and normoxic (control) plates for imaging, we observed changes in cell morphology in the presence of 1% oxygen. Hence, we normalized the fluorescence of the images with respect to the number of cells. We analyzed the images by the ImageJ software and calculated the integral density per unit area of the two treatment

groups. We observed the significantly higher amount of released dye in the hypoxic cells after 3 hours (Figure 4.6).

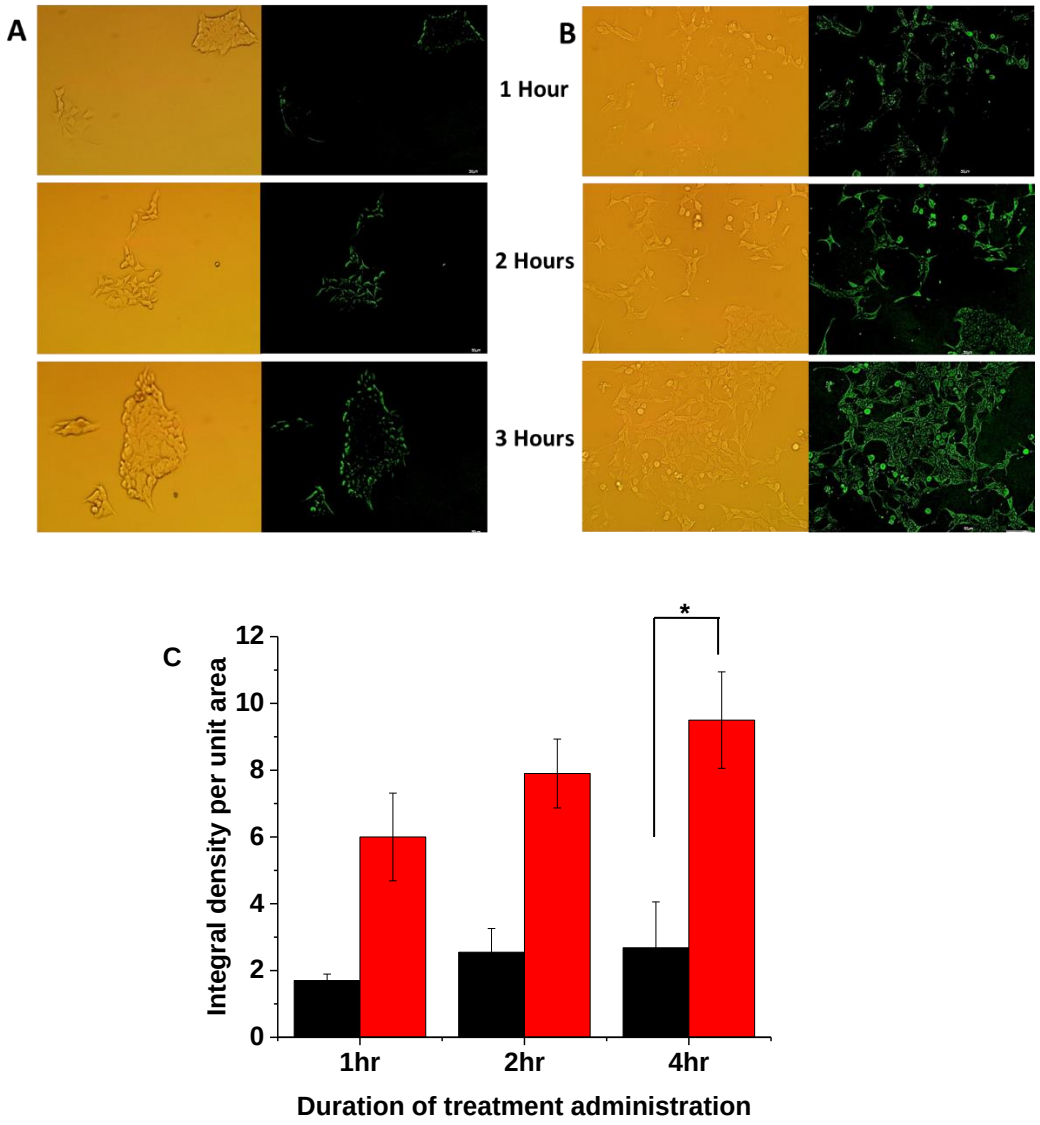

Figure 4.6. Confocal fluorescence microscopic images of the BxPC-3 cells incubated with carboxyfluorescein-encapsulated polymersomes under normoxic (Panel A) and hypoxic (Panel B) for 1, 2 and 3 hours. (C) Quantitative fluorescence integral density for the images shown in Panels A and B indicating uptake in cells cultured under normoxic (black) and hypoxic (red) conditions ($N = 3$, $*p < 0.05$).

After confirming the hypoxia-triggered release from the polymersomes, we proceeded to encapsulate the anticancer drugs gemcitabine and erlotinib using a combination of solvent exchange and pH-gradient methods.[113,82] Gemcitabine and erlotinib were encapsulated with 40 ± 6% and 28 ± 8% entrapment efficiency, respectively. The amount of gemcitabine and erlotinib encapsulated were 100 ± 15 μg and 60 ± 16 μg per mg of the polymer, respectively. For the cellular experiments, the treatment was determined based on the concentration of gemcitabine, as erlotinib is used as an adjuvant to enhance the overall effectiveness of therapy.[105] The buffer-encapsulated polymersomes showed more than 90% cell viability in monolayer as well as in spheroidal cultures of the BxPC-3 cells – indicating nontoxic nature of the drug carrier (Figure 4.7).

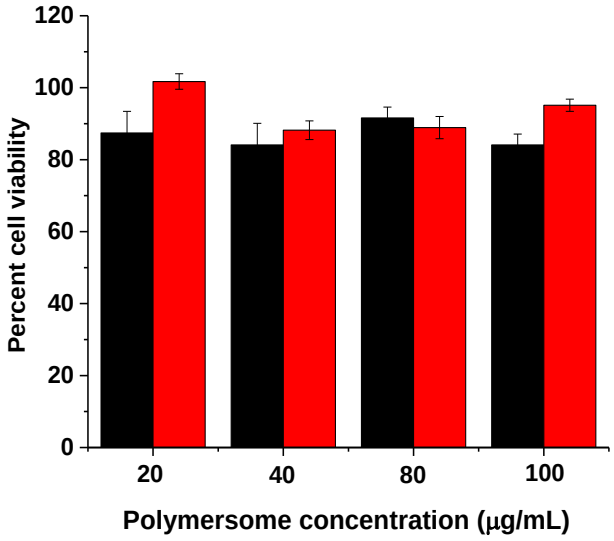

Figure 4.7. The viability of the BxPC-3 cells with polymersomes encapsulating phosphate buffer (pH = 7.4) under hypoxic (black bars) and normoxic (red bar) conditions (N = 4).

Subsequently, we treated the BxPC-3 cells with drug encapsulated polymersomes for 72 hours. The unencapsulated gemcitabine and erlotinib and polymersomes devoid of hypoxia-

responsive polymers were used as the controls. In normoxic monolayer cultures, treatment with the gemcitabine and erlotinib resulted in 38 ± 3% cell viability (Figure 4.8A). Under hypoxic conditions, the cell viability was more (58 ± 5%) showing that treatment was relatively less effective than under normoxic conditions. When the cells were treated with control polymersomes devoid of hypoxia treatment, cell viability was observed to be 65% under normoxic conditions and 71% under hypoxic conditions. We speculate that the decreased cell viability is a result of diffused drug in the cell culture media over the period of 72 hours. Treatment with hypoxia responsive polymersomes resulted in decrease in the cell viability to 59% under hypoxic conditions and 41% in normoxic conditions. Indicating significantly similar cell viability as observed with the free drug combination.

Although the monolayer cultures provide valuable information about the cellular function and viability, it does not simulate the three-dimensional architecture of the tumor tissues. To create a better mimic for the tumors, we cultured the BxPC-3 cells as three-dimensional spheroids in agar molds.[114,97] Spheroidal cultures also show presence of hypoxic cells in the core as observed in the solid tissues.[115,116] Hence, spheroids are better models for carrying out hypoxia responsive drug delivery studies *in-vitro*. The 15-day old spheroids were then treated with the polymersomes, analogous to the monolayer cultures (Figure 4.8B). The results indicated that cell viability was significantly reduced when the spheroids were treated with drug encapsulated polymersomes. The cell viability under normoxic conditions was unaffected by the hypoxia responsive polymersomes (black columns in Figures 4.8A and 4.8B, **Control P** and **Test P** groups). However, the cell viability for the hypoxic spheroids was substantially decreased (24 ± 4%) in the presence of the polymersome encapsulated drugs as compared to the free drugs (48 ± 2%). These results (Figure 4.8B) further confirmed hypoxia responsive characteristics of the polymersomes. We observed

that the cell viability was significantly reduced in spheroidal cultures as compared to monolayer cultures. We also observed 1.5X reduction in cell viability in spheroids treated with drugs encapsulated hypoxia responsive polymersomes as compared to free drug combination. We speculate that this difference may be due to the release of drug in hypoxic core of the spheroids.

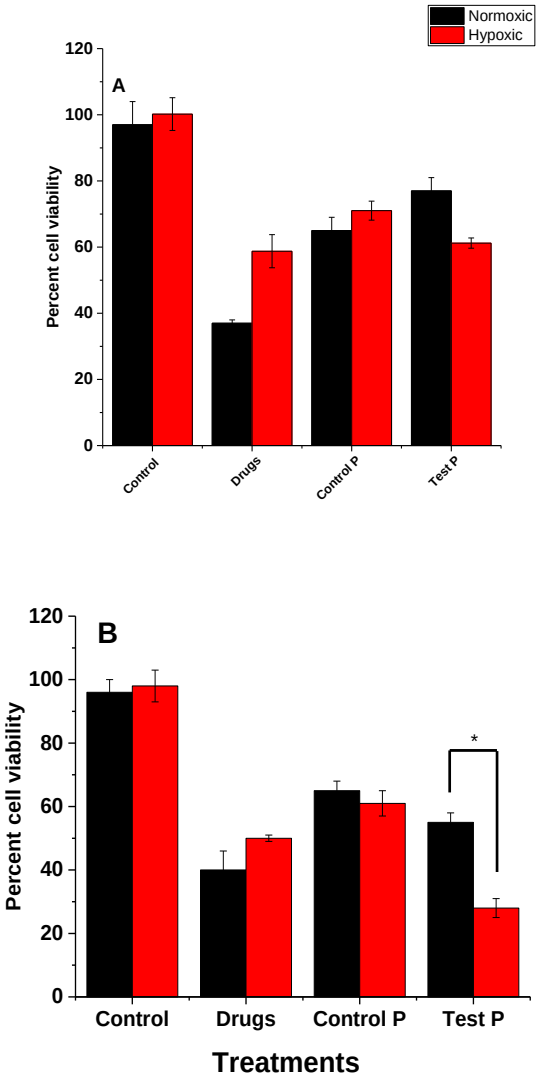

Figure 4.8. The viability of the BxPC-3 cells in monolayer (A) and spheroidal (B) cultures after treatment with the anticancer drugs (Drugs), drug encapsulated polymersomes without the hypoxia-responsive polymer (Control P), and the hypoxia-responsive vesicles (Test P) under normoxic (black bars) and hypoxic (red bars) conditions (N = 6, * $P < 0.05$).

4.4. Conclusion

In conclusion, our synthesized azobenzene incorporated, amphiphilic, PLA-PEG polymer self-assembled into polymeric vesicles. The polymersomes encapsulated the anticancer drugs gemcitabine and erlotinib with loading efficacy of 40 ± 6% and 28 ± 8% respectively. These polymersomes successfully released the encapsulated drugs to hypoxic pancreatic cancer cells, resulting in reduced cell viability in both monolayer and spheroidal cultures. Due to the presence of hypoxia-responsive subunit in these polymersomes, the vesicles can be used to image and deliver drugs to the hypoxic regions the tumors.

5. HYPOXIA RESPONSIVE ECHOGENIC POLYMERSOMES FOR DRUG DELIVERY TO HYPOXIC PANCREATIC CANCER CELLS[4]

5.1. Introduction

Hypoxia or lower oxygen concentrations are observed in solid tumor tissues.[93] The high interstitial fluidic pressures and irregular blood flow lead to hypoxic regions in the tumor tissues and help the progression of disease.[117] Cancers of breast, pancreas, cervix, rectum, head and neck show hypoxic zones in the solid tumors making them difficult to treat. [118] Clinical studies demonstrated resistance to chemo and radiotherapy in patients with hypoxic solid tumors. [119]

Cancer cells divide rapidly in the tumor tissues, but the blood vessels supplying nutrition to these cells grow at a relatively slower rate resulting in the development of hypoxic zones in oxygen deprived tumor tissue[120]. Hypoxic zones further assist in the remodeling of tumor extracellular matrix.[121] The overall remodeling of tumor extracellular matrix leads to changes in biochemical makeup at the tumor site which then allows tumor progress.[122]

The distinct biochemical changes at the tumor environment can be used as triggers for activating internal stimuli responsive drug delivery carriers and deliver drugs selectively at the tumor site.[79] Internal stimuli responsive nanoparticles interact with the biochemical environment around them and undergo chemical changes to weaken the barrier between the encapsulated drug and cancer cells leading to efficient drug delivery.[79] Biochemical triggers such as increased matrix

[4] This section is coauthored by Prajakta Kulkarni, Manas Haldar, Rayat Hossain, Matthew Confeld, Kara Gange, Lang Xia, Kaushik Sarkar, Sanku Mallik. Prajakta had primary responsibility to conduct all the experiments listed in the section, analyze the data and write the manuscript. Manas synthesized the hypoxia responsive polymer. Rayat and Matthew assisted in cellular studies. Dr. Gange, Lang and Dr. Sarkar were involved in ultrasound imaging studies. Dr. Mallik verified the data and edited the manuscript for publication.

metalloproteinase enzyme, glutathione, decreased pH have demonstrated effective ways to deliver the drug.[123] PEGylation of nanoparticles imparts long circulating characteristics to nanoparticles allowing passive targeting to the solid tumors.[124] PEGylated nanoparticles circulate through blood stream with minimal interaction with the reticuloendothelial system, and extravasate into the tumor tissues through leaky vasculature developed at the tumor site.[36] Stimuli responsive drug carriers experience biochemical changes in the surroundings and release the encapsulated drugs in tumor tissues in response to the biochemical surroundings. Internal stimuli responsive nanoparticles have been developed to release the drug in response to hallmarks of cancer such as lowered extracellular tumor pH, increased proteolytic enzymes in tumor extracellular matrix and increased levels of glutathione.[125] Although there are various stimuli responsive nanocarriers, hypoxia responsive drug delivery systems are less explored. Nanoparticles incorporating hypoxia responsive nitroimidazole derivative have demonstrated the ability to image and deliver drugs to hypoxic tumor tissues.[24] Azobenzene is another molecule that can undergo reduction in the reducing environment developed in the hypoxic tumors. Reduction of azobenzene group is a multi-step process in which the azo group is reduced to amine in a stepwise manner in oxygen-deprived conditions.[94] Azobenzene was used as a hypoxia responsive unit in micelles to release the drug under hypoxic conditions *in-vitro* and *in-vivo*.[89] Hypoxic regions are usually located far away from the source of nutrition.[126] PEGylated drug carriers extravasate through leaky vasculature developed in the tumor tissue.[127] However, reaching the hypoxic regions requires a further targeting or tissue penetrating capabilities.[128]

Cyclic peptide iRGD is known for its tissue-penetrating properties.[96] Nanoparticles conjugated to iRGD peptide have been observed to penetrate deep into the tumor tissue, and deliver the drug *in-vivo*.[129] It was observed in an *in-vivo* study, that chemotherapeutic drugs showed better

efficacy when co-administered with peptide iRGD.[130] Peptide iRGD has been conjugated to nanocarriers to improve tissue penetration and overall efficacy of the treatment.[130]

Echogenic nanoparticles allow imaging of the nanoparticles as they deliver the encapsulated drug at the targeted site.[131] In our previous studies, we have tested an azobenzene linked PLA-PEG polymer for its ability to form polymersomes and undergo reduction under hypoxic conditions. We hypothesize that azobenzene incorporated, iRGD functionalized, PEGylated polymersomes will penetrate deep inside tumor tissue to reach hypoxic regions of the tumor. In the hypoxic environment, azobenzene incorporated in polymersome membrane will undergo reduction and will destabilize the membrane integrity. Membrane destabilization further leads to the release of the encapsulated hydrophilic contents in the hypoxic tumor cells causing cytotoxic effects. We prepared azobenzene incorporated PLA-PEG polymer and blended it with peptide iRGD conjugated PLA-PEG polymer to form polymersomes by solvent exchange method. An anti-cancer drug, gemcitabine was encapsulated in the polymersomes. Pancreatic cancer cells BxPC-3 were cultured in the hypoxic and normoxic environment for testing hypoxia responsive characteristics of the prepared polymersomes. We observed the cell viability after the treatment with these polymersomes in monolayer and spheroidal cultures of pancreatic cancer cells BxPC-3. The depth of penetration assisted by iRGD peptide was evaluated in the layered cultures of BxPC-3 cells.

5.2. Materials and methods

5.2.1. Hypoxia responsive polymer

Hypoxia responsive azobenzene incorporated polymer was synthesized in our lab (Scheme 4.1). The polymer was characterized using NMR spectroscopy and GPC. (Figure C2, Figure C3)

5.2.2. Synthesis of hexynoic acid conjugated iRGD peptide

The peptide was synthesized using a microwave assisted, solid phase peptide synthesizer on a Rink amide resin (0.200 g, 0.1 mmol/g). The scale of synthesis was 0.1 mmol/g with amino acid sequence Hexynoic acid - Cys(Acm)-Arg(Pbf)-Gly-Asp(OBut)-Lys(Boc)-Gly-Pro-Asp(OBu^t)-Cys(Acm)-NH_2. Subsequently, a solution of thallium trifluoroacetate (55 mg, 0.1 mmol) in DMF (5 mL) was added, and the resulting resin was stirred for 3 hours. The resin was washed with DMF (3X), dichloromethane (3X), and then dried. The peptide was then cleaved from the resin by reacting with trifluoroacetic acid (19 mL), and distilled water (0.5 mL) for 3 hours. The resin was separated by filtering the solution through a Whatman filter paper. To the filtrate, 15 mL of cold diethyl ether was added, and the obtained precipitate was dried in a vacuum desiccator. The peptide was further analyzed by MALDI mass spectrometry and CD spectroscopy. (Figure B2)

5.2.3. Synthesis of PLA-PEG-N_3

Azide terminated PEG derivative (MW 2000, 400 mg) was taken into toluene (40 mL), and azeotropic distillation was performed for 6 hrs under nitrogen. Upon cooling the reaction mixture D, L- lactide (1400 mg) and tin (II) ethoxyhexanoate (20 mg) were added and refluxed for 14 hours. The pure polymer was isolated by precipitation in ice-cold ether and drying under vacuum (yield- 1.2 g, 67%). NMR: 1.48- 1.56 (m, 275 H), 3.6 (s, 172 H), 5.2-5.4 (m, 95 H).

5.2.4. Conjugation of iRGD peptide to PLA-PEG polymer

The polymer PLA-PEG-N_3(50mg) was ‘clicked’ with an excess of hexynoic acid conjugated iRGD peptide(8mg). The azide conjugated PLA-PEG polymer was dissolved in 3mL THF and added to aqueous solution of the iRGD peptide (3mg dissolved in 3mL of water). The copper catalyst was prepared by mixing the powder of copper (II) sulfate (72mg) with solution of

N,N,N', N', N''-Pentamethyldiethylenetriamine(PMDETA)(0.2mL) in water(3mL). The mixture was stirred for 2 hours at room temperature. The ascorbic acid solution was prepared in water. The copper catalyst (0.053M $CuSO_4$ solution in water and 2mmol PMDETA stirred for 2 hours) and sodium ascorbate (1.4 µmol) were added to the reaction mixture and stirred for 24 hours at room temperature. The sample was transferred to a dialysis cassette with a molecular cut-off of 3000. The reaction mixture was dialyzed against water for 72 hours to remove the catalyst and unreacted iRGD peptide. The product was then analyzed by CD spectroscopy.

5.2.5. Preparation of carboxyfluorescein encapsulated polymersomes

Hypoxia responsive polymer PLA_{5700}-Azobenzene-PEG_{2000} was dissolved in tetrahydrofuran to make 10mg/ml solution of the polymer. This solution was added dropwise to the stirring solution of carboxyfluorescein dye (100 mM) prepared in HEPES buffer (pH 7.4, 25 mM). After stirring the mixture for 1 hour, THF was evaporated by bubbling air through the mixture to form the carboxyfluorescein encapsulated polymersomes. Polymersomes were then sonicated for 1 hour. To remove the unencapsulated dye from the polymersomes, polymersome solution was subjected to overnight dialysis iso-osmolar HEPES buffer (pH 7.4, 25 mM), and were then passed through Sephadex G100 column to collect carboxyfluorescein encapsulated polymersomes.

5.2.6. Encapsulation of gemcitabine in polymersomes

Gemcitabine was encapsulated in polymersomes by the pH gradient method. Hypoxia responsive polymer and iRGD conjugated polymer were dissolved in THF to make 10 mg/mL stock solutions for each polymer. Lipid 1,2-dipalmitoyl-*sn*-glycero-3-phosphoethanolamine-N-lissamine rhodamine B sulfonyl ammonium salt (rhodamine lipid) was dissolved in chloroform to make a solution (0.01 mg/mL). To a vial, lissamine rhodamine lipid was added, and chloroform

was evaporated from the vial. To the same vial, hypoxia responsive polymer (2 mg, 200 µL), iRGD conjugated polymer (29 µg, 29 µL) were added. The molar ratio of the hypoxia responsive polymer, iRGD conjugated polymer and lissamine rhodamine lipid was maintained at 84:10:5:1 for drug encapsulated polymersomes. To prepare control formulation devoid of hypoxia responsive polymer, hypoxia responsive polymer was substituted with commercially available PLLA-PEG polymer (Polyscience). To prepare control formulation devoid of peptide iRGD, peptide conjugated polymer was substituted with the PLA_{5000}-PEG_{2000}-N3 polymer. In another vial, 2 mL citrate buffer (200 mM, pH 4) was added and was stirred. To a stirring buffer, polymer mixture in THF (200 µL) was added dropwise. The mixture was stirred at room temperature for 1 hour. The organic solvent was then evaporated by passing air through the mixture for 45 minutes. The solution was then sonicated using a bath sonicator (Aquasonic 250D, level 9) for 45 minutes, and kept at room temperature for 15 min. The size of the polymersomes was analyzed by differential light scattering (DLS). Un-encapsulated citrate buffer was neutralized with the addition of sodium bicarbonate solution (1mg, 100 µL of 10 mg/mL solution). Gemcitabine (0.4 mg of 1mg/mL aqueous solution) was added to the collected polymersomes to keep polymer: drug ratio - 5:1. The mixture was stirred for 4 hours to encapsulate gemcitabine by pH gradient developed across the polymersome membrane. To remove the unencapsulated gemcitabine, the polymersomes were again passed through Sephadex G100 column. The presence of gemcitabine was confirmed by UV spectrophotometric measurement at wavelength 269 nm. Percent entrapment and encapsulation efficiency of the polymersomes was calculated using following formula:

$$\text{Percent extrapment} = \frac{\text{gemcitabine before gel filtration (mg) - gemcitabine after gel filtration (mg)}}{\text{gemcitabine before gel filtration (mg)}} * 100$$

5.2.7. Preparation of echogenic polymersomes

Echogenic polymersomes were prepared by encapsulating mannitol (320 mM) in the polymersomes by solvent exchange method. To prepare gemcitabine encapsulated echogenic polymersomes, mannitol (320 mM) was incorporated in the citrate buffer (200 mM, pH 4). These polymersomes were then subjected to three freeze-thaw cycles and were freeze-dried to obtain a dry powder of polymersomes. To test the echogenicity, polymersomes were reconstituted in water to make 0.1 mg/mL solution.

5.2.8. Size analysis

Size analysis was carried out by dynamic light scattering (DLS using Malvern Zetasizer Nano-ZS90) and transmission electron microscopy (TEM). For DLS studies, Malvern zetasizer was used with disposable plastic cuvette. All the reported size analysis was performed on 1 mL of sample with six runs and six repeats. The size distribution was plotted taking size on x-axis and percent intensity on y- axis. Effect of hypoxia treatment on the size and morphology of polymersomes was studied by high-resolution TEM. Copper TEM grids (300-mesh, formvar-carbon coated, Electron Microscopy Sciences, Hatfield, Pennsylvania, USA) were prepared by applying a drop of 0.01% poly-L-lysine, allowing it to stand for 30 seconds, wicking off the liquid with torn filter paper, and allowing the grids to air dry. A drop of the suspension diluted 1:100 was placed on a prepared grid for 30 seconds and wicked off; grids were allowed to air dry again. Phosphotungstic acid 0.1%, pH adjusted to 7-8, was dropped onto the grid containing the sample, allowed to stand for 2 min, and wicked off. After the grids had been dry, images were obtained using a JEOL JEM-2100 LaB6 transmission electron microscope (JEOL USA, Peabody, Massachusetts) running at 200 keV. To observe the effect of hypoxia treatment on polymersomes, images were recorded before treatment and after 2 hours of hypoxia treatment (nitrogen gas was

bubbled through the mixture) in the presence of 100µM NADPH and 20µL of microsomes in a solution of 1mg/mL polymersomes.

5.2.9. Ultrasound scattering studies

5.2.9.1. Experimental setup to measure scattering

The scattering setup employed two spherically focused transducers with the same specifications (V310-SU, Olympus NDT), each having a central frequency of 5 MHz (Figure 5.1). The transmitting and receiving transducers were placed perpendicularly by two separate linear stages (433 series, 360-90, Newport) and immersed in a big water tank that was filled with DI water. A 20 mL cylindrical syringe was used as a sample chamber, in which polymersome suspension was filled. A function generator (Model AFG 3251; Tektronix) was utilized to generate a 32 cycle sinusoidal pulse of 5 MHz frequency at a PRF of 100Hz. This signal was then amplified using a 55dB power amplifier (Model A-300, ENI) and fed to the transmitting transducer. The polymersomes at the focal volume of the transducer scattered the input signal back which was received by the receiving transducer utilizing a pulser/receiver (DPR300, 475v, JSR) in through mode with a 40 dB gain. The amplified signals were then sent to an oscilloscope (TDS2012, Tektronix) to view them in real time. Voltage-time RF signals were averaged with every 64 sequences by the oscilloscope, and then they were transmitted and saved onto a desktop computer using the software Signal Express Tektronix Edition (version 2.5.1, Labview NI). For the data analysis of the scattered signals, 50 acquisitions in the averaging mode were saved.

5.2.9.2. Experimental procedure and data reduction

Polymersomes in the form of a dry powder were stored in the glass vial and placed in the refrigerator until ready for use. The scattering experiment was made by reconstituting the dry powder in phosphate buffered saline (PBS) solution for obtaining a concentration of 10 µg

polymer/mL PBS solution, and injecting 20 mL into the sample chamber. The measurement was repeated five times to guarantee the reliability of experimental data. The measurements for the control signal, i.e., without polymersomes and the response due to the polymersomes, were acquired as mentioned before. A customized FFT program for Matlab was used to get the average response in the frequency domain (50 voltage time acquisitions are used). The scattered response was converted into a dB scale by taking a unit reference. Fundamental, second and sub- harmonic scattered responses were extracted from the power spectrum. The final data is reported as an enhancement over the control.

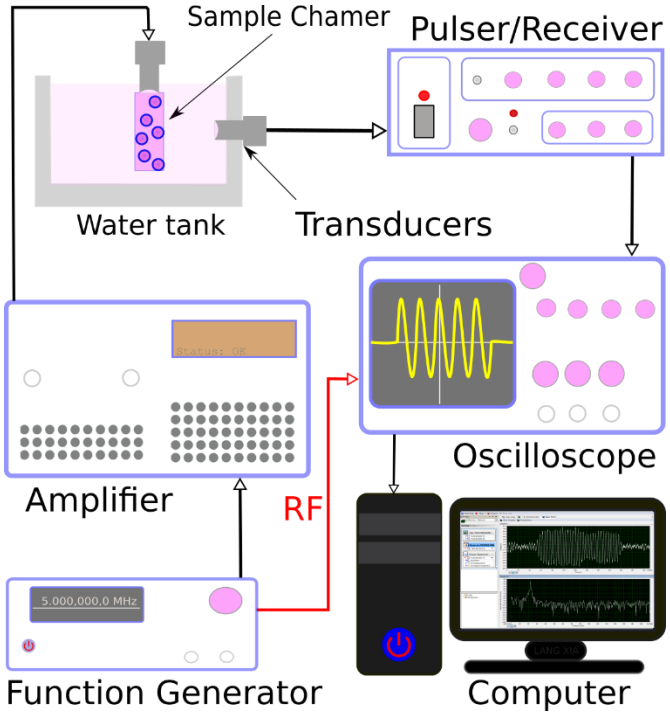

Figure 5.1. Experimental setup for measuring ultrasound scattering

5.2.10. Release studies

In a 6-dram glass vial, carboxyfluorescein encapsulated polymersomes (200 µL) were added to 1600 µL of iso-osmolar HEPES buffer (25 mM, pH 7.4). To this solution, 100 µL of rat

liver microsomes were added along with 100 µM NADPH. To observe the time-dependent release kinetics, polymersomes were subjected to treatment with normoxic and hypoxic treatment. The normoxic environment was created by bubbling air through the reaction mixture. Whereas, the hypoxic environment was created by bubbling nitrogen through the reaction mixture. Fluorescence (excitation wavelength: 480 nm, emission wavelength:515 nm) of released dye was measured every 15 minutes over a period of 2 hours. After exposure to hypoxic/normoxic conditions for 2 hours Triton (100µL) was added to disintegrate the polymersomes. The fluorescence emission intensity of disintegrated polymersomes after releasing all the fluorescent contents was considered as the was measured, and was used to calculate the cumulative percent release the encapsulated dye. The percent release was calculated using the following the formula and cumulative percent release profile was plotted as a function of time.

$$\text{Percent release} = \frac{(\text{Emission intensity after release-Intensity before release})}{(\text{Intensity after treatment with triton-Intensity before release})} \times 100$$

5.2.11. Cellular studies

Cellular studies were carried out with pancreatic cancer cell line BxPC-3 in RPMI media (supplemented with 10% FBS and 1% antibiotics). The cells were grown in monolayer and spheroidal cultures. Spheroids grown on 96 well agarose microwell plate were used for cell viability assay. To study the penetration ability of the polymersomes, BxPC-3 cells were grown as a layered culture on stacks of wet strengthened Whatman filter paper (number 114).

5.2.12. Ultrasound Imaging Methods/Instruments

A Terason t3200 diagnostic ultrasound (MediCorp LLC) instrument was used to image the echogenicity of polymersomes in the presence of normoxic and hypoxic cells. BxPC-3 cells were seeded on two 96 well plates (1000 cells per well) and were allowed to grow for one doubling time. One plate was incubated in a CO_2 incubator at 37˚C, while the other was incubated under

hypoxic conditions in hypoxic chamber supplemented with 1% oxygen. Cells in both the plates were treated with echogenic polymersomes (0.1 mg/mL), and cells were again incubated under normoxic and hypoxic conditions or 1 hour. A layer of Aquasonic 100 (Parker Laboratories) ultrasound gel was applied to a 16HL7 linear transducer (7-16 MHz; MediCorp, LLC). The transducer was placed over a 96 well plate that contained treated cells. The ultrasound scan properties were fixed at 0.6 mechanical index (MI), <0.4 thermal index, Omni Mean activated, level D image map, level 3 persistence, high frequency, TeraVision 2, 50 gain setting, dynamic range 64, 2 cm scan depth, and 37 Hz frame rate. The diagnostic ultrasound measured the amount of reflection from the solutions. A control group of cells did not receive treatment with polymersomes.

5.2.13. Cell viability studies in monolayer cultures

In a 96 well clear bottom plate, BxPC-3 cells (1000 each well) were seeded. Cells were allowed to attach to the surface and grow for 24 hours at 37°C in an incubator supplemented with 5% CO_2. Cells received treatment with iRGD conjugated hypoxia responsive polymersomes encapsulating gemcitabine (20 µM) for 72 hours. Polymersomes devoid of hypoxia responsive polymer (Control P1) and polymersomes without iRGD conjugation (Control P2) were used as controls. Gemcitabine (20µM) in aqueous solution was used as a positive control. After 72 hours of treatment, conditioned media was removed from the plate and was replaced with 180 µl media supplemented and 20 µl Alamar blue (Invitrogen). The plate was incubated in a CO_2 incubator at 37°C for 4 hours. After 4 hours, absorption was measured by spectrophotometer at 750 nm.

5.2.14. Cell viability study in 3-D cultures

BxPC-3 cell spheroids were prepared by seeding the 2x 10^6 cells in each 35 well agarose scaffold. To prepare agarose scaffold, agarose solution was prepared in water (2% W/V). This

solution was then sterilized using an autoclave for 45 minutes. A mold for spheroidal culture was purchased from Microtissues, and we prepared 35 well agarose scaffolds as per the manufacturer's protocol. The cells were seeded on 30 scaffolds and were incubated for seven days. The scaffolds were then divided equally into two groups (15 scaffolds per group). One group of the scaffold was allowed to grow under normoxic conditions, and another group was incubated in a hypoxic chamber maintained at an oxygen level of 1% (hypoxic conditions) for 24 hours. After establishing normoxic and hypoxic cultures, the scaffolds were treated with pure drug gemcitabine, gemcitabine encapsulating polymersomes devoid of hypoxia responsive polymer (Control P1), gemcitabine encapsulated hypoxia responsive polymersomes (Control P2), and gemcitabine encapsulated iRGD functionalized hypoxia responsive polymersomes (test). Treatment with encapsulating polymersomes was used as another control (Control). Scaffolds were divided equally into each of these treatment groups (3 scaffolds in each treatment group). Cell spheroids were treated under normoxic and hypoxic conditions with iso-osmolar polymersome formulations for 72 hours. After the treatment, cells in each spheroid scaffold were dissociated by using a recombinant Tryple solution (1mL for each scaffold). Cells were allowed to interact with Tryple for 10 min. Tryple was then removed from the surface of the scaffold. Scaffolds were then washed with 3mL of cell culture medium to harvest the cells. Cells harvested from each scaffold were then dissociated and plated directly in 6 wells of a 96 well plate. This step converted three-dimensional cell culture back to monolayer culture. It was crucial to keep the dilution of the cells exactly same for each treatment group in order to keep the relative ratios of cell viability in each treatment group. The cell viability was then measured by AlamarBlue assay.

5.2.15. Cellular uptake in layered cultures

To study the effect of the iRGD peptide on the depth of penetration *in-vitro*, we cultured BxPC-3 cells as layers rather than as a sphere. To grow layered cell culture, a stack of wet strengthened Whatman filter paper was used for ease of culturing and imaging the depth of penetration of this tissue penetrating polymersomes. Wet strengthened Whatman filter paper 114 was used for layered cell culture due to its desirable porosity, strength, and ability to be used as a cell culture scaffold.[132] We cut these papers as circles with 1-inch diameter using a commercially available punch. Papers were then wrapped in aluminum foil and were autoclaved for 45 minutes, and were then stored under UV lamp in a biosafety cabinet. To hold these papers in place, we designed an apparatus using CAD software Creo Parametric (Figure 5.2). The assembly was then 3-D printed using poly (lactic acid) as the material. The apparatus was designed to include four basic components- base container, paper stand, paper press attached to a media transfer tube and a lid.

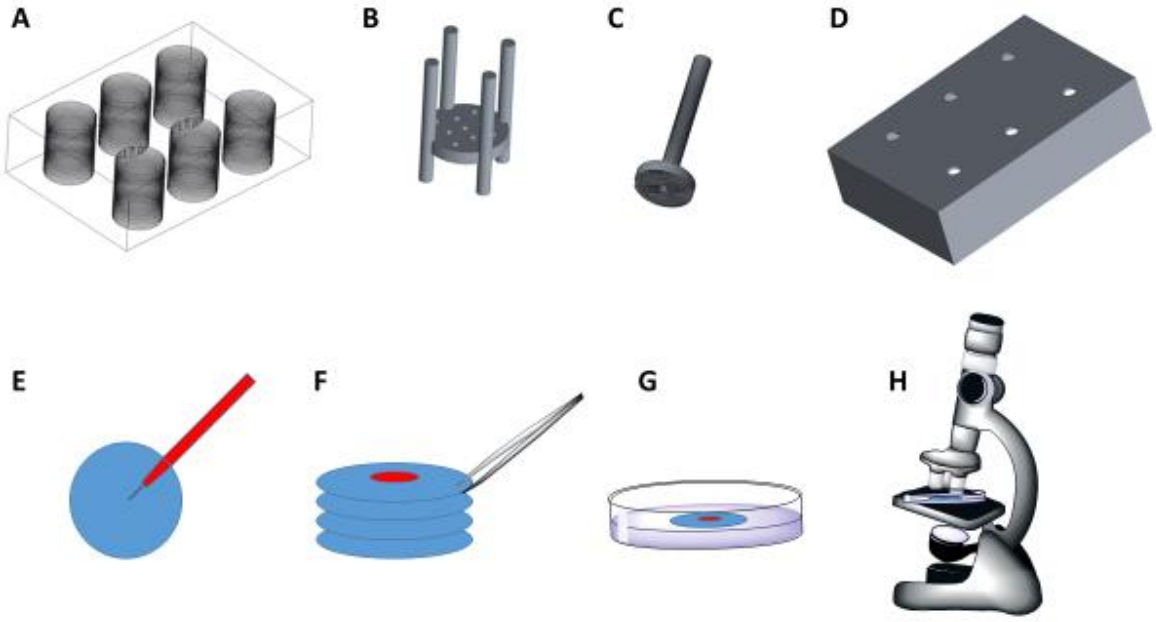

Figure 5.2. Cell culture apparatus six wells (A) in which a paper stack holder (B) was paced with a press on the top of the stack with a hollow tubing (C) enclosed by the cover (D). Whatman filter was inoculated with BxPC-3cells embedded in sodium alginate and agarose (E), and the filter papers were stacked together (F) and the stack was allowed to grow in the apparatus. For imaging, each stacked paper was separated (F) and placed in a clear glass bottom Petri plate (G) to image under laser scanning confocal microscope (H).

To culture the cells on paper, BxPC-3 cells were trypsinized, centrifuged and 100000 cells were suspended in 500µL cell culture medium. A solution of agarose and sodium alginate was prepared and autoclaved. This solution was allowed to cool to 40°C. Cells suspended in the media were added to agarose and sodium alginate solution (1:2). The cells were mixed well in the solution. The cell suspension (20µL) was then applied at the center of each paper. Layers of such papers were stacked together on the designed paper rack. Stacks (6) of 25 papers were prepared and assembled in the designed apparatus. The apparatus was then incubated under normoxic and hypoxic conditions for 8 days. After 8 days of incubation period, the cell stacks in received the treatments with 20µL of carboxyfluorescein encapsulated polymersomes with and without iRGD

functionalized polymersomes. Cell stacks were treated for 2 hours in respective incubation conditions (Normoxic/hypoxic). After 2 hours, paper racks were removed and were submerged in HBSS solution to wash excess of carboxyfluorescein. After washing the stacks three times, they were again submerged in cell culture medium before imaging. To image the cells with a confocal microscope, papers from the stack were peeled one at a time and fluorescence was measured in each paper layer. Fluorescence intensity and depth of penetration of polymersomes was measured after analyzing the images with ImageJ software.

5.3. Results and discussion

Azobenzene acts as a hypoxia responsive linker and undergoes reduction under hypoxic conditions in the presence of reducing environment.[110] We conjugated azobenzene linker to polymers PEG and PLA to yield a hypoxia responsive polymer (Figure 5.3A). The ratio of hydrophilicity to hydrophobicity in an amphiphilic polymer is critical for the formation of polymersome structure. We observed that the ratio of PEG to PLA was optimum for the formation of polymersomes (2:7). Spectra obtained from NMR spectroscopy and GPC chromatogram of the synthesized polymer confirmed the azobenzene conjugated polymer with PEG chain length with 2000 molecular weight and PLA with 5700.

Hexynoic acid conjugated to the peptide iRGD was synthesized using microwave assisted peptide synthesizer (liberty blue) (Figure 5.3B). The MALDI mass spectrum indicated the presence of the peptide (Expected mass: 1042.43, Observed mass: 1042.36). We conjugated this peptide to PLA-PEG-N_3 polymer by click chemistry employing copper complex as a catalyst (Figure 5.3 C). The obtained product was analyzed by CD spectroscopy.

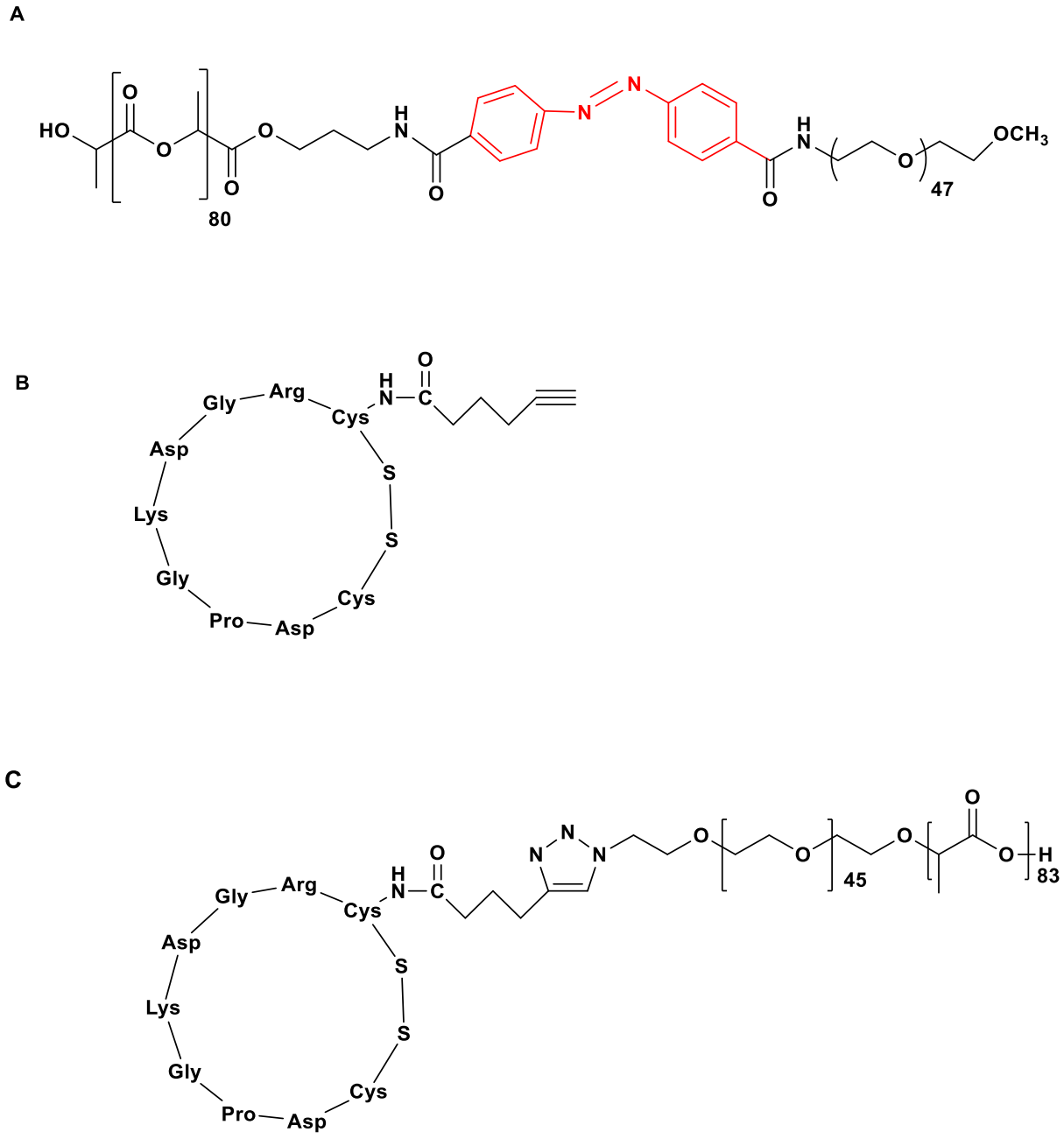

Figure 5.3. Structures for hypoxia responsive polymer (A), hexynoic acid conjugated iRGD peptide (B), and peptide iRGD conjugated PLA-PEG polymer (C).

We prepared tumor penetrating hypoxia responsive polymersomes by solvent exchange method. The polymer composition of the polymersomes was optimized by varying each component and testing it for its size and content release ability under hypoxic conditions. Targeting

polymer conjugated to cyclic peptide iRGD was 10 mol% of the polymer content in the optimized polymersome formulation yielding the final polymer composition as PLA-azobenzene-PEG - 90 mol%) and PLA-PEG-iRGD as 10 mol%. We observed that the polymersomes prepared by solvent exchange method were less than 200nm in size. Hypoxia treatment resulted in a reduction in size and increase in PDI value, indicating varied size distribution in the polymersomes (Figure 5.4, Table 5.1). To further investigate the changes in the polymersome membrane integrity, we imaged the polymersomes by TEM. TEM imaging indicated the spherical shape of the polymersomes under normoxic conditions. However, under hypoxic conditions, the polymersomes were disrupted indicating hypoxia responsive characteristics of the polymersomes. (Figure 5.5)

Table 5.1. Effect of hypoxia treatment on size of the polymersomes

Formulations encapsulating gemcitabine	**Size ± Std. dev.**	**PDI ± Std. dev.**
iRGD conjugated hypoxia responsive polymersomes before hypoxia treatment	178 ± 0.7	0.2 ± 0.02
iRGD conjugated polymersomes devoid of hypoxia responsive polymer before hypoxia treatment	96 ± 0.5	0.3 ± 0.02
iRGD conjugated hypoxia responsive polymersomes after hypoxia treatment	308 ± 60	0.7 ± 0.1
iRGD conjugated polymersomes devoid of hypoxia responsive polymer after hypoxia treatment	96 ± 4	0.4 ± 0.04

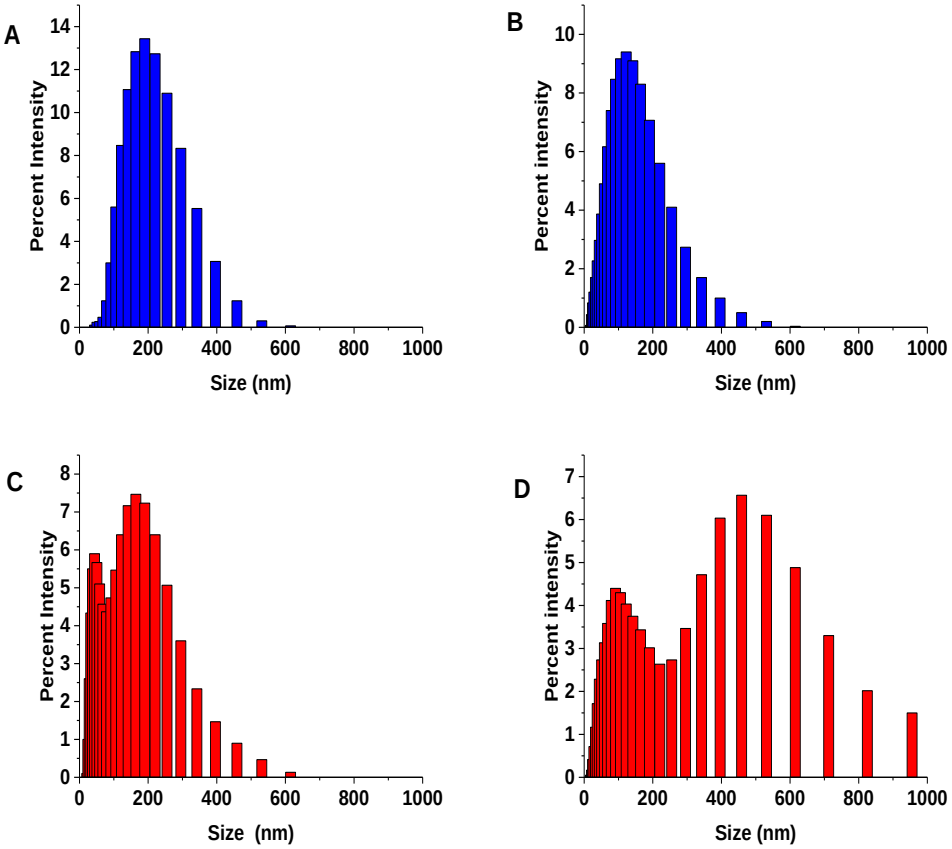

Figure 5.4. Size distribution profile for gemcitabine encapsulating iRGD conjugated polymersomes with (B, D) or without (A, C) hypoxia responsive polymer, after normoxic (blue) and hypoxic (red) treatment

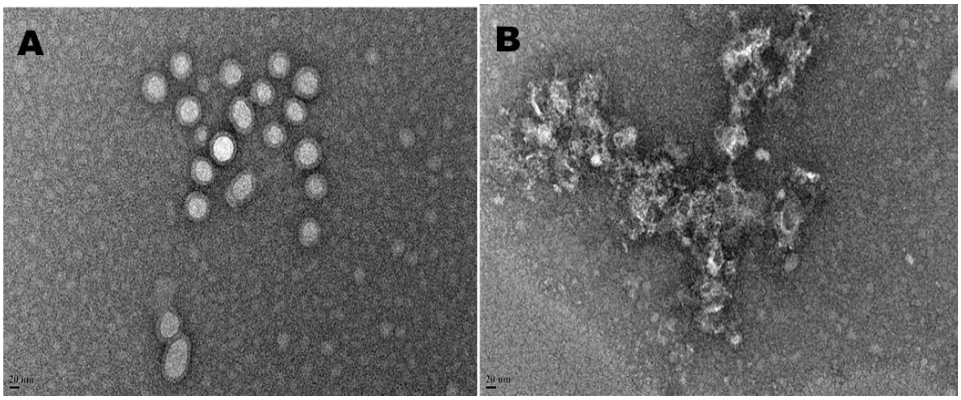

Figure 5.5. TEM images of polymersomes before (A) and after (B) hypoxia treatment.

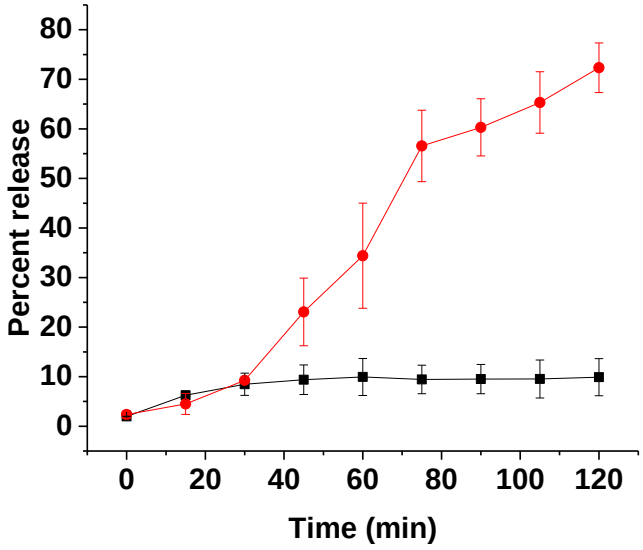

Figure 5.6. Release profile of the polymersomes after hypoxic (red) and normoxic treatment (black) in the presence of NADPH (100μM) and rat liver microsomes. (n=3)

The ability of the polymersomes to release encapsulated contents from the polymersomes under hypoxic conditions was studied by encapsulating a self-quenching dye carboxyfluorescein (100mM) in the polymersomes. The release of content was observed by fluorescence spectroscopy and the emission intensity was studied as a function of time (Figure 5.6). Polymersomes encapsulating carboxyfluorescein released 65-74% of the encapsulated dye after 2 hour exposure to hypoxic conditions in the presence of rat liver microsomes and NADPH (100 μM). Under normoxic conditions, the release of the dye from polymersomes was less than 10% indicating relative stability of the polymersomes in presence of oxygen. (Figure 5.6)

Echogenicity was induced in the polymersomes by encapsulating mannitol (320mM) in the polymersomes. We carried out 3 freeze and thaw cycles to incorporate bubble in the bilayer or the core. Entrapment of the air bubbles in the core or bilayer of the polymersomes allow imaging with diagnostic ultrasound imaging instrument. We freeze dried the polymersome solution and

reconstituted it with water for ultrasound imaging. Ultrasound images showed echogenicity concentrations as low as 0.1mg/ml.

To further study the echogenic characteristics and destruction threshold, we excited the polymersomes (0.1 mg/mL) with 100, 300, 500, 700, 1000 kPa excitation pressures. As it can be seen from Figure 5.7, the fundamental enhancement of polymersomes increased with increasing excitation pressures. The fundamental enhancement saturated at 700 kPa and decreased at 1000 kPa. This suggests possible destruction at the excitation pressure above 700 kPa.

We further analyzed echogenicity of the polymersomes at diagnostic ultrasound wavelengths. The reflection was observed in the polymersomes samples (0.1 mg/mL), but not in the control samples. Ultrasound contrast agents (microbubbles) exhibit stronger nonlinear response than the surrounding tissue, which is harnessed to improve contrast-to-tissue signal in medical ultrasound imaging such as harmonic imaging. However, harmonic imaging can often suffer from signal corruption due to nonlinear propagation effects in tissues and nonlinearity of the tissue itself at higher excitation amplitudes. Since subharmonic responses are unique to microbubbles and can be generated at relatively low excitation pressures, subharmonic imaging modalities are also being actively developed for potential clinical applications.

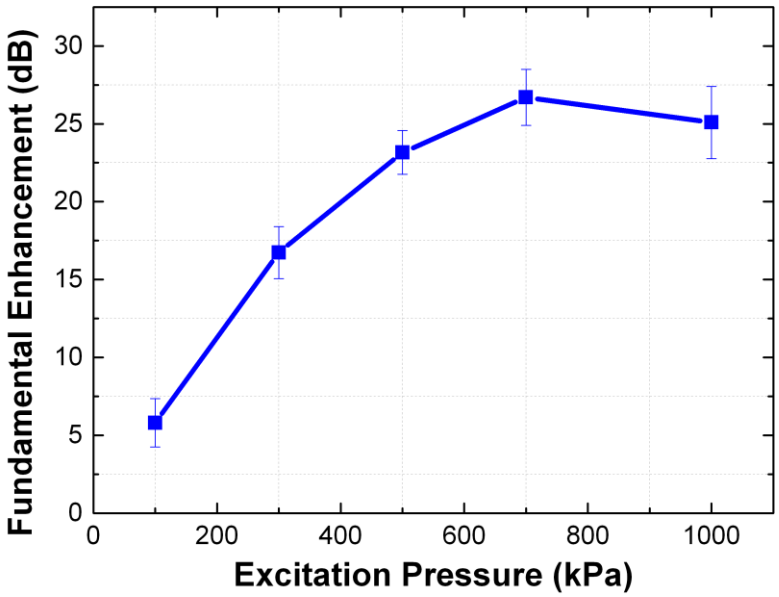

Figure 5.7. The subharmonic and second-harmonic enhancement of polymersomes are not prominent as compared to the fundamental response.

To observe the echogenicity in the cells, pancreatic cancer cells BxPC-3 were cultured under normoxic and hypoxic environment. Monolayer cultures of BxPC-3 cells were treated with echogenic polymersomes under hypoxia. We observed that after 1 hour of hypoxic treatment, polymersomes showed decreased gray scale value in the ultrasound images indicating decreased echogenicity. (Figure 5.8)

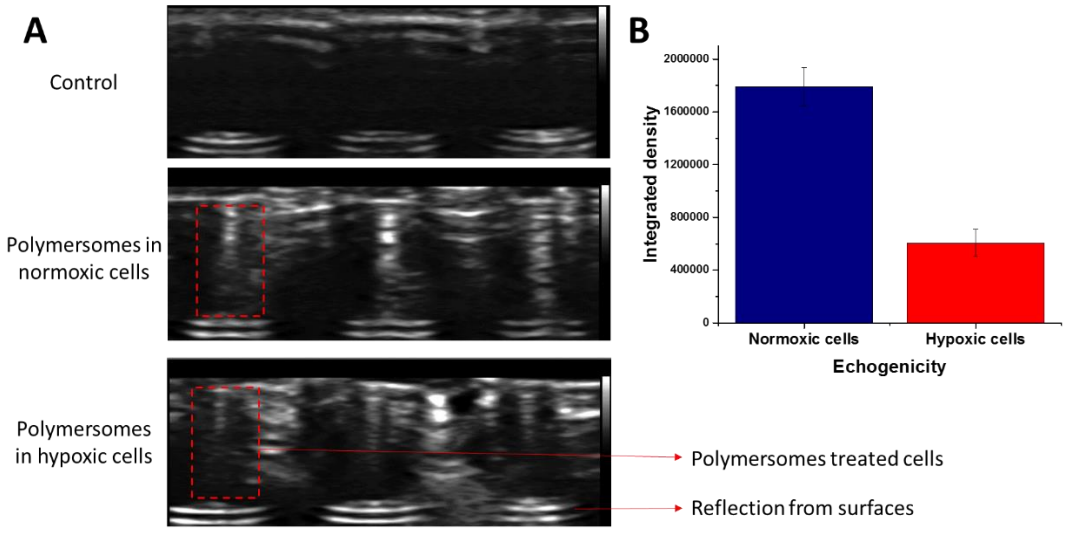

Figure 5.8. Ultrasound images of cells treated with polymersomes under normoxic and hypoxic conditions (A). Change in grayscale value observed by imageJ. (n=3) The gray scale value was reduced after the hypoxic treatment (B)

The images analyzed by imageJ showed a three-fold decrease in the echogenicity within 1 hour of hypoxia treatment suggesting disruption of polymer membrane and release of encapsulated contents after hypoxic exposure.

After confirming the echogenicity and stimuli responsiveness, we encapsulated cytotoxic drug gemcitabine in the polymersomes. The polymersomes entrapped up to 50% of the added gemcitabine by the pH gradient method. Peptide iRGD is also known for its anti-cancer and anti-metastatic properties.[133] Although we used a lower relative ratio of the peptide in the polymersomes, it was necessary to evaluate the cytotoxic nature of the drug carrier itself. We treated BxPC-3 cells with HBSS salt solution encapsulated polymersomes to observe the toxicity. We observed that after treatment with higher concentrations (100µg) of polymersomes, cell viability was as high as 80%. This indicated non-toxic nature of the polymersomes. (Figure 5.9)

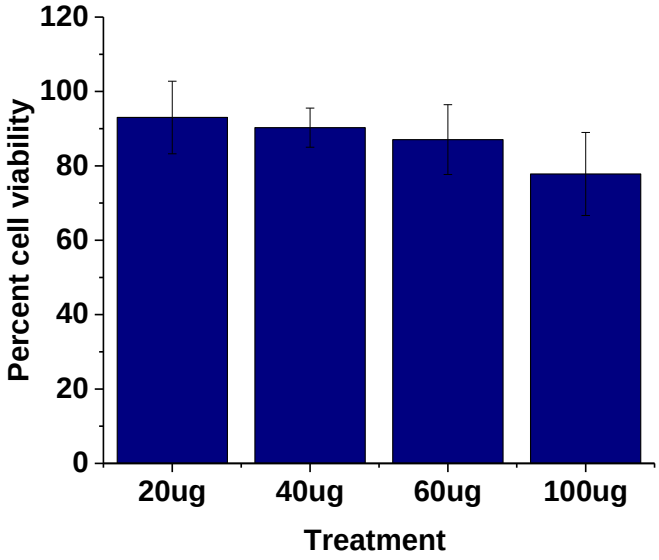

Figure 5.9. Cell viability after treatment with HBSS encapsulated 20µg, 40µg, 60µg and 100µg polymersomes

After confirming the safety of the drug carrier, we treated monolayer cultures of BxPC-3 cells with drug encapsulated test polymersomes (encapsulating 20 µM gemcitabine). Treatment with free drug gemcitabine (20 µM), and equimolar drug encapsulating polymersomes devoid of hypoxia responsive polymer (Control P1) and polymersomes without iRGD conjugation (Control P2) were used as controls. Additional negative control was used by encapsulating HBSS salt solution in the polymersomes.

Normoxic monolayer cultures indicated lowered cell viability as compared to that observed in the hypoxic cultures treated with gemcitabine. However, cells treated with drug encapsulating polymersomes showed higher cell viability indicating reduced drug release from the polymersomes under hypoxic conditions. We observed cell viability of 82% ± 5 in all normoxic BxPC-3 cell groups after the treatment with gemcitabine encapsulating control polymersome

formulations. This slight decrease in the cell viability may be due to leakage of gemcitabine in the cell culture media during the incubation period of 72 hours. (Figure 5.9A)

In hypoxic monolayer cultures of BxPC-3 cells, iRGD conjugated hypoxia responsive polymersomes showed a decrease in cell viability upto 25% which was significantly similar to the cytotoxicity observed after treatment with the free drug. Polymersomes devoid of hypoxia responsive polymer showed high cell viability which further confirmed stimuli responsive release of the drug from the polymersomes (Figure 5.9A).

In-vitro studies with monolayer cultures cannot give realistic predictions about the potency of the drugs.[134] Hence, three-dimensional cultures are better *in-vitro* models for testing efficacy and potency of drugs.[135] We cultured 3-D spheroids of BxPC-3 cells and treated them with test and control formulations

Although the less cytotoxic effect was observed in cells treated in normoxic monolayer cultures, spheroidal cultures grown in normoxic conditions showed a decrease in cell viability in the group of cells treated with hypoxia responsive polymersomes comprising hypoxia responsive polymer. Cell spheroids often exhibit hypoxia in the core.[135] We speculate that decrease in the cell viability under normoxic conditions may be due to iRGD assisted penetration and the hypoxia responsive release of the encapsulated drug in the core of spheroids.

Cell viability in spheroidal cultures indicated increased cytotoxic effect in the group of spheroids treated with iRGD functionalized drug carrying polymersomes (Figure 5.9B). We speculate that this increased cytotoxic effect was observed due to the ability of these polymersomes to penetrate deep inside the spheroids and gain access to more cells as compared to non-penetrating polymersomes.

To further confirm the iRGD assisted penetration depth, cell layers were cultured on the Whatman filter paper. When layered cultures were treated with the carboxyfluorescein encapsulating polymersomes, we observed that without iRGD, polymersomes penetrated 11 layers of the stacked cells. However, with surface functionalized iRGD peptide, polymersomes encapsulating carboxyfluorescein penetrated up to 18th layer indicating the ability to penetrate deep inside cellular layers (2.2 mm).

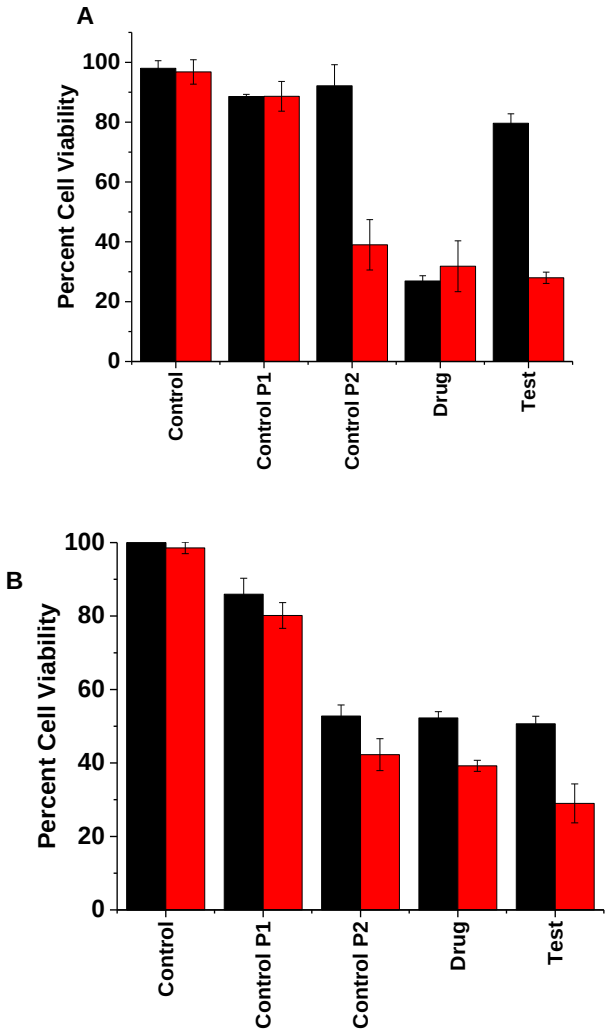

Figure 5.10. Cell viability in monolayer (A) and spheroidal (B) cultures of BxPC-3 cells after treatment with free drug gemcitabine, gemcitabine encapsulated control and test polymersomes under normoxic (Black) and hypoxic (Red) environment.

The depth of penetration of the iRGD conjugated polymersomes was tested in layered cell culture. We observed that polymersomes with iRGD functionalization penetrated deep inside the layers of cells as compared to polymersomes devoid of iRGD peptide (Figure 5.11).

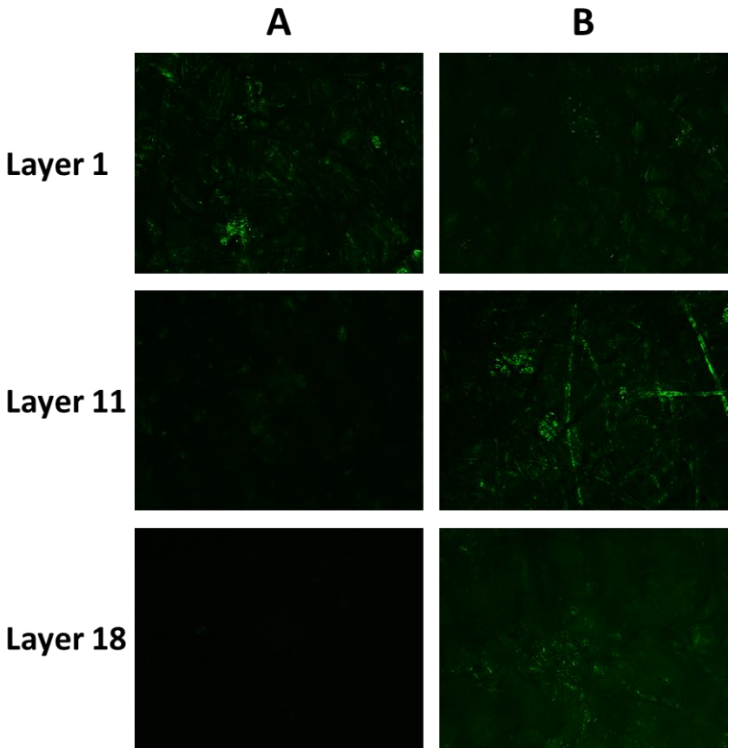

Figure 5.11. Depth of penetration of hypoxia responsive polymersomes before (A) and after (B) iRGD conjugation

5.4. Conclusion

Cyclic peptide iRGD functionalized hypoxia responsive polymersomes were prepared by solvent exchange method. These polymersomes significantly improved the depth of penetration while decreasing cell viability under hypoxic conditions. These polymersomes were observed to be echogenic in ultrasound imaging. These polymersomes, due to their echogenic and hypoxia responsive characteristics, can be used for imaging of hypoxia and deliver the drug to the hypoxic regions of the tumor tissues.

6. OVERALL SUMMARY AND FUTURE DIRECTIONS

Tumor microenvironment and irregularly developed vasculature in the tumor tissues provide various opportunities to target and deliver the chemotherapeutic agent at the tumor site with the help of nanotechnology. Stimuli responsive liposomes and polymersomes can be chemically engineered to deliver the drugs at the targeted tumor site. We developed and evaluated tumor microenvironment responsive PEGylated nanoparticles for their effectiveness as drug delivery carriers. We observed that the drugs were successfully delivered to tumor extracellular matrix when encapsulated in MMP-9 responsive liposomes. We also observed that lower levels of oxygen and reducing agents in tumor microenvironment can be used to deliver drugs to hypoxic tumor cells.

Overexpressed enzyme in tumor extracellular matrix - MMP-9 promotes tumor progression. MMP-9 digests collagen IV in the tumor extracellular matrix, and assists tumor cell migration, angiogenesis and metastasis. We synthesized a collagen mimetic lipopeptide, and incorporated it in a liposome (Chapter 1). We incorporated a reducible PEG lipid in the liposome to coat the liposome with PEG while in blood circulation and protect the collagen mimetic lipopeptide on the surface of liposomes. PEGylation of nanoparticles makes them long circulating by reducing the interactions between the nanoparticle and reticuloendothelial system. However, as the liposomes reach tumor extracellular matrix, this PEG layer is cleaved in response to overexpressed GSH in tumor extracellular matrix. Cleavage of PEG layer exposes the lipopeptide to overexpressed MMP-9 in the tumor tissue. The enzyme MMP-9 cleaves the lipopeptide, making the lipid bilayer unstable which allows leakage of the encapsulated content in the tumor extracellular matrix. We observed that these liposomes encapsulated drug gemcitabine and released it in pancreatic cancer cells in monolayer and spheroidal cultures. We also observed the

release of encapsulated dye carboxyfluorescein in the pancreatic cancer xenograft developed on Athymic female nude mice. Treatment with gemcitabine encapsulated liposomes resulted in decreased cell viability in pancreatic cancer cells PANC-1. Better control over tumor growth was observed after treatment with gemcitabine encapsulated MMP-9 responsive liposomes as compared to the conventional liposomes. These studies indicated the potential of the MMP-9 responsive liposomal drug carrier for clinical use. We have established the preliminary foundation for these studies by using biocompatible chemicals. The preliminary studies with animals would further help for power analysis and testing of the liposomal system *in-vivo* in mice. We have used an unsaturated lipid POPE for these liposomes. It would also be interesting to study the effect of a saturated lipid on drug delivery capability of drug release from the liposomes.

Recent studies on tumor microenvironment revealed its critical role in tumor progression. Hypoxia in the tumor microenvironment is a key player in modifying the biochemical levels at the tumor site. However, very few studies are focused on delivering the drugs to the hypoxic areas in the tumor tissues. We have developed hypoxia responsive liposomes (Chapter 2) and hypoxia responsive polymersomes (Chapter 3, Chapter 4) for drug delivery to hypoxic areas. We observed that azobenzene incorporated PEG conjugated lipid POPE and polymer PLA can be used for preparation of hypoxia responsive nanoparticles. Anti-cancer drug gemcitabine was used as a model drug for encapsulation into the nanoparticles. Cell viability in pancreatic cancer cells BxPC-3 was decreased after treatment with drug encapsulating hypoxia responsive liposomes and polymersomes. The peptide iRGD was observed to improve depth of penetration in the layered cultures of BxPC-3 (Chapter 2 and Chapter 4). We also observed that echogenic hypoxia responsive liposomes were traceable by diagnostic ultrasound imaging (Chapter 4). Future studies with polymersomes of varied polymer chain lengths would provide deeper understanding of effect

of chain length on stimuli responsive behavior. It is also necessary to observe the effect of these polymersomes on hypoxic tumors *in-vivo*. Echogenic polymersomes can be imaged using sub-harmonic ultrasound imaging apparatus to selectively track the polymersomes *in-vivo*. Combining multiple stimuli in a single tumor microenvironment responsive drug carrier may futher improve the drug delivery to the tumor tissues.

REFERENCES

1. Gu, F. X.; Karnik, R.; Wang, A. Z.; Alexis, F.; Levy-Nissenbaum, E.; Hong, S.; Langer, R. S.; Farokhzad, O. C., Targeted nanoparticles for cancer therapy. *Nano today* **2007,** *2* (3), 14-21.
2. Davis, M. E.; Shin, D. M., Nanoparticle therapeutics: an emerging treatment modality for cancer. *Nature reviews Drug discovery* **2008,** *7* (9), 771-782.
3. Brigger, I.; Dubernet, C.; Couvreur, P., Nanoparticles in cancer therapy and diagnosis. *Advanced drug delivery reviews* **2012,** *64*, 24-36.
4. Mura, S.; Nicolas, J.; Couvreur, P., Stimuli-responsive nanocarriers for drug delivery. *Nature materials* **2013,** *12* (11), 991-1003.
5. Rapoport, N., Physical stimuli-responsive polymeric micelles for anti-cancer drug delivery. *Progress in Polymer Science* **2007,** *32* (8), 962-990.
6. Danhier, F.; Feron, O.; Préat, V., To exploit the tumor microenvironment: passive and active tumor targeting of nanocarriers for anti-cancer drug delivery. *Journal of Controlled Release* **2010,** *148* (2), 135-146.
7. Whiteside, T., The tumor microenvironment and its role in promoting tumor growth. *Oncogene* **2008,** *27* (45), 5904-5912.
8. Maeda, H.; Sawa, T.; Konno, T., Mechanism of tumor-targeted delivery of macromolecular drugs, including the EPR effect in solid tumor and clinical overview of the prototype polymeric drug SMANCS. *Journal of controlled release* **2001,** *74* (1), 47-61.
9. Maeda, H.; Wu, J.; Sawa, T.; Matsumura, Y.; Hori, K., Tumor vascular permeability and the EPR effect in macromolecular therapeutics: a review. *Journal of controlled release* **2000,** *65* (1), 271-284.
10. Cho, K.; Wang, X.; Nie, S.; Shin, D. M., Therapeutic nanoparticles for drug delivery in cancer. *Clinical cancer research* **2008,** *14* (5), 1310-1316.
11. Motornov, M.; Roiter, Y.; Tokarev, I.; Minko, S., Stimuli-responsive nanoparticles, nanogels and capsules for integrated multifunctional intelligent systems. *Progress in Polymer Science* **2010,** *35* (1), 174-211.
12. Stuart, M. A. C.; Huck, W. T.; Genzer, J.; Müller, M.; Ober, C.; Stamm, M.; Sukhorukov, G. B.; Szleifer, I.; Tsukruk, V. V.; Urban, M., Emerging applications of stimuli-responsive polymer materials. *Nature materials* **2010,** *9* (2), 101-113.
13. Cheng, R.; Meng, F.; Deng, C.; Klok, H.-A.; Zhong, Z., Dual and multi-stimuli responsive polymeric nanoparticles for programmed site-specific drug delivery. *Biomaterials* **2013,** *34* (14), 3647-3657.
14. Li, J.; Wang, B.; Wang, Y.; Liu, P.; Qiao, W., Preparation and characterization of thermosensitive nanoparticles for targeted drug delivery. *Journal of Macromolecular Science, Part A* **2008,** *45* (10), 833-838.
15. Cabane, E.; Malinova, V.; Menon, S.; Palivan, C. G.; Meier, W., Photoresponsive polymersomes as smart, triggerable nanocarriers. *Soft Matter* **2011,** *7* (19), 9167-9176.
16. Chen, W.; Du, J., Ultrasound and pH dually responsive polymer vesicles for anticancer drug delivery. *Scientific reports* **2013,** *3*.
17. Qiu, Y.; Park, K., Environment-sensitive hydrogels for drug delivery. *Advanced drug delivery reviews* **2012,** *64*, 49-60.
18. Gao, W.; Chan, J. M.; Farokhzad, O. C., pH-responsive nanoparticles for drug delivery. *Molecular pharmaceutics* **2010,** *7* (6), 1913-1920.

19. Cook, J. A.; Gius, D.; Wink, D. A.; Krishna, M. C.; Russo, A.; Mitchell, J. B. In *Oxidative stress, redox, and the tumor microenvironment*, Seminars in radiation oncology, Elsevier: 2004; pp 259-266.
20. Cerritelli, S.; Velluto, D.; Hubbell, J. A., PEG-SS-PPS: reduction-sensitive disulfide block copolymer vesicles for intracellular drug delivery. *Biomacromolecules* **2007,** *8* (6), 1966-1972.
21. Lee, M. R.; Baek, K. H.; Jin, H. J.; Jung, Y. G.; Shin, I., Targeted enzyme-responsive drug carriers: studies on the delivery of a combination of drugs. *Angewandte Chemie International Edition* **2004,** *43* (13), 1675-1678.
22. De La Rica, R.; Aili, D.; Stevens, M. M., Enzyme-responsive nanoparticles for drug release and diagnostics. *Advanced drug delivery reviews* **2012,** *64* (11), 967-978.
23. Shannon, A. M.; Bouchier-Hayes, D. J.; Condron, C. M.; Toomey, D., Tumour hypoxia, chemotherapeutic resistance and hypoxia-related therapies. *Cancer treatment reviews* **2003,** *29* (4), 297-307.
24. Thambi, T.; Deepagan, V.; Yoon, H. Y.; Han, H. S.; Kim, S.-H.; Son, S.; Jo, D.-G.; Ahn, C.-H.; Suh, Y. D.; Kim, K., Hypoxia-responsive polymeric nanoparticles for tumor-targeted drug delivery. *Biomaterials* **2014,** *35* (5), 1735-1743.
25. Byrne, J. D.; Betancourt, T.; Brannon-Peppas, L., Active targeting schemes for nanoparticle systems in cancer therapeutics. *Advanced drug delivery reviews* **2008,** *60* (15), 1615-1626.
26. Tiwari, R.; Borgen, P.; Wong, G.; Cordon-Cardo, C.; Osborne, M., HER-2/neu amplification and overexpression in primary human breast cancer is associated with early metastasis. *Anticancer research* **1991,** *12* (2), 419-425.
27. Goldenberg, M. M., Trastuzumab, a recombinant DNA-derived humanized monoclonal antibody, a novel agent for the treatment of metastatic breast cancer. *Clinical therapeutics* **1999,** *21* (2), 309-318.
28. Viani, G. A.; Afonso, S. L.; Stefano, E. J.; De Fendi, L. I.; Soares, F. V., Adjuvant trastuzumab in the treatment of her-2-positive early breast cancer: a meta-analysis of published randomized trials. *BMC cancer* **2007,** *7* (1), 153.
29. Sudimack, J.; Lee, R. J., Targeted drug delivery via the folate receptor. *Advanced drug delivery reviews* **2000,** *41* (2), 147-162.
30. Hilgenbrink, A. R.; Low, P. S., Folate receptor-mediated drug targeting: From therapeutics to diagnostics. *Journal of pharmaceutical sciences* **2005,** *94* (10), 2135-2146.
31. Iyer, A. K.; Khaled, G.; Fang, J.; Maeda, H., Exploiting the enhanced permeability and retention effect for tumor targeting. *Drug discovery today* **2006,** *11* (17), 812-818.
32. (a) Sykes, E. A.; Chen, J.; Zheng, G.; Chan, W. C., Investigating the impact of nanoparticle size on active and passive tumor targeting efficiency. *ACS nano* **2014,** *8* (6), 5696-5706; (b) Lammers, T.; Hennink, W.; Storm, G., Tumour-targeted nanomedicines: principles and practice. *British journal of cancer* **2008,** *99* (3), 392-397.
33. (a) Yoo, J.-W.; Chambers, E.; Mitragotri, S., Factors that control the circulation time of nanoparticles in blood: challenges, solutions and future prospects. *Current pharmaceutical design* **2010,** *16* (21), 2298-2307; (b) Mohanraj, V.; Chen, Y., Nanoparticles-a review. *Tropical Journal of Pharmaceutical Research* **2007,** *5* (1), 561-573.
34. Choi, M.-R.; Stanton-Maxey, K. J.; Stanley, J. K.; Levin, C. S.; Bardhan, R.; Akin, D.; Badve, S.; Sturgis, J.; Robinson, J. P.; Bashir, R., A cellular Trojan Horse for delivery of therapeutic nanoparticles into tumors. *Nano letters* **2007,** *7* (12), 3759-3765.

35. Chambers, E.; Mitragotri, S., Long circulating nanoparticles via adhesion on red blood cells: mechanism and extended circulation. *Experimental Biology and Medicine* **2007,** *232* (7), 958-966.
36. Harris, J. M.; Chess, R. B., Effect of pegylation on pharmaceuticals. *Nature reviews Drug discovery* **2003,** *2* (3), 214-221.
37. Laverman, P.; Boerman, O. C.; Oyen, W. J.; Corstens, F. H.; Storm, G., In vivo applications of PEG liposomes: unexpected observations. *Critical Reviews™ in Therapeutic Drug Carrier Systems* **2001,** *18* (6).
38. Alconcel, S. N.; Baas, A. S.; Maynard, H. D., FDA-approved poly (ethylene glycol)–protein conjugate drugs. *Polymer Chemistry* **2011,** *2* (7), 1442-1448.
39. Barenholz, Y. C., Doxil®—the first FDA-approved nano-drug: lessons learned. *Journal of Controlled Release* **2012,** *160* (2), 117-134.
40. Yokoyama, M., Drug targeting with nano-sized carrier systems. *Journal of Artificial Organs* **2005,** *8* (2), 77-84.
41. Chandrawati, R.; Caruso, F., Biomimetic liposome-and polymersome-based multicompartmentalized assemblies. *Langmuir* **2012,** *28* (39), 13798-13807.
42. Wang, G., Liposomes as drug delivery vehicles. *Drug Delivery: Principles and Applications. Hoboken: John Wiley & Sons Inc* **2005**, 411-433.
43. Sharma, A.; Sharma, U. S., Liposomes in drug delivery: progress and limitations. *International journal of pharmaceutics* **1997,** *154* (2), 123-140.
44. Gregoriadis, G., Engineering liposomes for drug delivery: progress and problems. *Trends in biotechnology* **1995,** *13* (12), 527-537.
45. Gabizon, A.; Martin, F., Polyethylene glycol-coated (pegylated) liposomal doxorubicin. *Drugs* **1997,** *54* (4), 15-21.
46. Meyerhoff, A., US Food and Drug Administration approval of AmBisome (liposomal amphotericin B) for treatment of visceral leishmaniasis. *Clinical Infectious Diseases* **1999,** *28* (1), 42-48.
47. Moribe, K.; Maruyama, K., Reviews on PEG coated liposomal drug carriers. *Drug Delivery Syst.* **2001,** *16* (3), 165-171.
48. Discher, B. M.; Won, Y.-Y.; Ege, D. S.; Lee, J. C.; Bates, F. S.; Discher, D. E.; Hammer, D. A., Polymersomes: tough vesicles made from diblock copolymers. *Science* **1999,** *284* (5417), 1143-1146.
49. Meng, F.; Zhong, Z.; Feijen, J., Stimuli-responsive polymersomes for programmed drug delivery. *Biomacromolecules* **2009,** *10* (2), 197-209.
50. Fleige, E.; Quadir, M. A.; Haag, R., Stimuli-responsive polymeric nanocarriers for the controlled transport of active compounds: Concepts and applications. *Adv Drug Deliver Rev* **2012,** *64* (9), 866-884.
51. Ganta, S.; Devalapally, H.; Shahiwala, A.; Amiji, M., A review of stimuli-responsive nanocarriers for drug and gene delivery. *J Control Release* **2008,** *126* (3), 187-204.
52. Radhakrishnan, K.; Tripathy, J.; Raichur, A. M., Dual enzyme responsive microcapsules simulating an "OR" logic gate for biologically triggered drug delivery applications. *Chem commun* **2013,** *49* (47), 5390-2.
53. de, l. R. R.; Aili, D.; Stevens, M. M., Enzyme-responsive nanoparticles for drug release and diagnostics. *Adv. Drug Delivery Rev.* **2012,** *64* (11), 967-978.
54. Coleman, J. D.; Thompson, J. T.; Smith, R. W., 3rd; Prokopczyk, B.; Vanden, H. J. P., Role of Peroxisome Proliferator-Activated Receptor β/δ and B-Cell Lymphoma-6 in

Regulation of Genes Involved in Metastasis and Migration in Pancreatic Cancer Cells. *PPAR Res* **2013,** *2013*, 121956.
55. Tauro, J. R.; Gemeinhart, R. A., Matrix metalloprotease triggered delivery of cancer chemotherapeutics from hydrogel matrixes. *Bioconjugate chem* **2005,** *16* (5), 1133-9.
56. Molineux, G., PEGylation: engineering improved pharmaceuticals for enhanced therapy. *Cancer Treat Rev* **2002,** *28* (Suppl. A), 13-16.
57. Liu, D.-L.; Chang, X.; Dong, C.-M., Reduction- and thermo-sensitive star polypeptide micelles and hydrogels for on-demand drug delivery. *Chem commun* **2013,** *49* (12), 1229-1231.
58. Ge, Z.; Li, J.; Liu, S., PEG-sheddable polyplex micelles as smart gene carriers based on MMP-cleavable peptide-linked block copolymers. *Chem commun* **2013**.
59. Määttä, M.; Soini, Y.; Liakka, A.; Autio-Harmainen, H., Differential expression of matrix metalloproteinase (MMP)-2, MMP-9, and membrane type 1-MMP in hepatocellular and pancreatic adenocarcinoma: implications for tumor progression and clinical prognosis. *Clin Cancer Res* **2000,** *6* (7), 2726-2734.
60. (a) Yingyuad, P.; Mevel, M.; Prata, C.; Furegati, S.; Kontogiorgis, C.; Thanou, M.; Miller, A. D., Enzyme-Triggered PEGylated pDNA-Nanoparticles for Controlled Release of pDNA in Tumors. *Bioconjugate chem* **2013,** *24* (3), 343-362; (b) Koo, A. N.; Lee, H. J.; Kim, S. E.; Chang, J. H.; Park, C.; Kim, C.; Park, J. H.; Lee, S. C., Disulfide-cross-linked PEG-poly(amino acid)s copolymer micelles for glutathione-mediated intracellular drug delivery. *Chem commun* **2008,** (48), 6570-6572; (c) Ren, T.-B.; Xia, W.-J.; Dong, H.-Q.; Li, Y.-Y., Sheddable micelles based on disulfide-linked hybrid PEG-polypeptide copolymer for intracellular drug delivery. *Polymer* **2011,** *52* (16), 3580-3586; (d) Zhang, A.; Zhang, Z.; Shi, F.; Ding, J.; Xiao, C.; Zhuang, X.; He, C.; Chen, L.; Chen, X., Disulfide crosslinked PEGylated starch micelles as efficient intracellular drug delivery platforms. *Soft Matter* **2013,** *9* (7), 2224-2233.
61. Abbott, A., Cell culture: biology's new dimension. *Nature* **2003,** *424* (6951), 870-872.
62. Phung, Y. T.; Barbone, D.; Broaddus, V. C.; Ho, M., Rapid generation of in vitro multicellular spheroids for the study of monoclonal antibody therapy. *J Cancer* **2011,** *2*, 507.
63. Longati, P.; Jia, X.; Eimer, J.; Wagman, A.; Witt, M.-R.; Rehnmark, S.; Verbeke, C.; Toftgård, R.; Löhr, M.; Heuchel, R. L., 3D pancreatic carcinoma spheroids induce a matrix-rich, chemoresistant phenotype offering a better model for drug testing. *BMC cancer* **2013,** *13* (1), 1-13.
64. Celano, M.; Calvagno, M. G.; Bulotta, S.; Paolino, D.; Arturi, F.; Rotiroti, D.; Filetti, S.; Fresta, M.; Russo, D., Cytotoxic effects of gemcitabine-loaded liposomes in human anaplastic thyroid carcinoma cells. *BMC cancer* **2004,** *4* (1), 63.
65. (a) Sarkar, N.; Banerjee, J.; Hanson, A. J.; Elegbede, A. I.; Rosendahl, T.; Krueger, A. B.; Banerjee, A. L.; Tobwala, S.; Wang, R.; Lu, X.; Mallik, S.; Srivastava, D. K., Matrix metalloproteinase-assisted triggered release of liposomal contents. *Bioconjugate chem* **2008,** *19* (1), 57-64; (b) Elegbede, A. I.; Banerjee, J.; Hanson, A. J.; Tobwala, S.; Ganguli, B.; Wang, R.; Lu, X.; Srivastava, D. K.; Mallik, S., Mechanistic studies of the triggered release of liposomal contents by matrix metalloproteinase-9. *J Am Chem Soc* **2008,** *130* (32), 10633-42.
66. Li, S.-D.; Huang, L., Stealth nanoparticles: high density but sheddable PEG is a key for tumor targeting. *J control release* **2010,** *145* (3), 178.

67. Estrela, J. M.; Ortega, A.; Obrador, E., Glutathione in cancer biology and therapy. *Crit Rev Clin Lab Sci* **2006,** *43* (2), 143-181.
68. Pompella, A.; Visvikis, A.; Paolicchi, A.; Tata, V. D.; Casini, A. F., The changing faces of glutathione, a cellular protagonist. *Biochem pharm* **2003,** *66* (8), 1499-1503.
69. Banerjee, J.; Hanson, A. J.; Gadam, B.; Elegbede, A. I.; Tobwala, S.; Ganguly, B.; Wagh, A. V.; Muhonen, W. W.; Law, B.; Shabb, J. B.; Srivastava, D. K.; Mallik, S., Release of liposomal contents by cell-secreted matrix metalloproteinase-9. *Bioconjugate chem* **2009,** *20* (7), 1332-9.
70. (a) Akers, W. J.; Xu, B.; Lee, H.; Sudlow, G. P.; Fields, G. B.; Achilefu, S.; Edwards, W. B., Detection of MMP-2 and MMP-9 activity in vivo with a triple-helical peptide optical probe. *Bioconjugate chem* **2012,** *23* (3), 656-63; (b) Knapinska, A.; Fields, G. B., Chemical biology for understanding matrix metalloproteinase function. *Chembiochem : a European journal of chemical biology* **2012,** *13* (14), 2002-20.
71. Nahire, R.; Paul, S.; Scott, M. D.; Singh, R. K.; Muhonen, W. W.; Shabb, J.; Gange, K. N.; Srivastava, D. K.; Sarkar, K.; Mallik, S., Ultrasound enhanced matrix metalloproteinase-9 triggered release of contents from echogenic liposomes. *Mol Pharm* **2012,** *9* (9), 2554-64.
72. Choi, M.-R.; Stanton-Maxey, K. J.; Stanley, J. K.; Levin, C. S.; Bardhan, R.; Akin, D.; Badve, S.; Sturgis, J.; Robinson, J. P.; Bashir, R., A cellular Trojan Horse for delivery of therapeutic nanoparticles into tumors. *Nano lett* **2007,** *7* (12), 3759-3765.
73. (a) Han, L. F.; Chen, Q. B.; Hu, Z. T.; Piao, J. G.; Hong, C. Y.; Yan, J. J.; You, Y. Z., Stimuli-triggered growth and removal of a bioreducible nanoshell on nanoparticles. *Macromolecular rapid communications* **2014,** *35* (6), 649-54; (b) Cai, X.; Dong, C.; Dong, H.; Wang, G.; Pauletti, G. M.; Pan, X.; Wen, H.; Mehl, I.; Li, Y.; Shi, D., Effective gene delivery using stimulus-responsive catiomer designed with redox-sensitive disulfide and acid-labile imine linkers. *Biomacromolecules* **2012,** *13* (4), 1024-34.
74. Chen, F.; Ohashi, N.; Li, W.; Eckman, C.; Nguyen, J. H., Disruptions of occludin and claudin-5 in brain endothelial cells in vitro and in brains of mice with acute liver failure. *Hepatology (Baltimore, Md.)* **2009,** *50* (6), 1914-23.
75. Sutherland, R. M., Cell and environment interactions in tumor microregions: the multicell spheroid model. *Science* **1988,** *240* (4849), 177-184.
76. Sasaki, T.; Ohno, T., Cytotoxicity tests on eye drop preparations by LDH release assay in human cultured cell lines. *Toxicol in Vitro* **1994,** *8* (5), 1113-1119.
77. Cosco, D.; Bulotta, A.; Ventura, M.; Celia, C.; Calimeri, T.; Perri, G.; Paolino, D.; Costa, N.; Neri, P.; Tagliaferri, P.; Tassone, P.; Fresta, M., In vivo activity of gemcitabine-loaded PEGylated small unilamellar liposomes against pancreatic cancer. *Cancer Chemother. Pharmacol.* **2009,** *64* (5), 1009-20.
78. Brusa, P.; Immordino, M. L.; Rocco, F.; Cattel, L., Antitumor activity and pharmacokinetics of liposomes containing lipophilic gemcitabine prodrugs. *Anticancer res* **2007,** *27* (1A), 195-199.
79. Ganta, S.; Devalapally, H.; Shahiwala, A.; Amiji, M., A review of stimuli-responsive nanocarriers for drug and gene delivery. *Journal of Controlled Release* **2008,** *126* (3), 187-204.
80. O'brien, M.; Wigler, N.; Inbar, M.; Rosso, R.; Grischke, E.; Santoro, A.; Catane, R.; Kieback, D.; Tomczak, P.; Ackland, S., Reduced cardiotoxicity and comparable efficacy in a phase III trial of pegylated liposomal doxorubicin HCl (CAELYX™/Doxil®) versus

conventional doxorubicin for first-line treatment of metastatic breast cancer. *Annals of oncology* **2004,** *15* (3), 440-449.
81. Torchilin, V., Tumor delivery of macromolecular drugs based on the EPR effect. *Advanced drug delivery reviews* **2011,** *63* (3), 131-135.
82. Kulkarni, P. S.; Haldar, M. K.; Nahire, R. R.; Katti, P.; Ambre, A. H.; Muhonen, W. W.; Shabb, J. B.; Padi, S. K.; Singh, R. K.; Borowicz, P. P., MMP-9 Responsive PEG cleavable nanovesicles for efficient delivery of chemotherapeutics to pancreatic cancer. *Molecular pharmaceutics* **2014,** *11* (7), 2390-2399.
83. Höckel, M.; Vaupel, P., Tumor hypoxia: definitions and current clinical, biologic, and molecular aspects. *Journal of the National Cancer Institute* **2001,** *93* (4), 266-276.
84. Vaupel, P.; Kallinowski, F.; Okunieff, P., Blood flow, oxygen and nutrient supply, and metabolic microenvironment of human tumors: a review. *Cancer research* **1989,** *49* (23), 6449-6465.
85. Höckel, M.; Schlenger, K.; Aral, B.; Mitze, M.; Schäffer, U.; Vaupel, P., Association between tumor hypoxia and malignant progression in advanced cancer of the uterine cervix. *Cancer research* **1996,** *56* (19), 4509-4515.
86. Brown, J. M.; Giaccia, A. J., The unique physiology of solid tumors: opportunities (and problems) for cancer therapy. *Cancer research* **1998,** *58* (7), 1408-1416.
87. Kadonosono, T.; Yamano, A.; Goto, T.; Tsubaki, T.; Niibori, M.; Kuchimaru, T.; Kizaka-Kondoh, S., Cell penetrating peptides improve tumor delivery of cargos through neuropilin-1-dependent extravasation. *Journal of Controlled Release* **2015,** *201*, 14-21.
88. Sugahara, K. N.; Teesalu, T.; Karmali, P. P.; Kotamraju, V. R.; Agemy, L.; Girard, O. M.; Hanahan, D.; Mattrey, R. F.; Ruoslahti, E., Tissue-penetrating delivery of compounds and nanoparticles into tumors. *Cancer cell* **2009,** *16* (6), 510-520.
89. Perche, F.; Biswas, S.; Wang, T.; Zhu, L.; Torchilin, V., Hypoxia-Targeted siRNA Delivery. *Angewandte Chemie International Edition* **2014,** *53* (13), 3362-3366.
90. Kamath, S.; Kummerow, F.; Narayan, K. A., A simple procedure for the isolation of rat liver microsomes. *Febs Letters* **1971,** *17* (1), 90-92.
91. Derda, R.; Laromaine, A.; Mammoto, A.; Tang, S. K.; Mammoto, T.; Ingber, D. E.; Whitesides, G. M., Paper-supported 3D cell culture for tissue-based bioassays. *Proceedings of the National Academy of Sciences* **2009,** *106* (44), 18457-18462.
92. Brown, J. M.; Wilson, W. R., Exploiting tumour hypoxia in cancer treatment. *Nature Reviews Cancer* **2004,** *4* (6), 437-447.
93. Vaupel, P.; Harrison, L., Tumor hypoxia: causative factors, compensatory mechanisms, and cellular response. *The oncologist* **2004,** *9* (Supplement 5), 4-9.
94. Kiyose, K.; Hanaoka, K.; Oushiki, D.; Nakamura, T.; Kajimura, M.; Suematsu, M.; Nishimatsu, H.; Yamane, T.; Terai, T.; Hirata, Y., Hypoxia-sensitive fluorescent probes for in vivo real-time fluorescence imaging of acute ischemia. *Journal of the American Chemical Society* **2010,** *132* (45), 15846-15848.
95. Ruoslahti, E., Peptides as targeting elements and tissue penetration devices for nanoparticles. *Advanced Materials* **2012,** *24* (28), 3747-3756.
96. Teesalu, T.; Sugahara, K. N.; Ruoslahti, E., Tumor-penetrating peptides. *Front Oncol* **2013,** *3* (216), b3.
97. Lee, J.; Lilly, G. D.; Doty, R. C.; Podsiadlo, P.; Kotov, N. A., In vitro toxicity testing of nanoparticles in 3D cell culture. *Small* **2009,** *5* (10), 1213-1221.

98. Helmlinger, G.; Yuan, F.; Dellian, M.; Jain, R. K., Interstitial pH and pO2 gradients in solid tumors in vivo: high-resolution measurements reveal a lack of correlation. *Nature medicine* **1997,** *3* (2), 177-182.
99. Vaupel, P.; Schlenger, K.; Knoop, C.; Höckel, M., Oxygenation of human tumors: evaluation of tissue oxygen distribution in breast cancers by computerized O2 tension measurements. *Cancer research* **1991,** *51* (12), 3316-3322.
100. Carmeliet, P.; Jain, R. K., Angiogenesis in cancer and other diseases. *nature* **2000,** *407* (6801), 249-257.
101. Semenza, G. L., Hypoxia and cancer. *Cancer and Metastasis Reviews* **2007,** *26* (2), 223.
102. Zhong, H.; De Marzo, A. M.; Laughner, E.; Lim, M.; Hilton, D. A.; Zagzag, D.; Buechler, P.; Isaacs, W. B.; Semenza, G. L.; Simons, J. W., Overexpression of hypoxia-inducible factor 1α in common human cancers and their metastases. *Cancer research* **1999,** *59* (22), 5830-5835.
103. Duffy, J. P.; Eibl, G.; Reber, H. A.; Hines, O. J., Influence of hypoxia and neoangiogenesis on the growth of pancreatic cancer. *Mol Cancer* **2003,** *2* (1), 12.
104. Li, D.; Xie, K.; Wolff, R.; Abbruzzese, J. L., Pancreatic cancer. *The Lancet* **2004,** *363* (9414), 1049-1057.
105. Moore, M. J.; Goldstein, D.; Hamm, J.; Figer, A.; Hecht, J. R.; Gallinger, S.; Au, H. J.; Murawa, P.; Walde, D.; Wolff, R. A., Erlotinib plus gemcitabine compared with gemcitabine alone in patients with advanced pancreatic cancer: a phase III trial of the National Cancer Institute of Canada Clinical Trials Group. *Journal of clinical oncology* **2007,** *25* (15), 1960-1966.
106. Perche, F.; Biswas, S.; Wang, T.; Zhu, L.; Torchilin, V., Hypoxia-Targeted siRNA Delivery. *Angewandte Chemie* **2014,** *126* (13), 3430-3434.
107. Burris, H. r.; Moore, M. J.; Andersen, J.; Green, M. R.; Rothenberg, M. L.; Modiano, M. R.; Cripps, M. C.; Portenoy, R. K.; Storniolo, A. M.; Tarassoff, P., Improvements in survival and clinical benefit with gemcitabine as first-line therapy for patients with advanced pancreas cancer: a randomized trial. *Journal of clinical oncology* **1997,** *15* (6), 2403-2413.
108. Ciardiello, F.; Tortora, G., EGFR antagonists in cancer treatment. *New England Journal of Medicine* **2008,** *358* (11), 1160-1174.
109. Letchford, K.; Burt, H., A review of the formation and classification of amphiphilic block copolymer nanoparticulate structures: micelles, nanospheres, nanocapsules and polymersomes. *European journal of pharmaceutics and biopharmaceutics* **2007,** *65* (3), 259-269.
110. Chevalier, A.; Piao, W.; Hanaoka, K.; Nagano, T.; Renard, P.-Y.; Romieu, A., Azobenzene-caged sulforhodamine dyes: a novel class of 'turn-on'reactive probes for hypoxic tumor cell imaging. *Methods and Applications in Fluorescence* **2015,** *3* (4), 044004.
111. Gabizon, A.; Catane, R.; Uziely, B.; Kaufman, B.; Safra, T.; Cohen, R.; Martin, F.; Huang, A.; Barenholz, Y., Prolonged circulation time and enhanced accumulation in malignant exudates of doxorubicin encapsulated in polyethylene-glycol coated liposomes. *Cancer research* **1994,** *54* (4), 987-992.
112. Du, Y.; Chen, W.; Zheng, M.; Meng, F.; Zhong, Z., pH-sensitive degradable chimaeric polymersomes for the intracellular release of doxorubicin hydrochloride. *Biomaterials* **2012,** *33* (29), 7291-7299.

113. Howse, J. R.; Jones, R. A.; Battaglia, G.; Ducker, R. E.; Leggett, G. J.; Ryan, A. J., Templated formation of giant polymer vesicles with controlled size distributions. *Nature materials* **2009,** *8* (6), 507-511.
114. Justice, B. A.; Badr, N. A.; Felder, R. A., 3D cell culture opens new dimensions in cell-based assays. *Drug discovery today* **2009,** *14* (1), 102-107.
115. Yoshii, Y.; Waki, A.; Yoshida, K.; Kakezuka, A.; Kobayashi, M.; Namiki, H.; Kuroda, Y.; Kiyono, Y.; Yoshii, H.; Furukawa, T., The use of nanoimprinted scaffolds as 3D culture models to facilitate spontaneous tumor cell migration and well-regulated spheroid formation. *Biomaterials* **2011,** *32* (26), 6052-6058.
116. Durand, R. E.; Olive, P. L., Evaluation of bioreductive drugs in multicell spheroids. *International Journal of Radiation Oncology* Biology* Physics* **1992,** *22* (4), 689-692.
117. Heldin, C.-H.; Rubin, K.; Pietras, K.; Östman, A., High interstitial fluid pressure—an obstacle in cancer therapy. *Nature Reviews Cancer* **2004,** *4* (10), 806-813.
118. Teicher, B. A., Hypoxia and drug resistance. *Cancer and Metastasis Reviews* **1994,** *13* (2), 139-168.
119. Vaupel, P.; Kelleher, D. K.; Höckel, M. In *Oxygenation status of malignant tumors: pathogenesis of hypoxia and significance for tumor therapy*, Seminars in oncology, Elsevier: 2001; pp 29-35.
120. Brahimi-Horn, M. C.; Chiche, J.; Pouysségur, J., Hypoxia and cancer. *Journal of molecular medicine* **2007,** *85* (12), 1301-1307.
121. Gilkes, D. M.; Semenza, G. L.; Wirtz, D., Hypoxia and the extracellular matrix: drivers of tumour metastasis. *Nature Reviews Cancer* **2014,** *14* (6), 430-439.
122. Pupa, S. M.; Ménard, S.; Forti, S.; Tagliabue, E., New insights into the role of extracellular matrix during tumor onset and progression. *Journal of cellular physiology* **2002,** *192* (3), 259-267.
123. MacEwan, S. R.; Callahan, D. J.; Chilkoti, A., Stimulus-responsive macromolecules and nanoparticles for cancer drug delivery. *Nanomedicine* **2010,** *5* (5), 793-806.
124. Immordino, M. L.; Dosio, F.; Cattel, L., Stealth liposomes: review of the basic science, rationale, and clinical applications, existing and potential. *International journal of nanomedicine* **2006,** *1* (3), 297.
125. Hanahan, D.; Weinberg, R. A., The hallmarks of cancer. *cell* **2000,** *100* (1), 57-70.
126. Kizaka-Kondoh, S.; Inoue, M.; Harada, H.; Hiraoka, M., Tumor hypoxia: a target for selective cancer therapy. *Cancer science* **2003,** *94* (12), 1021-1028.
127. Maeda, H.; Bharate, G.; Daruwalla, J., Polymeric drugs for efficient tumor-targeted drug delivery based on EPR-effect. *European Journal of Pharmaceutics and Biopharmaceutics* **2009,** *71* (3), 409-419.
128. Wilson, W. R.; Hay, M. P., Targeting hypoxia in cancer therapy. *Nature Reviews Cancer* **2011,** *11* (6), 393-410.
129. Gu, G.; Gao, X.; Hu, Q.; Kang, T.; Liu, Z.; Jiang, M.; Miao, D.; Song, Q.; Yao, L.; Tu, Y., The influence of the penetrating peptide iRGD on the effect of paclitaxel-loaded MT1-AF7p-conjugated nanoparticles on glioma cells. *Biomaterials* **2013,** *34* (21), 5138-5148.
130. Sugahara, K. N.; Teesalu, T.; Karmali, P. P.; Kotamraju, V. R.; Agemy, L.; Greenwald, D. R.; Ruoslahti, E., Coadministration of a tumor-penetrating peptide enhances the efficacy of cancer drugs. *science* **2010,** *328* (5981), 1031-1035.
131. Diou, O.; Tsapis, N.; Fattal, E., Targeted nanotheranostics for personalized cancer therapy. *Expert opinion on drug delivery* **2012,** *9* (12), 1475-1487.

132. Derda, R.; Tang, S. K.; Laromaine, A.; Mosadegh, B.; Hong, E.; Mwangi, M.; Mammoto, A.; Ingber, D. E.; Whitesides, G. M., Multizone paper platform for 3D cell cultures. *PloS one* **2011,** *6* (5), e18940.
133. Sugahara, K. N.; Braun, G. B.; de Mendoza, T. H.; Kotamraju, V. R.; French, R. P.; Lowy, A. M.; Teesalu, T.; Ruoslahti, E., Tumor-penetrating iRGD peptide inhibits metastasis. *Molecular cancer therapeutics* **2015,** *14* (1), 120-128.
134. Khoruzhenko, A., 2D-and 3D-cell culture. *Biopolymers and Cell* **2011,** *27* (1), 17-24.
135. Tung, Y.-C.; Hsiao, A. Y.; Allen, S. G.; Torisawa, Y.-s.; Ho, M.; Takayama, S., High-throughput 3D spheroid culture and drug testing using a 384 hanging drop array. *Analyst* **2011,** *136* (3), 473-478.
136. Banerjee, J.; Hanson, A. J.; Muhonen, W. W.; Shabb, J. B.; Mallik, S., Microwave-assisted synthesis of triple-helical, collagen-mimetic lipopeptides. *Nature protocols* **2010,** *5* (1), 39-50.

APPENDIX A. SUPPORTING INFORMATION FOR 2

A1. Synthesis and characterization of Lipopeptide

The lipopeptide LP [$CH_3(CH_2)_{16}$CONH-GPQGIAGQR$(GPO)_4$GG-COOH] was synthesized by employing microwave assisted solid phase peptide synthesizer (Liberty, CEM Corporation, Matthews, SC) by following the protocol previously established in our laboratory[136]. The lipopeptide was purified by reverse phase HPLC (Shimadzu Scientific Instruments) using a diphenyl semi-preparatory column (Grace Vydac, 300 Å pore diameter silica, 5 μm particle size, 10 mm × 250 mm) as the stationary phase. A linear gradient (0−70%) of acetonitrile (with 0.1% trifluoroacetic acid) in water (with 0.1% trifluoroacetic acid) was used at a flow rate of 8 mL/min over 60 min. The chromatogram was recorded at 235 nm using a UV detector. After freeze drying the eluents, the peptide was characterized employing MALDI-TOF mass spectrometry with an AB 4800 MALDI TOF/TOF mass analyzer. An observed mass of 2332.3 Da in MALDI spectra confirmed the LP (calculated mass: 2332.2 Da). The collagen mimetic triple helical structure of the lipopeptide was assessed by CD spectrometry employing a Jasco J-815 CD spectrometer with a quartz cuvette of 1 mm path length. The positive peak at 222 nm and the negative peak at 198 nm confirmed the triple helical structure of collagen mimetic peptide. For the CD spectroscopic studies, 32 accumulations were recorded for each spectra.

A2. Synthesis of POPE-SPDP derivative

To a stirred solution of POPE (100 mg, 0.139 mmol) in dichloromethane (10 mL), diisopropylethyl amine (33 μL, 0.167 mmol) was added followed by SPDP-OSu (46 mg, 0.1462 mmol). Upon stirring overnight under an inert atmosphere, the reaction mixture was washed with water, dried over Na_2SO_4 and the solvent was evaporated under reduced pressure. The residue was

subjected to flash chromatography (R_f = 0.7 in 15% MeOH in CH_2Cl_2) to afford pure product as a waxy white solid (104 mg, 82%).

^{1}H NMR ($CDCl_3$,400 MHz): δ 0.81-0.89 (m, 6H), 1.2-1.4 (m, 41 H), 1.6 (br s, 4 H), 1.95- 2.05 (q, 4H), 2.25-2.35 (m, 4H), 2.6-2.8 (m, 6H), 3.0-3.1 (m, 2H), 3.41 (s, 2H), 3.8-3.95 (m, 4H), 4.3-4.4 (m, 2H), 5.2 (s, 1H), 5.3-5.4 (m, 2H), 7.12 -7.2 (t, 1H), 7.68-7.8 (m, 2H), 8.4 (d, 2H).

A3. Synthesis of POPE-S-S-PEG

The product obtained in the previous reaction (35 mg, 0.038 mmol) was reacted with PEG-SH (MW: 5000, 191 mg, 0.038 mmol) in dichloromethane (8 mL) under inert condition for 12 h. The volume of the reaction mixture was reduced under reduced pressure and then subjected to PLC (R_f = 0.8 in 15% MeOH in CH_2Cl_2). The pure product was isolated as a white waxy solid (125 mg, 56%). ^{1}H NMR ($CDCl_3$,400 MHz): δ 0.81-0.89 (m, 6H), 1.19-1.42 (m, 45H), 1.51-1.62 (m, 4H), 1.95-2.05 (q, 4H), 2.24-2.32 (m, 4H), 2.57-2.67 (m, 2H), 2.85-2.9 (t, 1H), 2.91-2.96 (t, 1H), 3.01-3.09 (m, 2H), 3.4-3.5 (m, 2H),3.52-3.75 (m, 307 H)3.8-3.86 (m, 2H), 3.86-4.0 (m, 4H), 4.1-4.2 (m, 1H), 4.32-4.4 (m, 1H), 5.15-5.25 (s, 1H), 5.3-5.4 (m, 2H). ^{13}C NMR ($CDCl_3$,100MHz): δ 13.90, 14.31, 19.27, 22.87, 25.06, 27.43, 29.51, 29.56, 29.87, 29.93, 32.10, 34.3, 59.22, 70.75, 72.13, 129.87, 130.168. MALDI mass spectra also confirmed the conjugation of PEG (Figure A1).

A4. Calculation for percent entrapment of gemcitabine

To calculate percent drug entrapment, absorbance of liposomes was measured at 268 nm (λmax of gemcitabine) before passing through Sephadex column (A1) and after collecting the eluent (A2). Dilution factor (d) was taken into consideration while calculating percent entrapment of the drug.

$$\text{Percent Entrapment} = \frac{\text{A1-A2d}}{\text{A1}} \times 100$$

A5. Calculation for amount of gemcitabine entrapped in nanovesicles

Gemcitabine was loaded in nanovesicles by pH gradient method. Citrate buffer (pH 4) encapsulated nanovesicles were incubated with gemcitabine, maintaining lipid:drug ratio of 10:1 (for example, 1 mg lipid containing vesicles were incubated with 0.1 mg of gemcitabine). Percent drug entrapment was calculated by using equation given in SC1. Percent entrapment of 50% was calculated, indicating that 50 µg of gemcitabine is encapsulated in nanovesicles containing 1 mg equivalent of lipid.

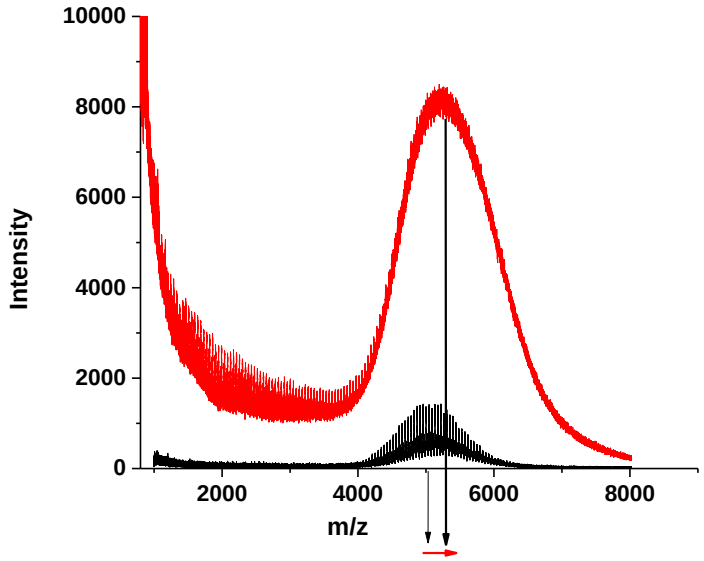

Figure A1. Overlay plot of MALDI spectra indicating increase in mass of PEG5000 (black) after successful synthesis of POPE-SS-PEG5000 (red)

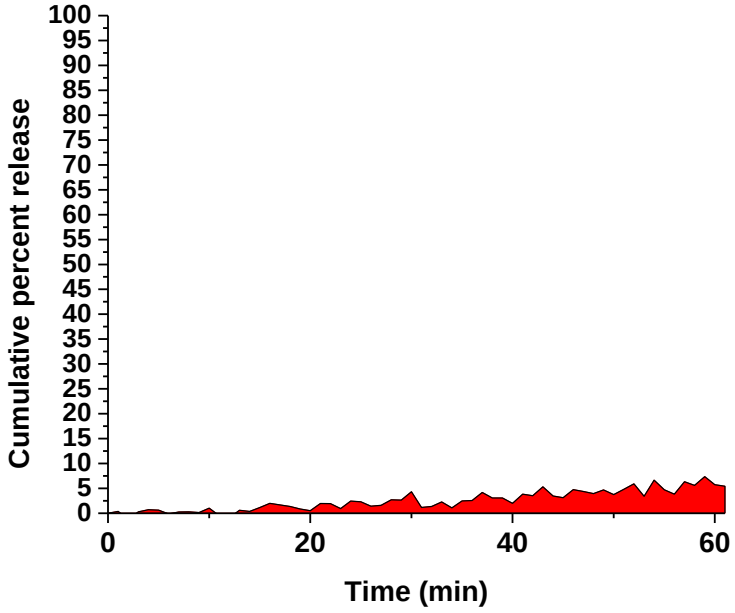

Figure A2. Cumulative percent release of carboxyfluorescein from nanovesicles was observed to be less than 5 (area represented in red) in 60 min in the presence of 10% human serum which was suggestive of stability of nanovesicles in circulation.

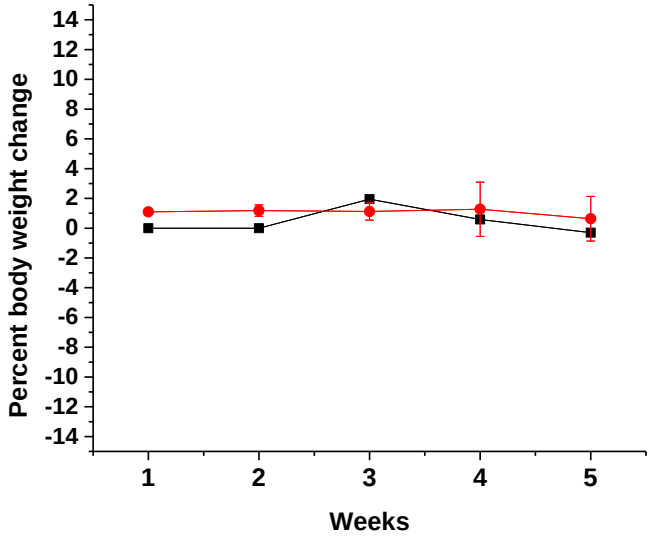

Figure A3. Body weight changes for mice under study were monitored over 5 weeks during the treatment. Weight loss of more than 15% was set as reference for toxicity. However, no significant weight loss was observed in control (black) as well as gemcitabine nanovesicles treated group (red).

Table A1. Release studies at 37 ºC

Treatment	Time (min)	Percent release
GSH (2 µM)	60	15
GSH (50 µM)	60	22
MMP-9 (2 µM)	60	43
MMP-9 (2 µM) and GSH (50 µM)	60	58

Table A2. Release from liposomes in conditioned media of cells

Conditioned media of cell line	Percent release in 1 hour
Brain endothelial cell line (does not secret MMP-9)	15
PANC-1	28

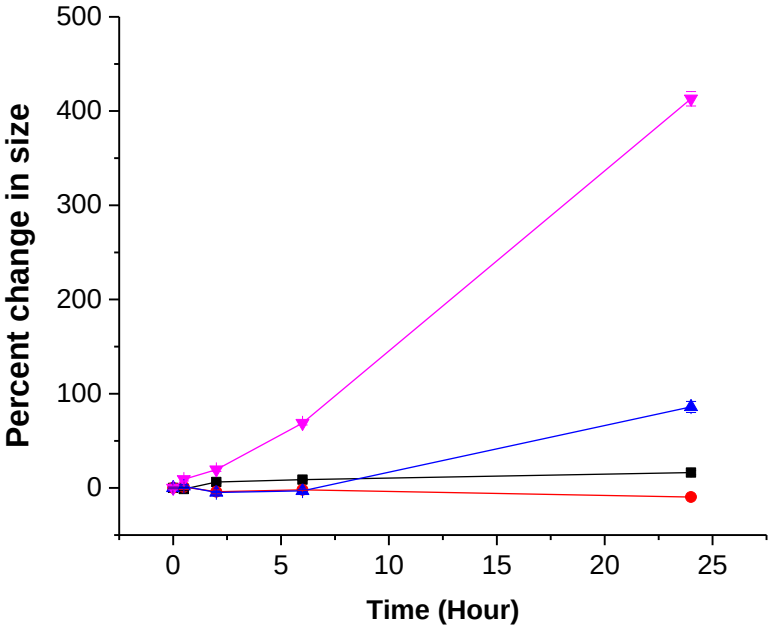

Figure A4. Effect of MMP-9 and GSH treatments on the size of nanovesicles at 37 ºC. Nanovesicles treated with MMP-9 (2 µM) and GSH (50 µM) showed significant increase in size in 24 hours (magenta triangles). Nanovesicles receiving only MMP-9 (2 µM) treatment also showed some increase in size within 24 hours (blue triangles). No substantial change in size was observed when nanovesicles received no treatment (black squares). Treatment with GSH (50 µM) showed a slight decrease in size over 24 hours (red circles).

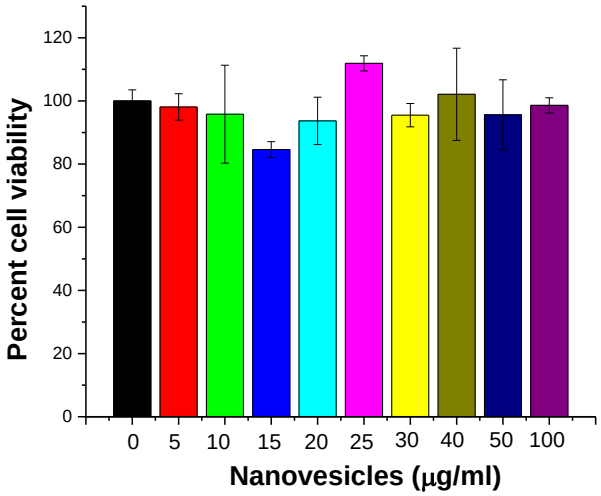

Figure A5. Toxicity of nanovesicles. Nanovesicles did not show any toxicity when incubated with MIAPaca-2 cells for 72 hours

APPENDIX B. SUPPORTING INFORMATION FOR 3

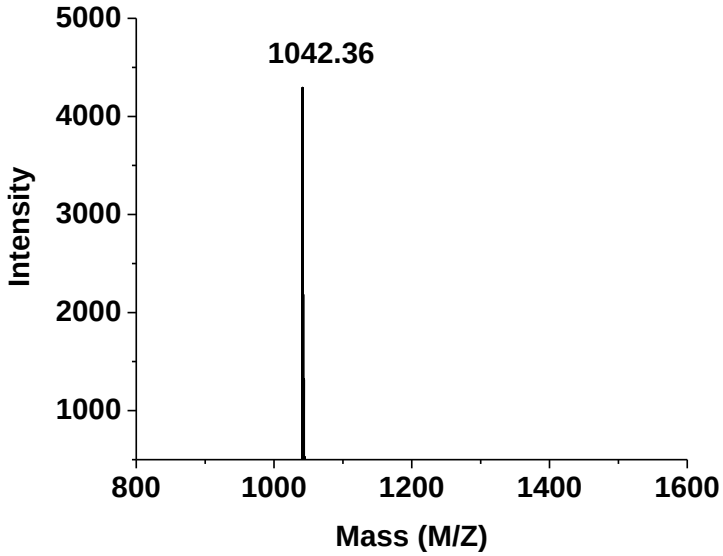

Figure B1. MALDI Mass spectrum for hexynoic acid conjugated iRGD peptide

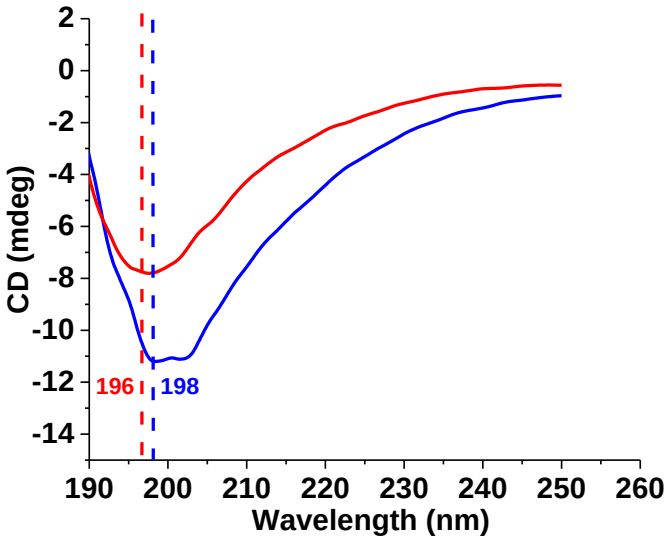

Figure B2. CD Spectra of iRGD peptide before (Blue) and after (Red) treatment with GSH (2mM)

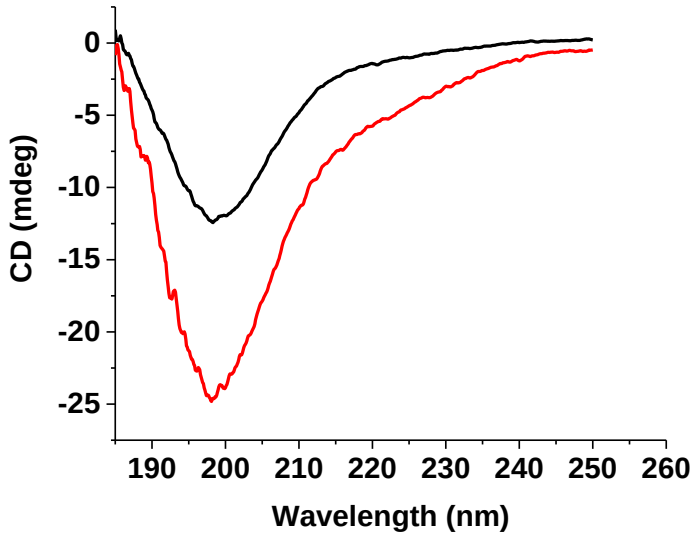

Figure B3. CD Spectra of hexynoic acid conjugated iRGD peptide before (Red) and after (Black) click reaction with DSPE-PEG-N3

APPENDIX C. SUPPORTING INFORMATION FOR 4

C1. Hypoxia responsive characteristic of azobenzene linker

To assess the hypoxia responsive characteristics of the azobenzene linker, the compound was dissolved in THF: water (1:5) to make 1 mg/mL solution. Microsomes (20 µg) and NADPH (100 µM) were added to the solution. This solution was then subjected to hypoxia treatment for 2 hours by bubbling nitrogen gas through the mixture. The UV spectrum was recorded before and after hypoxia treatment. To record the spectrum, the suspension was filtered through 0.2 µ filter, and UV spectra were recorded from 200 nm to 400 nm. We observed the shift in λ_{max} from 330 nm to 290 nm for the azobenzene linker after the treatment. We also observed a peak at 230 nm after treatment under hypoxic conditions. We speculate that emergence of the peak at 230 nm may be due to release of aniline from azobenzene molecule after hypoxia treatment.

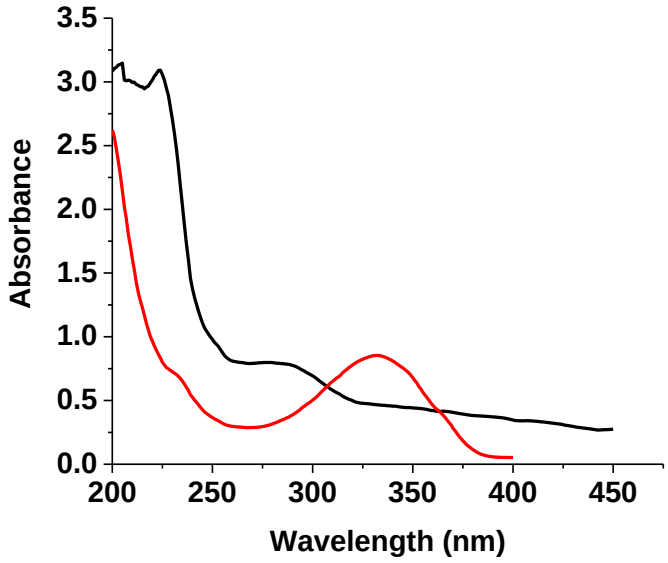

Figure C1. UV absorption spectra of responsive polymer before (red) and after (black) hypoxia treatment.

C2. Analysis of hypoxia responsive polymersomes by NMR spectroscopy

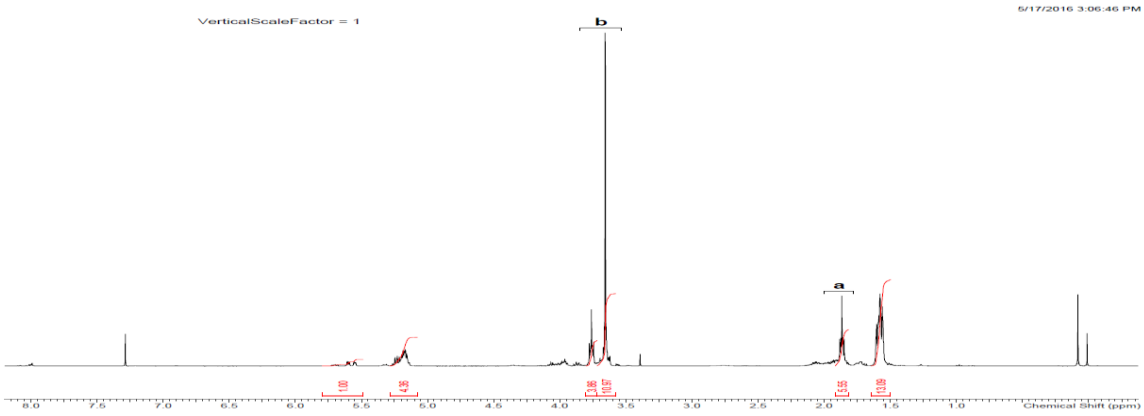

Figure C2. NMR spectrum of hypoxia responsive polymer. Integration of peaks a and b were used to determine chain lengths of PLA and PEG polymers

C3. GPC of synthesized hypoxia responsive polymers

GPC was carried out using Agilent 1120 system equipped with Ultrahydrogel 120 (Waters) column. Polystyrene standards (molecular weights: 1000, 2500, 3350, 5000, 9000) were used for calibration. Solutions of polystyrene standards and the synthesized hypoxia responsive polymer were prepared in trifluoroacetic acid. GPC was run using TFA (100%) as mobile phase with UV detection (230 nm). A standard curve was generated from the polystyrene standards, and molecular weight for the synthesized polymer was calculated from this plot. The molecular weight for the synthesized polymer was observed to be 7,400.

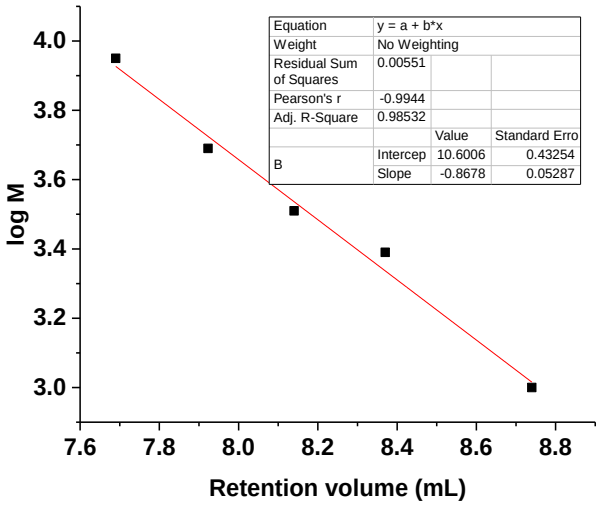

Figure C3. Calibration curve for the polystyrene molecular weight standards. The fitted straight line is shown in red along with the fitting parameters.

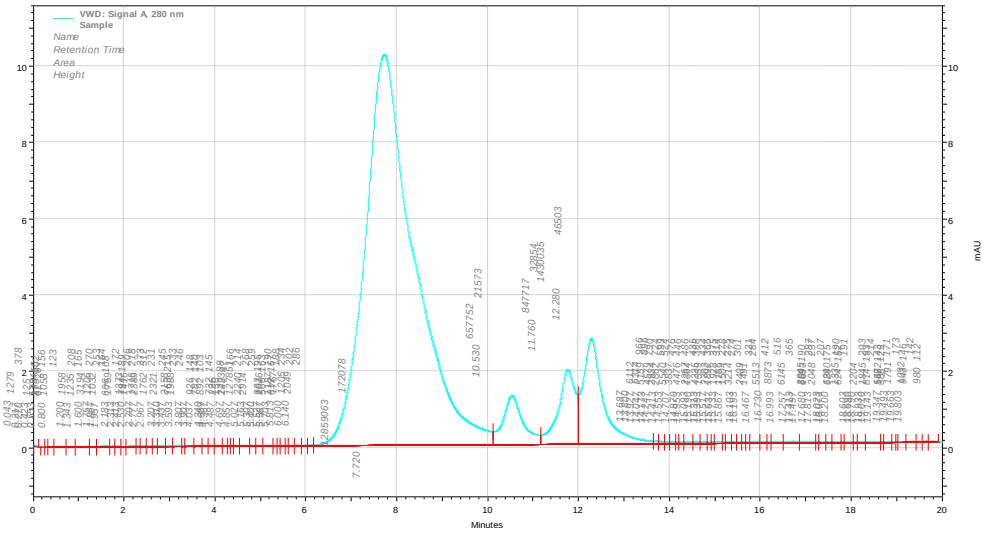

Figure C4. GPC Chromatogram of hypoxia responsive polymer.

C4. Cellular uptake in control polymersomes

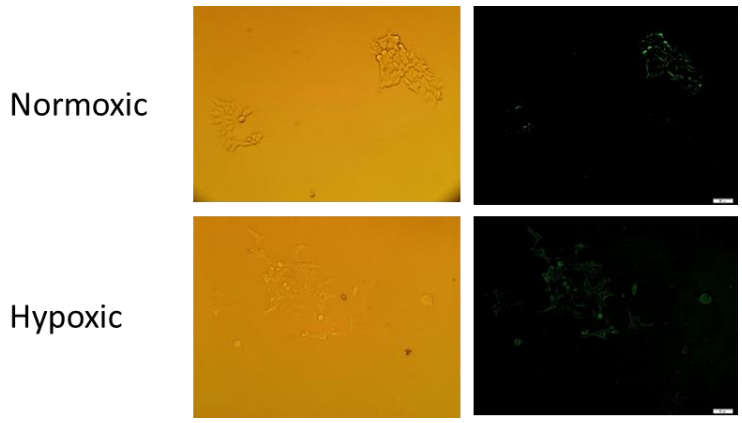

Figure C5. Cellular uptake of Control P polymersomes in normoxic and hypoxic BxPC-3 cells.

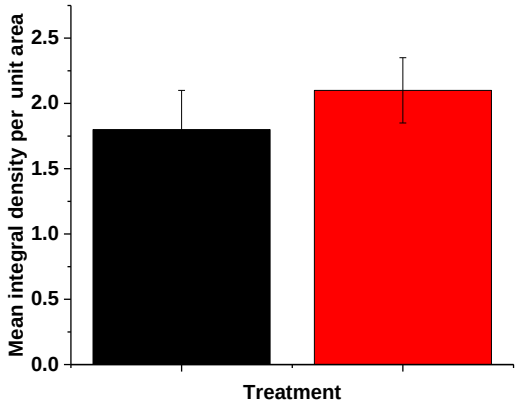

Figure C6. Cellular uptake of Control polymersomes (prepared from PLLA-PEG) in normoxic (black) and hypoxic (red) BxPC-3 cells did not show significant difference.

C5. Laser scanning confocal imaging for stained polymersome vesicles

A hydrophobic dye FM1-43 (Biotium) was encapsulated in the polymersome bilayer (20 µg/mg of polymer). To prepare large vesicles, polymersomes were briefly sonicated (5 min) in a bath sonicator (Aquasonic 500D, level 9). The polymersomes were passed through a gel filtration

column (Sephadex G-100), and the collected polymersomes were used for imaging. Confocal images were recorded using Olympus confocal laser scanning microscope with a 60X objective. The images indicated formation of vesicles (Figure C7).

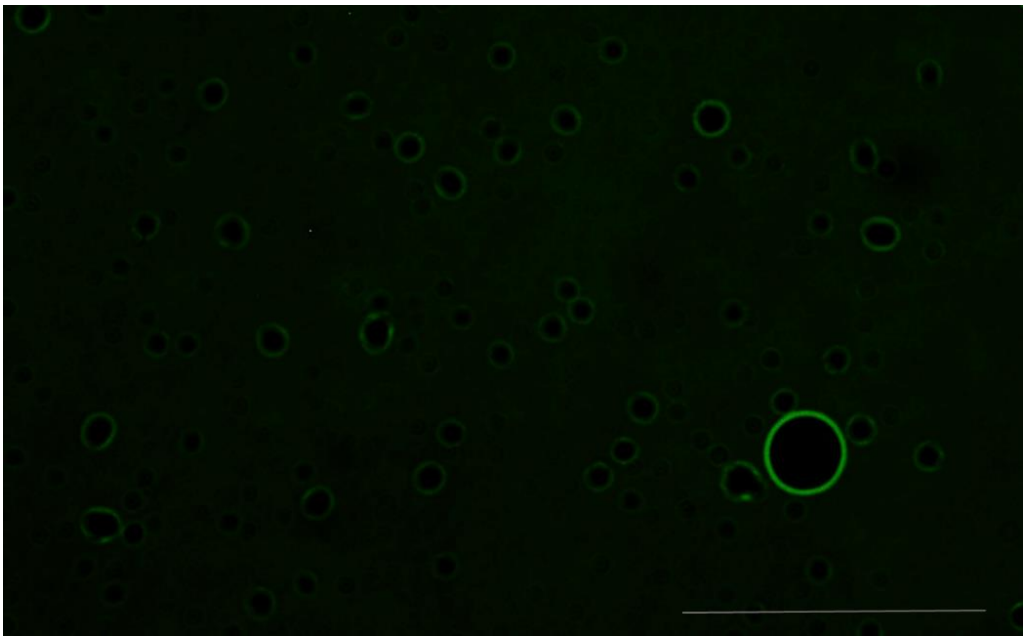

Figure C7. Large polymersome vesicles (green) stained with FM1-43. Scale bar indicates 10 µm.

C6. UV spectra of gemcitabine, erlotinib and hypoxia responsive polymer

To record the UV spectrum of the polymer (1mg), it was dissolved in 100µL THF, and was added to 1mL phosphate buffer (4mM, pH 7.4). THF was then evaporated by passing air through the mixture. To a 96 well plate, 20µL of the polymer solution was added to 180µL of phosphate buffer (4mM, pH 7.4). UV spectrum was recorded for the polymer in the range of 200nm to 400nm. Erlotinib (20µM) and gemcitabine (20µM) solutions were prepared in 4mM phosphate buffer (pH 7.4) for recording UV spectra.

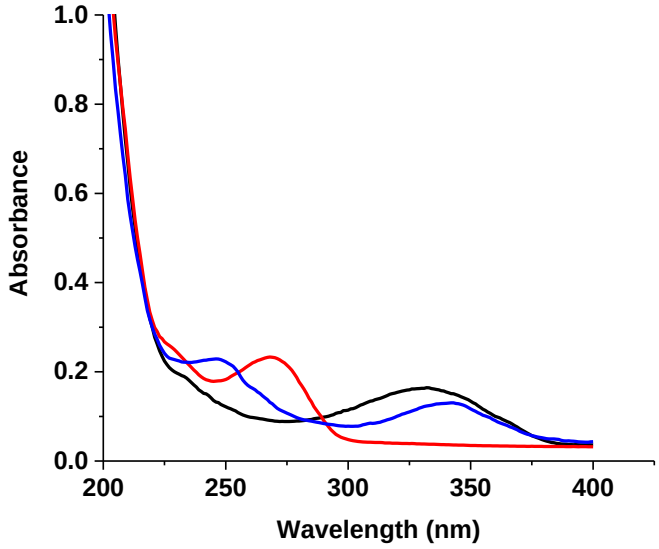

Figure C8. UV spectra of polymer (black), gemcitabine (red) and erlotinib (blue).